ELECTROCHEMICAL PROCESSING OF POLYTHIOPHENE FILMS WITH ENHANCED STRUCTURAL ORDER

A Thesis
Presented to
The Academic Faculty

By
Handoko Tirto Santoso

In Partial Fulfillment
Of the Requirements for the Degree
Master of Science in Mechanical Engineering

Georgia Institute of Technology
December 2011

ELECTROCHEMICAL PROCESSING OF POLYTHIOPHENE FILMS WITH ENHANCED STRUCTURAL ORDER

Approved by
Dr. Baratunde Cola, Co-Advisor
Mechanical Engineering
Georgia Institute of Technology

Dr. Kyriaki Kalaitzidou, Co-Advisor
Mechanical Engineering
Georgia Institute of Technology

Dr. Samuel Graham
Mechanical Engineering
Georgia Institute of Technology

Date Approved: July 8, 2011

To my father and mother, Johan Hadi Santoso and Yunita Lestari Santoso

ACKNOWLEDGEMENTS

Researching in Georgia Institute of Technology was a great life experience to shape my leadership, communication, problem solving and technical skill. The journey was full of challenge and I would not be able to finish it without the support of my advisors, family, friends, and loved ones. I would like to express my thankfulness to all who have helped me.

I would like to thank Dr. Baratunde Cola for being my advisor, sponsor, mentor, and role model. He did not only give me useful advices when I encountered problems on my research, but also shared his thought about planning early and making decision about the future. Everything started from one lunch with him. He told me that if I can learn to put my determination and perseverance in one thing, it will help me a lot in the future.

Dr. Kyriaki Kalatizidou was my academic advisor since my undergraduate research. She told me about the tremendous prospect in the polymer composite world and gave me insights about some powerful research applications which gave me inspiration and motivation for my work.

Dr. Virendra Singh, a friend and a mentor, always helped me with a lot of technical problems and taught me on doing experiments. He was also my chemistry trainer, without him, I would not be able to finish this thesis.

Thanks to Yaodong Liu for preparing the four-probe system and performing XRD on all of my samples, Dr. Satish Kumar from PTFE for letting me use his equipments, NEST group for a great discussion, and Dr. Samuel Graham for reviewing this thesis.

I owe a special gratitude for my girlfriend, Jessica Kamal, for her understanding and patience during my study as well as for giving me a lot of motivations. My parents, my brother, and my sister who always encourage and support me in everything I do, I thank them deeply.

Lastly, but the most important, I would like to give my special gratitude to my lovely God for giving me a healthy body and mind to endure and finish my study. Thank you.

TABLE OF CONTENTS

LIST OF TABLES

LIST OF FIGURES

LIST OF SYMBOLS AND ABBREVIATIONS

PTh	Polythiophene
PA	Polyaniline
PAL	Polyacetelyne
PPy	Polypyrrole
ICP	Intrinsically conducting polymer
SS	Stainless steel
CMC	Critical micelles concentration
SDBS	Sodium dodecylbenzenesulfonate
SDS	Sodium dodecyl sulfate
BFEE	Boron trifluoride diethyl etherate
DTBP	2,6-Di-tert-butylpyridine
WAXS	Wide-angle X-ray scattering
TGA	Thermogravimetric analysis
CP	Chronopotentiometry
CV	Cyclic voltammetry
CA	Chronoamperometry
XPS	X-ray photoelectron spectroscopy
σ	Conductivity
n	Density of charge
q	Charge
μ	Mobility of the carries

$t_{Polymer}$	Thickness of polymer film
Q	Net charge
η	Charge efficiency
M	Molar mass of thiophene
F	Faraday constant
n	Number of electrons transfer per monomer
δ	Doping level
ρ	Polymer density
$\boldsymbol{\varrho}$	Sheet resistivity
G	Volume correction factor
V	Potential
I	Current
d	Molecular spacing from XRD
λ	Wavelength of XRD laser
β	Full width at half maximum (FWHM)
θ	Bragg's angle
τ	Crystallite size
η	Charge efficiency of polymerization
Wp	Weight of the polymer
M	Molar mass of the monomer
k_B	Boltzmann constant
T	Absolute temperature
E	Dielectric constant

λ_B	Bjerrum length
r	Radius of an ion
$E_{coulomb}$	Coulombic energy
A	Area of the electrode

SUMMARY

Intrinsically conducting polymers (ICPs) with high mechanical strength and electrical conductivity are attractive for several applications spanning the fields of energy, defense, and transportation. Electrochemically processed polythiophene (PTh) films are a class of ICPs that have been demonstrated recently to possess electrical conductivities as high as 1,300 S/cm and stronger than common types of processed aluminum foils. While these results are promising, the electrical conductivity of PTh is still low compared to metals and the effects of important process conditions such as electrode resistance, distance between working and counter electrodes, and thiophene concentration on the structure and physical properties of electrochemically processed PTh films must be investigated in detail. In this work, electrode resistance and inter-electrode distance were demonstrated to be inversely proportional to the charge efficiency for PTh film growth. A critical concentration of thiophene that produced films with the highest conductivity was also revealed. Anionic surfactants sodium dodecyl sulfate (SDS) and sodium dodeclybenzene sulfonate (SDBS) were used, with and without a proton scavenger, in the Lewis acid boron trifluoride diethyl etherate (BFEE) electrolyte, which allows polymerization of thiophene at low oxidation potentials, to enhance the ordering and conjugation length of PTh through stabilization of the radical cation of thiophene via the dodecyl chain of the anionic surfactants. X-ray diffraction spectra revealed enhanced order and packing when surfactant was used during the processing of PTh films, and measured electrical conductivities were increased by as much as 300% because of the surfactant-mediated structural improvements. Necking behavior observed in tensile test of PTh films with anionic surfactant additives also suggests chain alignment and increased chain length.

1. INTRODUCTION

The optical, electrical, and mechanical properties of conjugated or intrinsically conducting polymers (ICPs) can be tailored by using different electrolytes, monomers, reduction-oxidation potentials, and dopants, which makes ICPs excellent candidates for a wide variety of applications. The discovery of electrical conductivity in polyacetylene upon doping with electron acceptors and electron-donors like iodine or arsenic pentafluoride by Heeger, MacDiarmid, and Shirakawa [1, 2] in 1977 was awarded the Chemistry Noble Prize in 2000. Intensive studies of different polymers, such as polyacetylene (PAL), polyaniline (PA), polypyrrole (PPy), and polythiophene (PTh), have been done since the seminal work of Heeger, MacDiarmid, and Shirakawa. Unlike conducting polymer composites that are a physical mixture of an insulating polymer and conductive fillers, ICPs can possess conductivities that are several orders of magnitude higher than conducting polymer composites because of the delocalization of π-bonded electrons in the polymer backbone [3]. ICPs are semiconductor with electrical conductivities in the range of metal (1-10^5 S/cm) with doping.

ICPs, such as PAL, PA, PPy, and PTh, have received a great deal of attention due to their broad application potential including but not limited to thermoelectric materials [4, 5], electrochromic displays [6, 7], light-emitting diodes [8, 9], photovoltaic cells [10, 11], and field-effect transistors [12, 13]. Several studies in the area of organic electronic devices attracted researchers because the organic materials have the potential to be more facile and economical to manufacture and more cost effective compared to inorganic electronics [14, 15]. The flexibility of polymer electronics is also attractive.

Conductivity of a solid at a macroscopic scale is represented by Eq. 1.1

$$\sigma = n\, q\, \mu \qquad \text{Eq. 1.1}$$

where, n is the density of charge, q is the charge, and μ is the mobility of the carries. ICPs are semiconductor materials with conductivities in the range of 10^{-2} to 10^{3} S/cm. The charge density in metals is much higher than in ICPs. However, the charge mobility in metals is lower than that of ICPs because charge mobility in metals is limited by a high rate of collision [16]. The current density in ICPs, unlike metal, is limited by the number of dopants in its conjugated polymer chain, so the charge transport in the polymer must be fast in order to have a high conductivity. It is well known that the molecular structure of polymers, i.e. chain-alignment, is an important factor in determining the physical properties of the polymer [17]. This is also true in ICPs, where chain alignment has been shown in several studies to affect the mechanical strength and electrical conductivity. While much progress has been made on understanding the structure-property relationship in ICPs, significant efforts are still required to improve the electrical and mechanical properties of ICPs in order for them to be used in various applications, which has been proven to be a daunting challenge [8, 18-20]. Therefore, the work in this thesis is focused on improving the molecular alignment and optimizing the conditions for scaling up the synthesis of PTh films, which have been demonstrated to posses the best combination of mechanical and electrical properties in an air-stable ICP [21-23].

PTh can be prepared by electrochemical polymerization [24-28] or chemical oxidation [20, 29]. Electrochemical polymerization typically yields films with more oriented structure than the chemical oxidation method because more cross-linking occurs during chemical oxidation [30]. In addition, a free-standing film can be electropolymerized directly on the working electrode without any post-processing. The thickness, morphology, and the rate of reaction can be controlled instrumentally via the electrochemical parameters. Electrochemical deposition also

has the advantage of providing fast and accurate information on the characteristics and properties of deposited film [30].

Electrochemical routes offer the ability to control molecular arrangement; yet the insolubility of thiophene in aqueous solution creates a challenge where limited electrolytes are available. Nonaqueous organic solvents like acetonitrile (CH_3CN), with different supporting salts have been used as the reaction medium for thiophene electropolymerization [6, 27, 31, 32]. However, polymer films synthesized in acetonitrile have relatively low conductivity (10-20 S/cm) and poor mechanical strength because the oxidation potential of the monomer (1.7 V vs. SCE) is higher than the potential required to overoxidize the PTh – this is the so called PTh paradox [33]. Alternatively, PTh films deposited in aqueous acid solutions such as H_3PO_4 [34] and $HClO_4$ [35] at lower oxidation potential, 1.05 V and 0.9 V, respectively, have poor film conductivity (0.1 – 1 S/cm) due to low doping level. Thiophene is unstable in strong acidic solvents, so an acid-initiated additive polymerization may take place resulting in a non-conjugated polymer. Solvated Lewis acid boron trifluoride diethyl etherate (BFEE) was used recently to synthesize PTh films with electrical conductivities as high as 100 S/cm and tensile strength of 140 MPa [26]. The drawback of using BFEE is that the solution is moisture sensitive and the presence of water during electropolymerization can degrade the quality of the synthesized PTh due to the formation of hydrogenated thiophene ring [36].

The electrical conductivity and mechanical properties of PTh films produced electrochemically depends on the oxidation potential applied during deposition, thiophene radical cation stability in the solution, and the amount and type of doping in the film. The addition of surfactants into the polymerization medium has been shown to lower the oxidation potential of thiophene [37] and stabilize charged species such as anion or cation radicals [19, 38].

Additionally, the anionic surfactants sodium dodecyl sulfate (SDS) and sodium dodecylbenzenesulfonate (SDBS) mixed into electropolymerization medium were shown to orient the molecular structure of polypyrrole under the controlled current density and surfactant concentration [39].

This thesis addresses a method of controlling the electropolymerization and enhancing molecular ordering of PTh films to have exceptional electrical and mechanical properties. While PTh films are attractive for several applications, the findings and techniques presented in this study of PTh films can be used to guide the electrochemical synthesize of different ICPs that may be more attractive for a broader set of applications (e.g., poly (3-hexylthiophene) or poly (3,4-ehylenedioxylthiophene)); thus one may consider the PTh films studied here as "model systems" for the electropolymerization process of ICPs with similar chemical structure. The goals of this thesis are accomplished by first presenting a review of the theoretical background for PTh electropolymerization and its associated experimental technique and characterization methods, then, systematically studying the effect of electrode and electrolyte preparation, inter-electrode distance, and thiophene concentration. A significant effort is devoted to understand the effects of anionic surfactants and 2,6-di-tert-butylpyridine (DTBP) mixed in BFEE on the structural order, quality, electrical, and mechanical properties of PTh films.

1.1 Charge Transport in Polythiophene Films

The addition or removal of electrons in conjugated polymer distorts the molecular structure producing specific energy levels called solitons, polarons, and bipolarons, depending on the doping level and the polymer structure [40]. The solitons conduction mechanism is suitable for ICPs with degenerate ground states such as polyacetylene. The polyheterocyclic polymers,

i.e. PTh and PPy, only have one ground state, so polaron(s) and bipolaron(s) are the more likely conduction mechanisms in the polymers. Polaron(s) and bipolaron in the PTh are shown in Figure 1.1.

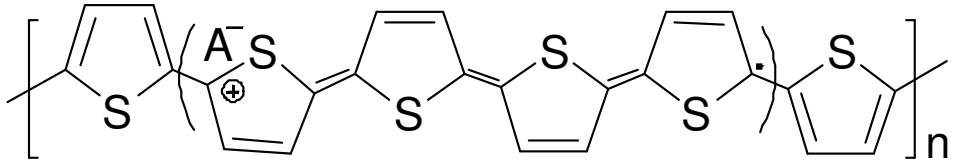

POLARON

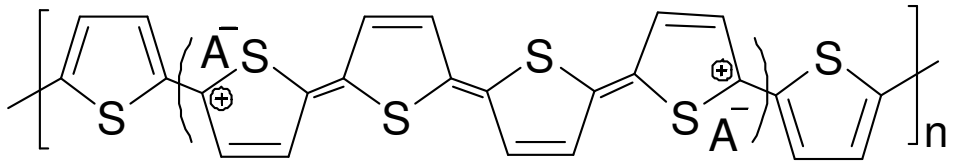

BIPOLARON

Figure 1.1: Polaron and bipolaron of PTh.

The process of formation of the polaron and bipolaron state is explained here based on the oxidation route which removes an electron from the polymer chain. When an electron is removed from the backbone, a free radical cation and a positive charge are produced; this is called a polaron (see Figure 1.1). The positive charge is then satisfied by the counter ion from the electrolyte. This process creates two non-degenerate ground states, aromatic and quinoid thiophene shown in Figure 1.2. The number of polarons increases to a certain extent with further doping and two nearby polarons combine and form a bipolaron that is more energetically favorable [40, 41]. A large number of bipolarons is generated at high doping levels and the overlapping produces bipolaron energy bands shown in Figure 1.3. In the undoped state, the PTh bandgap is 2.2 eV and PTh is insulating. Upon further doping, the highest occupied molecular orbital (HOMO) shifts upward by 0.61 eV and the lowest unoccupied molecular orbital (LUMO)

shifts downward by 0.71 eV to form bipolaron state, which makes the PTh conductive. The bipolaron states overlap at higher doping concentration and form bipolaron bands (0.19 to 0.21 eV) that lower the effective band gap, increasing the conductivity of the film further [42].

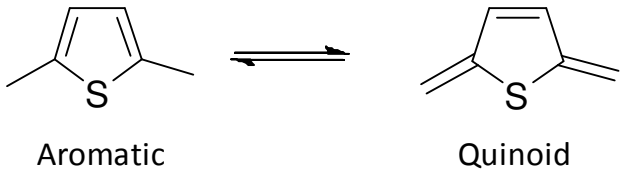

Figure 1.2: Aromatic and quinoid form of thiophene.

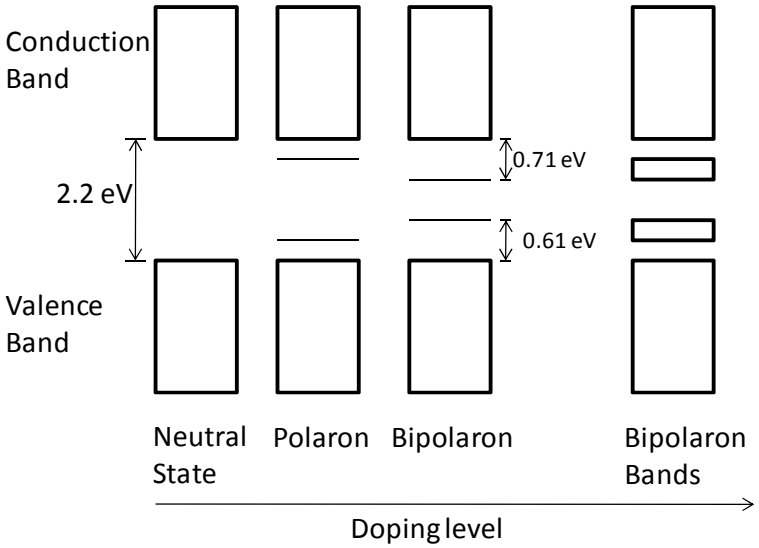

Figure 1.3: Band structure of ICPs with one ground state.

The concept of polarons and bipolarons is used to explain the mechanism of intra-chain charge mobility. These mechanism only explain part of the charge transport in ICP because the length of a conjugated polymer chain is usually in the range of 30 to 60 units[11] which corresponds to 15.6 to 31.2 nm for PTh; therefore, charge transport between chains must also be considered. This transport is best described by a "hopping" process similar to the process in redox polymers where electrons travel between occupied and unoccupied sites of one redox state

as shown in Figure 1.4 [11]. Intra-chain charge carrier transport is faster than inter-chain transport. Therefore, films with highly ordered and long conjugated polymer chains are expected to produce the highest electrical conductivities.

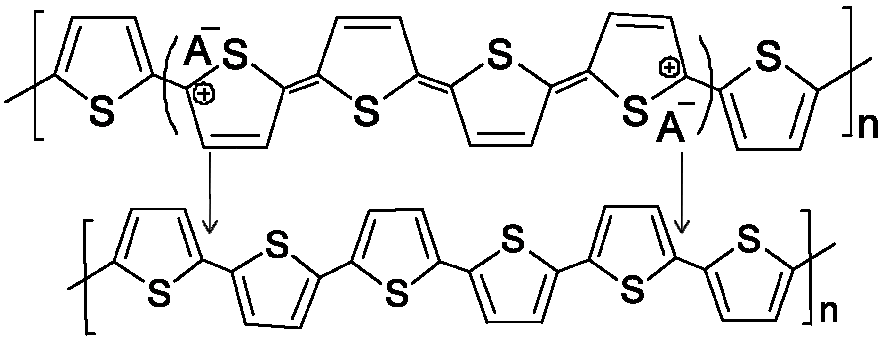

Figure 1.4: Inter-chain charge transport from bipolaron to neutral state chain.

1.2 Electropolymerization of Thiophene

The concept of doping distinguishes ICPs from all other types of polymers. The doping of conducting polymer is different than the doping process used in the semiconductor industry; the doping reaction in ICPs are redox reactions where p-doping is the oxidation doping reaction and n-doping is the reduction doping reaction. The doping charge is supplied by the electrode to the polymer, while oppositely charged ions migrate from the electrolyte to balance the electronic doping charge; this process resembles an electrochemical cell.

The electrolytic cell system used for polymer deposition in this study is shown Figure 1.5. Potential or current was applied to the cell to start the electrochemical process. There are three methods of deposition: galvanostatic or chronopotentiometry (CP), potentiostatic or chronoamperometry (CA), and potentiodynamic or cyclic voltammetry (CV). When ICP films are grown with CV, the polymers undergo constant changes between the doped (reduction or

oxidation) and neutral state which causes formation of disordered chains resulting in films with decreased electrical conductivities in the films. However, CV is very useful for investigating the preliminary polymerization conditions. It was used it this study for this purpose. CP and CA are more suitable for producing films with well-ordered structures compare with CV because the polymer does not undergo redox cycles and the ICP is in the doped state during the entire deposition.

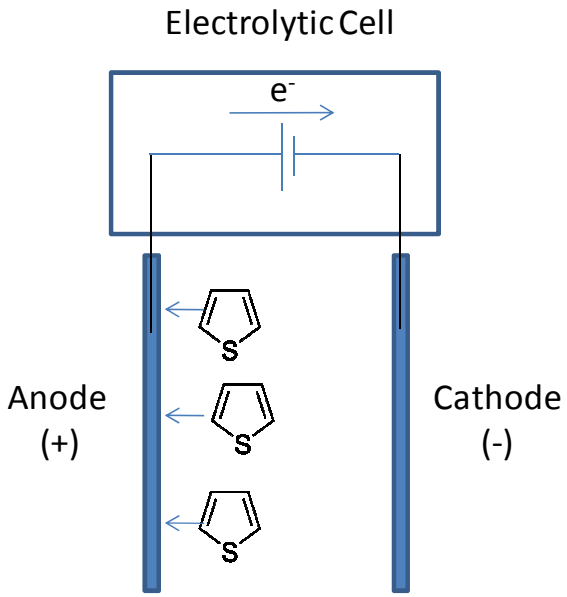

Figure 1.5: Electrolytic cell used to deposit PTh film.

The mechanism of the electrochemical polymerization remains the same for both CP and CA [43]. In the beginning, the dimerization process [44], shown in Figure 1.6, occurs on the electrode first because PTh has a very high rate constants of dimerization [44, 45]. CP is used to maintain constant current during deposition, which controls the diffusion rate of the monomer on the working electrode. The main features of electropolymerization using CP are that the potential decreases initially in a short period then increases to reach a maximum, and this is followed by a continuous decrease in potential. The initial decrease in potential is related to the charging of the

double layer capacitance. The increase in potential that follows is due to nucleation of ICP on the working electrode. Charged oligomers on the electrode catalyze the oxidation of monomers as the film increases in thickness and this process decreases the oxidation potential. Figure 1.7 shows a typical plot of potential versus time for the deposition of PTh using CP. CA is used to maintain constant potential during deposition providing constant thermodynamics during deposition. The current decreases initially in a short period with CA deposition as the double layer capacitance is established. The current increases to a maximum during nucleation of the ICP film, which follows the formation of the double layer. The nucleation step is followed by successive oxidation of monomer, which decreases the current. Figure 1.8 shows a typical plot of current versus time for deposition using CA. The last step of polymerization using CP and CA deposition is the solid-state polymerization process [43] where some time is required for the formation of a continuous film after the electrochemical process is stopped.

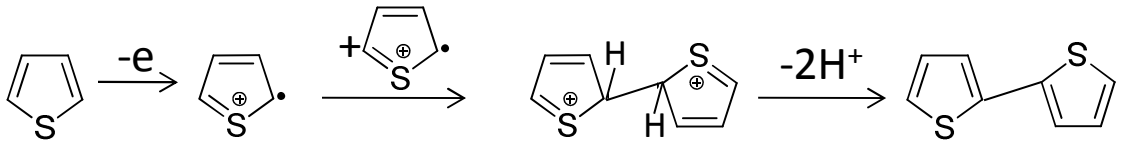

Figure 1.6: Dimerization of PTh.

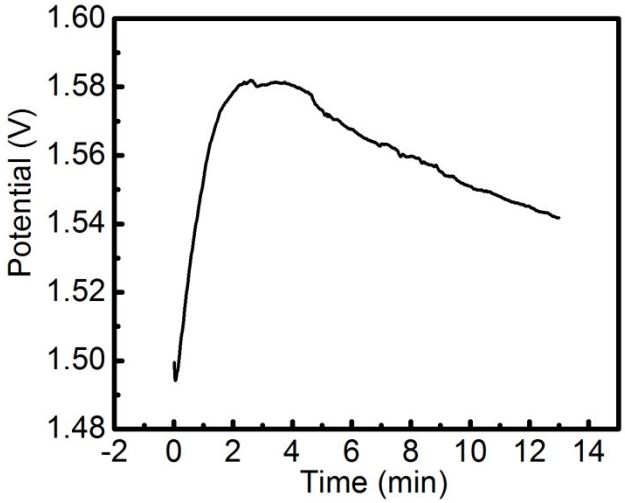

Figure 1.7: Chronopotentiogram of 50 mM thiophene in BFEE with 5 mm inter-electrode distance at 1 mA/cm^2.

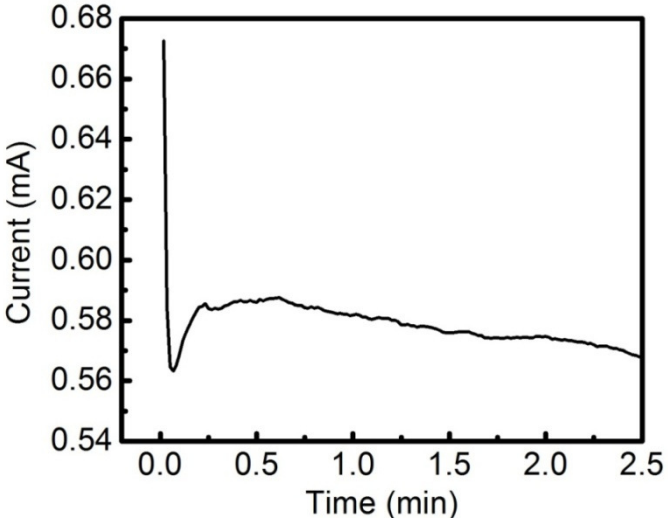

Figure 1.8: Chronoamperogram of 30 mM thiophene in BFEE with 5 mm inter-electrode distance at 1.3 V.

Deposition of PTh with CP and CA was conducted at a constant current of 1 mA/cm^2 and constant potential of 1.3 V, respectively, to compare the effect of this processing choice on the ability to control the deposition process. Figure 1.9 shows that potential and current during deposition of PTh in our experimental system is more reproducible with CP processing than with

CA processing. This result suggested that it is easier to control electrode kinetics than thermodynamics in our experimental setup. Figure 1.10a shows that the thickness of PTh films has more variability under the same conditions for deposition with CA than with CP. Films produced using CP also had higher electrical conductivities than films produced with CA (see Figure 1.10b). Therefore, galvanostat or CP was used here to study the physical properties of PTh films and produce PTh films with improved electrical and mechanical properties.

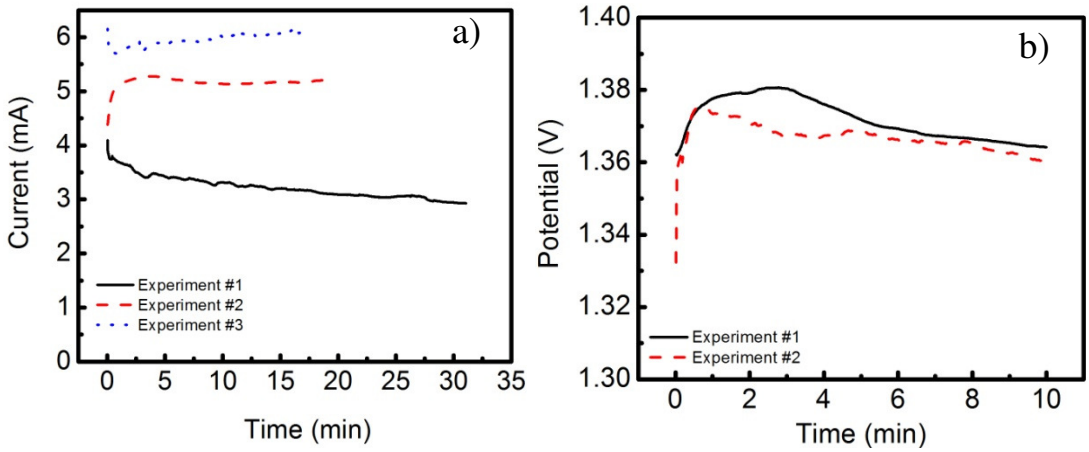

Figure 1.9: a) CA and b) CP comparison of 50 mM thiophene in BFEE with 10 cm^2 working electrode area with total charge of 6 C at 5 mm inter-electrode distance.

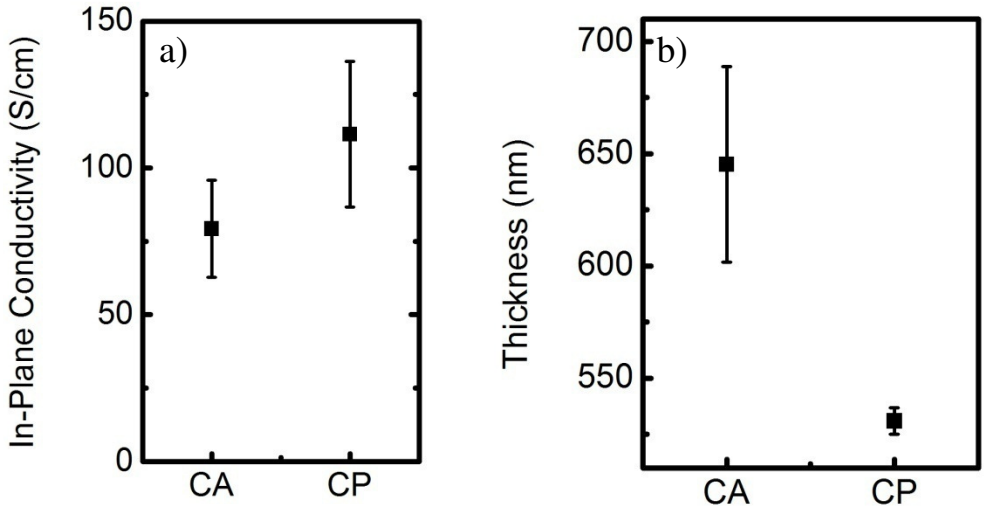

Figure 1.10: a) In-plane conductivity and b) thickness of 50 mM thiophene in BFEE with 10 cm^2 working electrode area with total charge of 6 C at 5 mm inter-electrode distance using CP at 1 mA/cm^2 and CA at 1.3 V. The data points are the average of three samples for CA and two samples for CP.

2. PROCESS OF MAKING POLYTHIOPHENE FILMS

2.1 Electrochemical Deposition of Thiophene

PTh films can be electropolymerized by reduction or oxidation routes. However, there is a major disadvantage using the reduction route because the polymer is synthesized in its neutral insulating form limiting attainable film thickness to about 100 nm [6]. The oxidation route enables film thickness up to hundreds of microns with a proper synthesis route [25]. PTh films were grown by either constant current (1 and 0.5 mA/cm^2) or constant potential (1.3 V) process in a one-compartment three-electrode cell using a Basi Epsilon C3. CV was performed from 1600 mV to -700 mV with a scan speed of 200 or 20 mV/s (the slower scan rate of 20 mV/s was used when necessary to observe electrochemical properties of additives with slow diffusion rates). Faster scan rate produces thinner film and fewer defects than slower scan rate, so it can be used when the CV was run before the deposition using CP or CA. On the other hand, lower scan rate can give more accurate reading from the CV. The reference electrode was Ag/AgCl, and 5 × 2 cm and 5.5 × 2.5 cm stainless steel (SS) sheets (AISI 304 with 0.025 mm thickness purchased from Alfa Aesar) were used as the working and counter electrode, respectively. The polished SS electrodes were placed in acetone for 30 min, sonicated using a Branson 3510 sonicator, and dried under vacuum for 30 min prior to each experiment. The electrode contact resistance was measured to be 0.6 Ω. All solutions were deaerated by bubbling argon gas for 30 min and maintained at a low overpressure during the polymerization. Thiophene monomer (> 99%) purchased from Sigma Aldrich was mixed in BFEE solvent during the deoxygenization process. BFEE was sonicated with the anionic surfactant for 30 min to break the ionic bond in studies where surfactant was used. Here, all electropolymerization experiments were performed at 21 ±

1 ^{0}C. Polymer films were washed with acetone before and after being peeled from the electrode. The clean films were dried for 8 hours under vacuum before any characterization.

CV scans of 50 mM thiophene in BFEE with a scan rate of 20 mV/s show the electrochemical properties of the system (see Figure 2.1). The oxidation from 0.02 V to 1 V corresponds to the oxidation of the polymer and the strong oxidation peak above 1 V indicates oxidation of the monomer. The oxidation of the polymer initiated at low potential (0.02 V) shows that the polymer is already formed on the working electrode because the CV was started from 1.6 V to -0.7 V. The oxidation potential of the monomer being higher than that of the polymer results in the so called PTh paradox [33]. This paradox leads to overoxidation of the polymer when the potential is large enough to oxidize the monomer and grow the polymer (as discussed below the use of BFEE reduces the magnitude of this overoxidation potential and its effects on film properties significantly compared to other electrolytes). The current density increased after the first CV cycle, which indicates polymer growth occurred on the working electrode during the first cycle. This increase in current produced a shift in oxidation potential to larger values. The change in oxidation current reached steady state in CV testing after the second cycle. Figure 2.2 shows that BFEE and SS are not electroactive and that BFEE with thiophene and anionic surfactants has a higher electrical conductivity than that BFEE without thiophene and anionic surfactants.

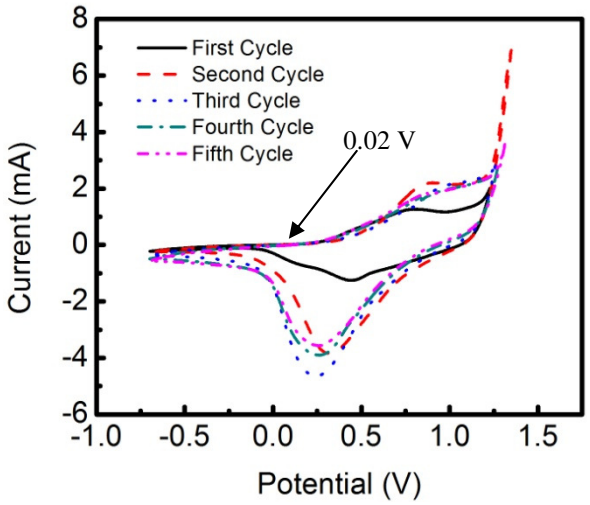

Figure 2.1: CV of 50 mM thiophene in BFEE at 5 mm inter-electrode distance using 20 mV/s scan rate.

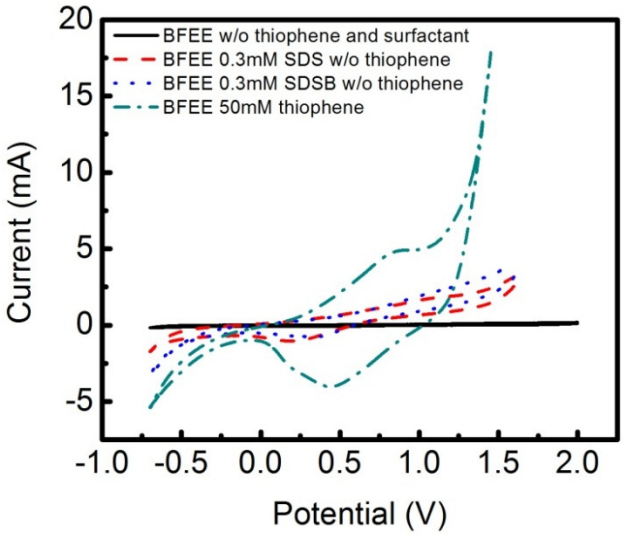

Figure 2.2: CV of electrochemical system in different electrolyte at 5 mm inter-electrode distance using scan rate of 200 mV/S

2.2 Boron Trifluoride Diethyl Etherate (BFEE) Electrolyte

The development of BFEE was first reported by Gasselin in 1894. It is a Lewis adduct between boron trifluoride and diethyl ether in 1:1 ratio, and a colorless, fuming liquid. The

conductivity of BFEE is 2.97×10^{-4} S/cm [46]. The conductivity of BFEE likely arises from the presence of polar molecules $[(C_2H_5)_3O^+]BF_4^-$ [47] or $H^+BF_3OH^-$ species, which result from complexation with low quantities of water [48]. BFEE is a solvated Lewis acid which helps to increase the stability of thiophene monomer in solution and reduce the aromaticity of thiophene, which decrease the oxidation potential of thiophene monomer. The oxidation potential of thiophene in BFEE has been reported to be as low as 1.3 V, which is 24% lower than the oxidation potential of thiophene in acetonitrile [26].

BFEE is an extremely moisture sensitive solvent. The exposure of the solution with air needs to be controlled in order to obtain consistent results and synthesize polymer films with high quality. Despite storing the solution under argon in a sealed container, the BFEE condition changed overtime in this work. In addition, different batches of the same type of BFEE purchased from Alfa Aesar resulted in PTh films with different properties. Therefore, in this study, the effects of different polymerization parameters were studied using the same batch from the manufacturer.

Another approach to control the quality of the BFEE used here was to freshly distill the BFEE before experiments. BFEE received from Alfa Aesar is reported to have less than 0.1% water; however, even small variations in water content can lead to inconsistent electrochemical behavior and make it difficult to synthesize PTh films with reproducible properties. The process used here to distill BFEE at 123-128 ^oC is shown in Figure 2.3. All glassware was rinsed with deionized water (DI) water then dried at 100 ^oC for 2 hours under vacuum before distillation. The first 10 mL of the distillation product was discarded.

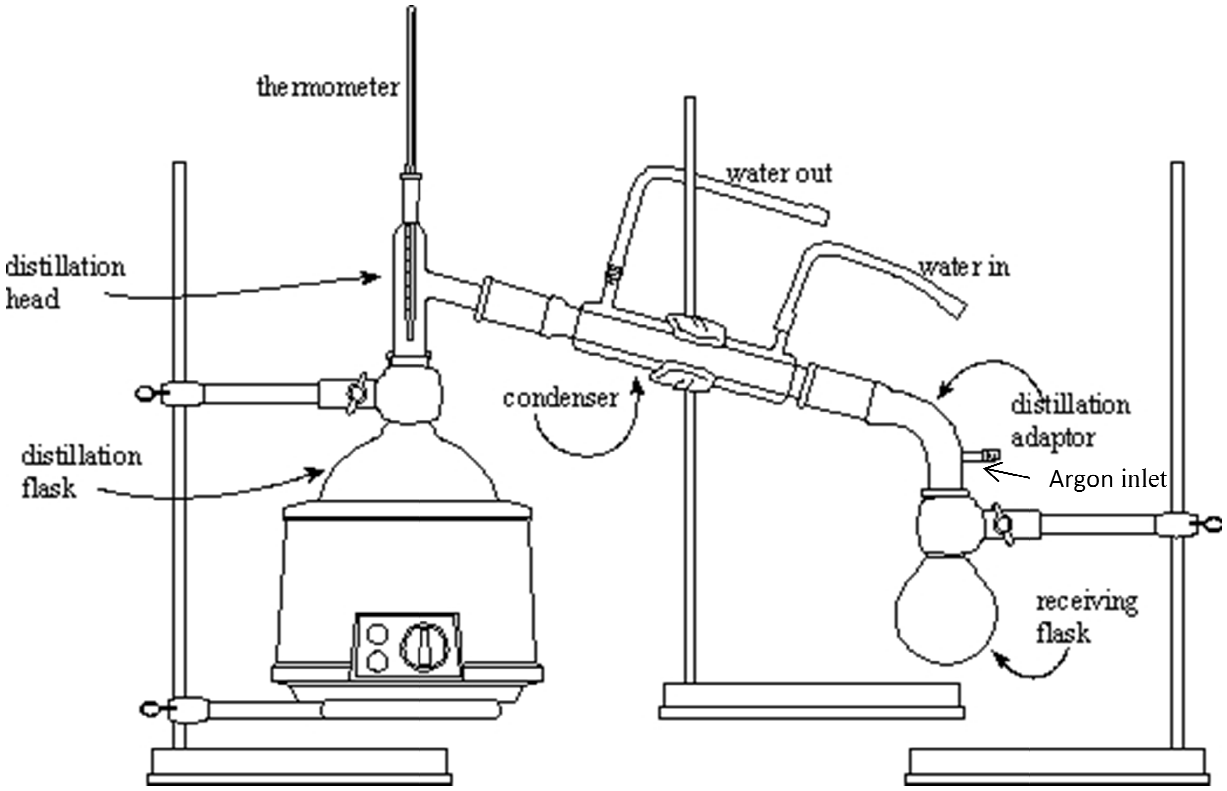

Figure 2.3: Setup to distill BFEE

BFEE was freshly distilled each time when combined with the proton scavenger DTBP in this work. The unknown concentration of water in BFEE supplied from the manufacturer would make isolating the effect of DTBP on the anodic route of PTh polymerization difficult because DTBP has been known as a proton scavenger that has high specificity towards protons in cationic polymerization, i.e. protons from water [49].

BFEE was stored between 2-8 ^{o}C because ether has a low boiling point. Due to the low boiling point, fumes are produced whenever BFEE makes contact with air, so all experiments involving BFEE were performed in a working chemical hood. BFEE is a toxic material that requires special care for handling and disposal. In addition, BFEE is a corrosive material, so the person used proper protective equipment (i.e. lab coat, goggles, gloves) when working with

BFEE. A respirator was used here when conducting experiments with BFEE and is recommended.

2.3 Selection and Preparation of Electrode

The selection of metal electrode is important because it affects the quality of the film [24]. The metal electrode has to be electrochemically stable within the applied potential used during the deposition, otherwise no film will be deposited because the kinetics of the metal dissolution are faster than the diffusion and polymerization of thiophene [50]. Platinum (Pt) and stainless steel (SS) are electrochemical stabile in BFEE at the potential window for deposition. However, PTh films deposited on Pt are difficult to peel from the substrate, which creates defects that reduce the strength of the film [24]. PTh films adhered well to Pt because of the electron shell configuration of Pt that has one electron on the most outer shell, which is removed easily to create a bond with thiophene. There is less electronic interaction when PTh is deposited on SS, and such films have been measured to be stronger than aluminum [24].

Surface finish of the electrode plays an important role in the quality of the PTh films. The films were difficult to peel from unpolished electrode which can create defects on the films, so a standardize approach to polish the surface of the electrode was developed. Polishing the SS can reduce the defects, i.e. microcracks, impurities due to oxygen layers, and extrusion lines from the processing, which affect surface processes such as adsorption, nucleation, and growth [51]. The SS sheet was polished on both sides using a Dremel MultiMax at a speed setting of 5 with oscillating motion using successively 1, 0.3, and 0.05 μm aluminum oxide powders purchased from Leco; this was then followed by a final polishing step with a colloidal silica suspension purchased from Struers to achieve a mirror-finish. The polishing time was 4 minutes on each side

with each grain size, so the total polishing time was 32 min per electrode. Then, the SS was cut in 5.5 × 3 cm size for use as the working and counter electrodes. A SS electrode before and after polishing with a reflection of an object is shown in Figure 2.4.

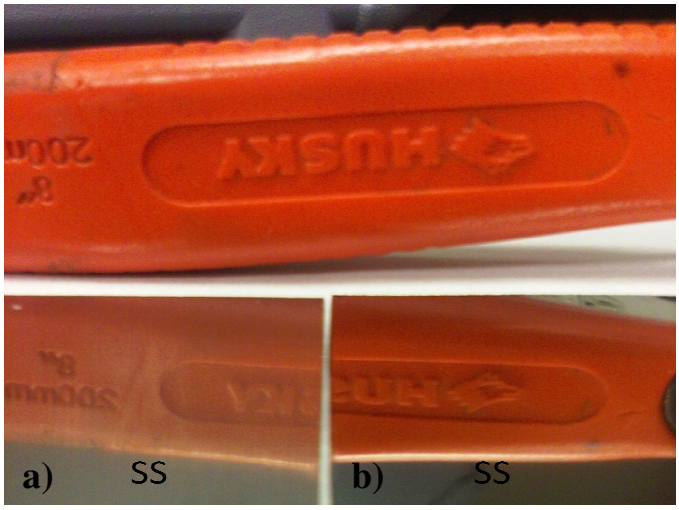

Figure 2.4: a) Unpolished and b) polished SS Sheet. The top photo is the object reflected in a) and b)

The SS working and counter electrodes were connected to a potentiostat/galvanostat by copper tape and stainless steel wire as shown in Figure 2.5a. The size of the copper tape is large enough to cover almost one side of the SS; the copper tape is covered with Kapton® tape to prevent oxidation. The next step was to make sure that the contact resistance was consistent. A screw and bolt were used to clamp the copper tape to the SS to produce a consistent contact resistance of 0.6-1 Ω. The screw and bolt were covered by Kapton® tape to prevent them for making contact with the other electrode. The working electrode was sized smaller than the counter electrode to reduce the effects of fringe capacitance and to improve charge quantity from the counter electrode. The side of the electrodes was covered with Kapton® tape as shown in Figure 2.5b to fix the electrode area at 5 × 2 cm.

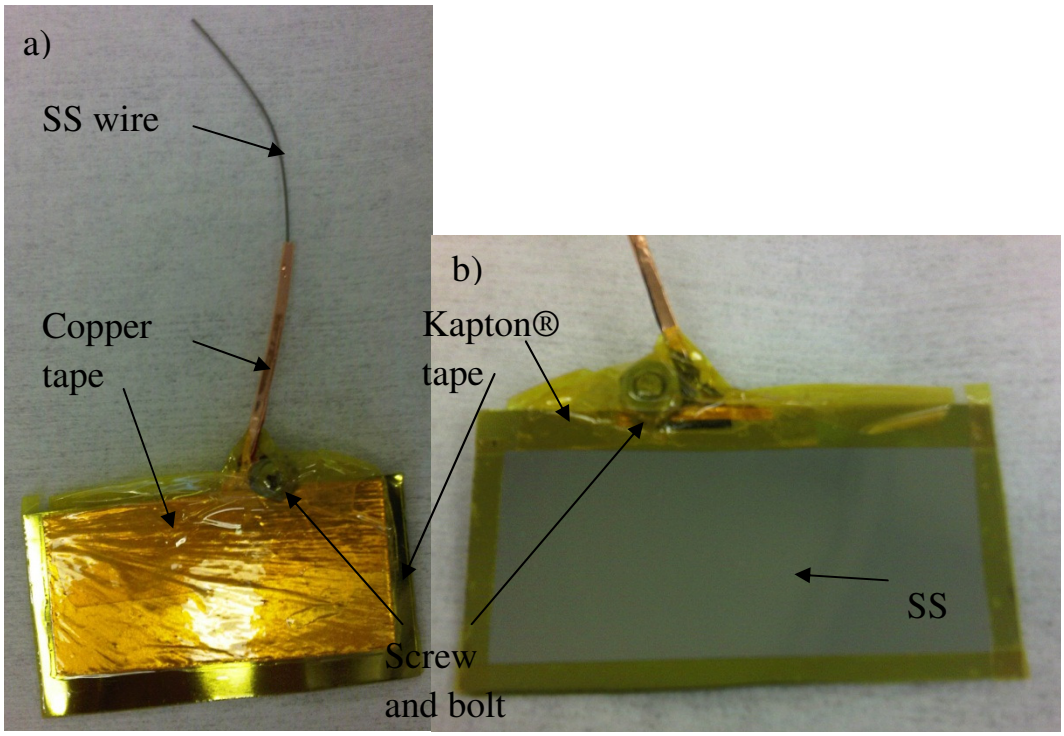

Figure 2.5: a) Back of the working electrode (the back of the counter electrode was configured similarly) and b) front of the working electrode.

Contact resistance at the electrode-lead wire junction has a significant effect on efficiency of the electrochemical deposition process. Figure 2.6 shows the cyclic voltammogram (CV) and chronoamperogram (CA) of 30 mM thiophene in BFEE with 5 mm inter-electrode distance for two different electrode contact resistances. The current density is smaller and the monomer oxidation potential is higher for higher contact resistance. The CA plot agreed with the CV plot that the current density decreased at higher contact resistance; this result in a significantly longer deposition time. This behavior agrees with Ohm's law; current is inversely proportional to resistance.

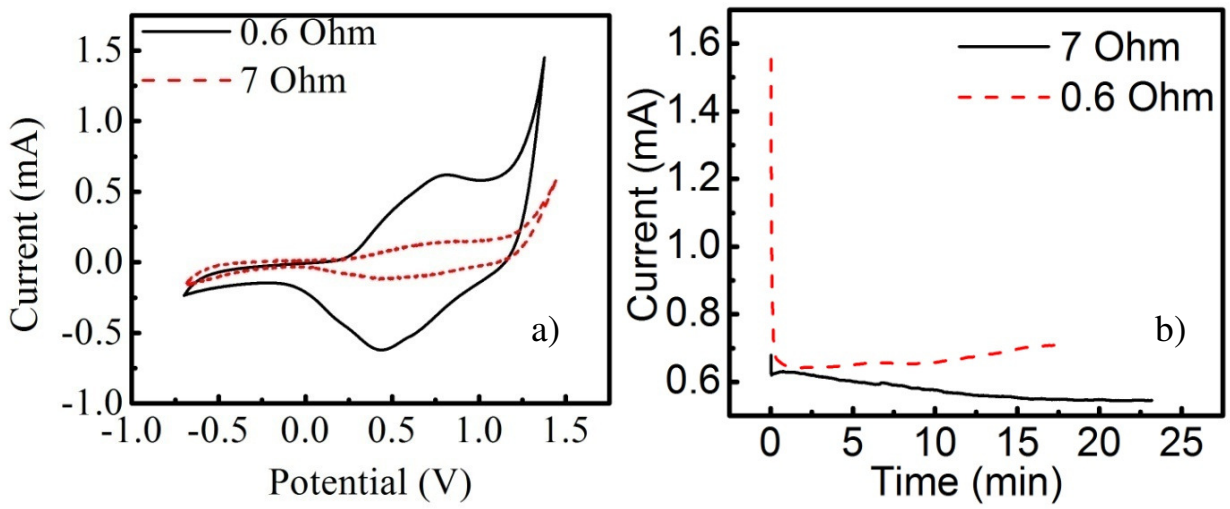

Figure 2.6: a) CV using 200 mV/s scan rate and b) CA of 30 mM thiophene in BFEE at 5 mM inter-electrode distance with different contact resistance of electrode. The potential of CA was 1.3 V with total charge of 800 mC.

2.4 Control of Film Thickness

The amount of charge passed at the working electrode during the polymerization was controlled in order to control the film thickness. Eq. 2.1 shows that the thickness of the polymer is proportional to *Q*, the net charge, which can be expressed as

$$t_{polymer} = \frac{\eta QM}{FA(n+\delta)\rho} \qquad \text{Eq. 2.1}$$

where η is the charge efficiency, *M* is the molar mass of thiophene, *F* is the Faraday constant, *A* is the electrode area, *n* is the number of electrons transferred per monomer (n=2), δ is the doping level, and ρ is polymer density [24, 52]. The thickness of PTh films were predicted using Eq. 2.1 and linear interpolation to reduce the number of experiments required to calibrate different experiments to produce a specific film thickness. Figure 2.7 shows the trend of thickness at 0.5 and 1 mA/cm^2. The total net charge of the film is calculated as the current, which is constant, multiplied by the total deposition time. For example, to make a film with 1.3 µm thickness, one

can perform deposition at 0.5 mA/cm^2 with total charge of 7.8 C as a starting guess and measure the thickness. If the film was measured to be 1.6 μm thick, the total charge would be reduced to say 6 C in a second experiment to create another data point. If the second film has measured thickness of 0.71 μm, then a linear interpolation can be used to estimate the total charge required to produce a film with 1.3 μm thickness.

Using the same charge at different current densities produced films of different thickness. 7.8 C was needed to produce a 1.3 μm film using 1 mA/cm^2, but only 6.9 C was needed to produce a film with the same thickness at 0.5 mA/cm^2 because the polymer produced at this lower current density allows more time for monomers or oligomers to rearrange during deposition to produce a more compact film with higher electrical conductivity (see Figure 2.7). A higher current density also resulted in a higher oxidation potential, which can produce shorter conjugated chains due to cross-linking. A critical value of current density for producing PTh films with high electrical conductivity has been reported [27]. At very low current density, a longer polymerization time is required to produce a specific film thickness, and in this period of time the positive effect of longer time for rearrangement competes with negative effects of side reactions that form oligomers and ultimately shorter chains. A current density of 0.5 mA/cm^2 was used to synthesize films in this study because improvements in molecular structure and electrical conductivity were produced choosing this current density over a current density of 1 mA/cm^2 as shown in Figure 2.7. The electrical conductivity increased as the total charge increased due to the longer deposition time, which incorporates more dopants in the film. The modest increase in electrical conductivity from a total charge of 6.8 C to 8 C shown in Figure 2.7a is expected because of the modest increase in total charge – larger increases in total charge shown in Figure 2.7b produced larger changes in electrical conductivity. Films synthesized using

0.5 mA/cm^2 were found to have better molecular ordering than films synthesized using 1 mA/cm^2; this is shown and discussed in Chapter 6.

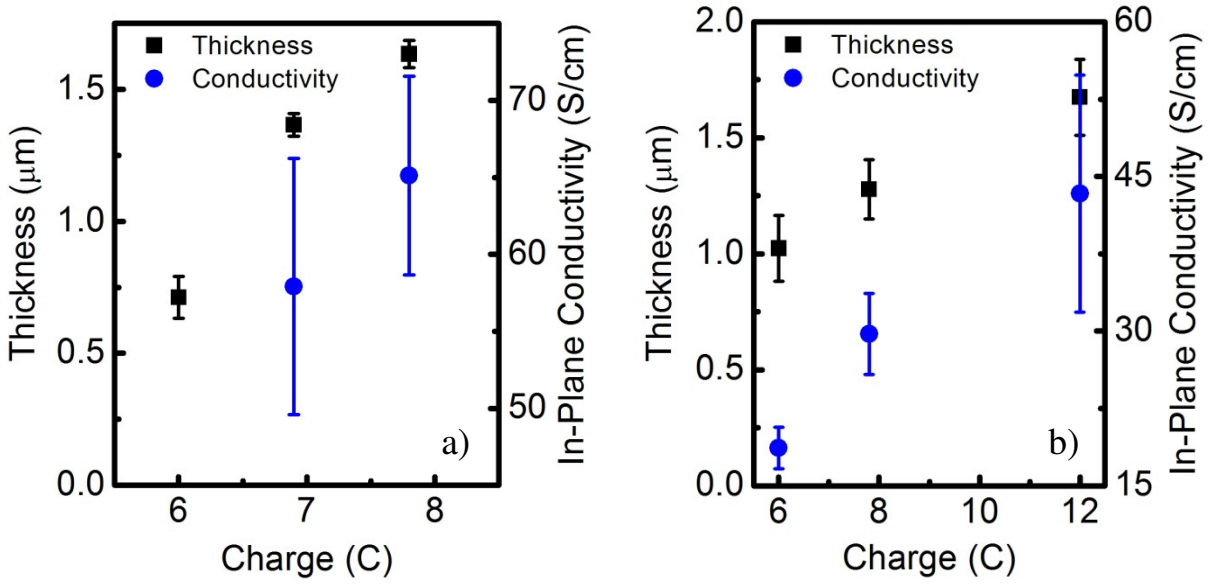

Figure 2.7: Film thickness and in-plane conductivity of PTh film synthesized with different current densities for different total charge. a) 0.5 mA/cm^2 and b) 1 mA/cm^2. Each data point is an average of two measurements on samples coming from one film.

3. POLYTHIOPHENE CHARACTERIZATION

PTh films were synthesized in 5 × 2 cm sheets and cut as shown in Figure 3.1 to enable characterization with various techniques. One square in the sample map below represents 0.25 cm^2. Note that the outer squares were unused to avoid fringe capacitance effect on film properties except for samples used in mechanical testing where the outer squares were used for gripping. Measuring electrical conductivity and mechanical properties of polymer films are simple, indirect techniques to quantify changes in structural order because both of these properties depend significantly on the packing and alignment of polymer chains. Improvement in physical properties of PTh films is expected to correlate to improvement in the molecular order of the film, which is the main objective of this study.

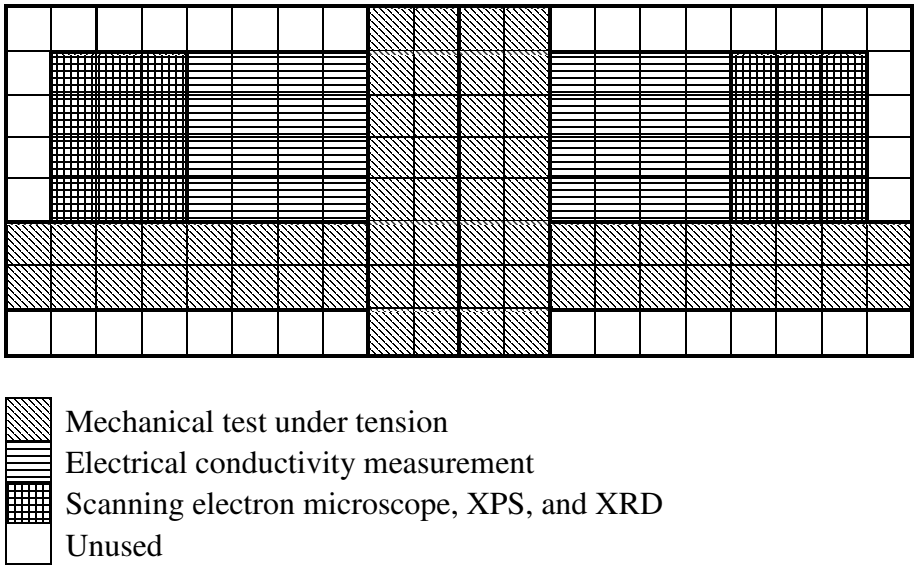

Figure 3.1: Sample map of 5 × 2 cm PTh film.

3.1 In-Plane Conductivity Measurement by Four-Probe Technique

The inline four-point probe technique is a method for measuring sheet resistivity where four-needle like electrodes in a linear array are brought in contact with the sample, and current flows to the material via the outer two electrodes while the two electrodes in the middle measure the electric potential as shown in Figure 3.2 [53]. This method of measuring resistivity does not include the contact resistance, because there is no potential drop across the voltage measurement.

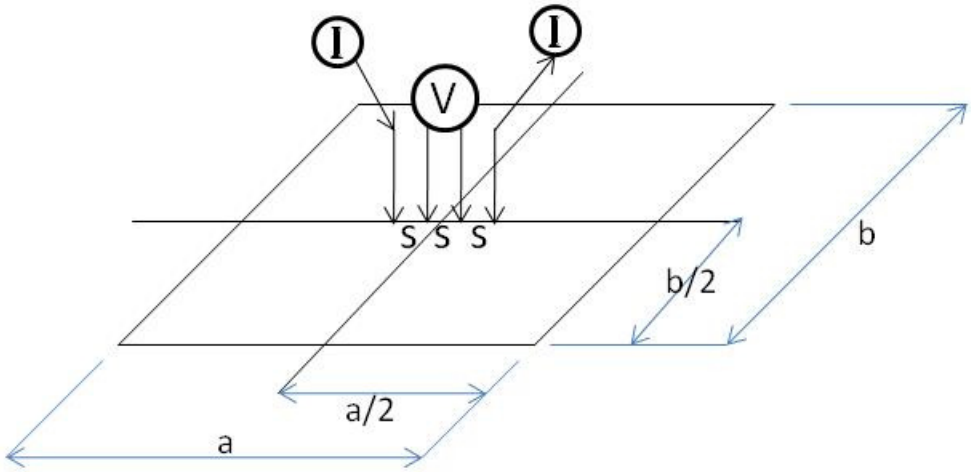

Figure 3.2: Four-probe measurement on rectangular surface.

Sheet resistivity was calculated using Eq. 3.1 where *G* is the correction factor for a thin rectangular film (1.27×10^{-5}) times the thickness of the film [53]. Three measurements, each in transversal and longitudinal directions of the film were performed on a 1×1 cm film – note that the measured conductivity values presented in this thesis are isotropic in the plane of the PTh films as confirmed by measurements in the transverse and longitudinal directions. The voltage was recorded at twenty different current values generated with 1 second delay using Keithley 2400 multimeter for each measurement. The slope of the V-I plot was used in Eq. 3.1, and then the in-plane conductivity was calculated as the inverse of resistivity as shown in Eq. 3.2

$$\varrho = G\frac{V}{I} \qquad \text{Eq. 3.1}$$

$$\sigma = \frac{1}{\varrho} \qquad \text{Eq. 3.2}$$

Electrical conductivity measurements were always performed on the surface of the films that was in contact with the electrode for consistency. However, measurement of the electrical conductivity on the surface of the films in contact with the solution side gave similar results. Figure 3.3 shows that the conductivity measured on the electrode or solution side of the same film with thickness of 1.3 µm is the same suggesting that the measured in-plane conductivities are representative of bulk film properties.

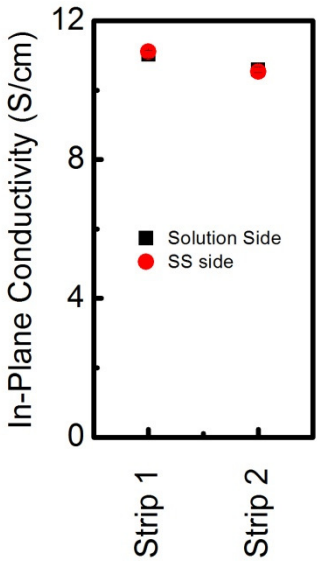

Figure 3.3: Conductivity measurement of PTh films synthesized using 50 mM thiophene in BFEE at 5 mm inter-electrode distance with 1 mA/cm^2. The film was cut into two 1 × 1 cm strips. Strip 1 was measured on the solution side first, then the SS side. Strip 2 was measured on the SS side, then the solution side.

The oxidation state of Pth is not stable in the air because of large free energy (1.19 V) associated with the two half reactions of water and PTh [54]. Therefore, the reduction reaction of an oxidized PTh film may occur very quickly. The PTh films were stored in a vacuum chamber (dry atmosphere) and always transported in a desiccator to prevent dedoping of the films via exposure to moisture in air. Electrical conductivities of PTh films were always measured the day after film deposition in approximately 8 hours to establish a consistent time frame.

As discussed in section 2.2 of Chapter 2, BFEE is a moisture sensitive solution and cannot be stored for long times. This produces PTh films with electrical conductivities that show batch-to-batch variation. Therefore, the absolute value of electrical conductivity is only compared between films synthesized with the same BFEE batch supplied from the manufacturer. Trends and percent improvements in electrical conductivity are compared when considering films made in different batches.

3.2 Mechanical Properties under Tension

A 0.5 × 2 cm strip of film was loaded under tension using TA Instrument QA 800 with a stretching rate of 2 mm/s and clamping pressure of 2 psi applied at room temperature 23 ± 1 ^{o}C. The strain-stress behavior of the films was analyzed to obtain the tensile strength, tensile modulus, and elongation at break. Tensile strength is the maximum stress the material can withstand under unaxial loading, and tensile modulus or Young's modulus is calculated using the initial linear slope of the strain-stress curve as shown in Figure 3.4. The elongation at break reported in this study assumes that the polymer deforms uniformly. When the polymer exhibits necking behavior, the change in shape factor is not incorporated, so the value may be overestimated. The measurement of strain during the necking region is challenging due to the

size of the sample, which is very small. Observations of necking behavior are reported in this work as evidence of increased chain alignment and chain length in PTh films.

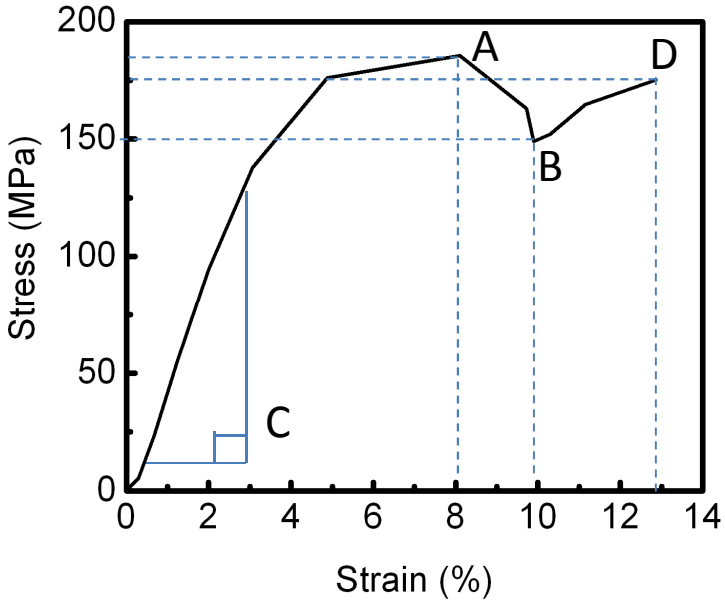

Figure 3.4: Strain-stress curve of PTh film with necking. (A) Tensile strength, (B) necking, (C) Young's or tensile modulus, and (D) fracture point.

The thickness of films was held constant because it is known that mechanical properties of electropolymerized ICP films depend on their thickness [55]. Mechanical properties can reveal useful information about the bulk properties of the polymer film; however, the relatively thin PTh films synthesized here exhibit surface roughness including small bumps that can comprise a significant fraction of the film thickness as shown in Figure 3.5, and such roughness introduces variability in the thickness measurements and thus on the determination of the mechanical properties of the films.

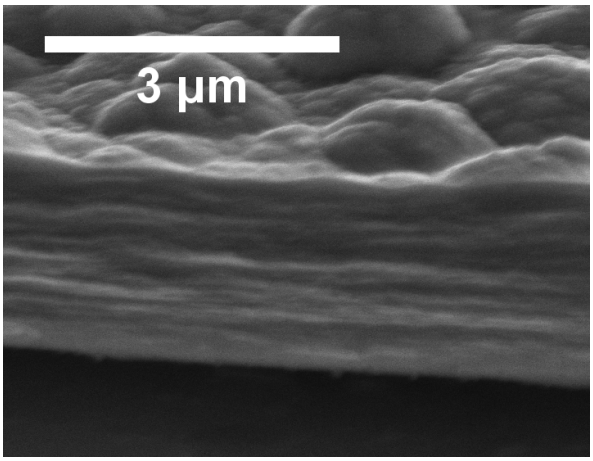

Figure 3.5: Cross section of PTh film.

3.3 Thermal, Chemical, and Structural Analysis

Thermogravimetric analysis (TGA) is often used to measure the weight change of polymer films as a function of temperature, which relates to the thermal stability of the films, and was used here for this purpose. The reader is referred to [22] or additional information on TGA and its use to characterize thermal properties of ICPs. The TA Instrument SDT Q600 was used to perform TGA from 20 ^{0}C to 600 ^{0}C with a temperature ramp rate of 10 ^{0}C/min under nitrogen flowing at 100 mL/min. The film was cut to small pieces (total sample weight = 0.5 mg) and placed in an aluminum pan covered with an aluminum lid. The aluminum pan filled with PTh pieces is placed on the sensitive balance inside a heat chamber with thermocouple. The weight of the sample is recorded as the temperature increases.

X-rays photoelectron spectroscopy (XPS) is a quantitative and qualitative technique to provide elemental composition and chemical bonding structure on the surface (5-50 nm) of a solid [56]. XPS measures the kinetic energy of photoelectrons and the number of electron that are ejected after the surface is exposed to X-rays. Because ICPs films lose electrons when bombarded with the X-ray source, a flood gun was applied for charge neutralization at the

surface of PTh films. The XPS used in this study was Thermo Fisher Scientific K Alpha. The X-rays source is a monochromatic Al K_α with spot size of 400 µm. At least 10 cycles were used to perform high resolution scan of sulfur and oxygen to verify the incorporation of anionic surfactant in PTh films.

Wide angle x-ray scattering (WAXS) in transmission mode with Rigaku Micromax 002 X-ray generator (λ = 0.15418 nm) and R-axis IV++ detector system was used to examine the structure of polymer films. WAXS is a commonly used technique for characterizing the structure of polymer films and the reader is referred to [31, 36]. for an in-depth discussion on the use of WAXS for polymer film characterization. The total exposure time was two hours for each sample. The X-ray pattern is not clear with only 30 minutes exposure time because the film was too thin. The molecular spacing, *d*, of PTh was calculated using Bragg's law as shown in Eq. 3.3, where θ is the Bragg's angle, and λ is the wavelength of the X-ray generator.

$$d = \frac{\lambda}{2 \sin(\theta)} \qquad \text{Eq. 3.3}$$

Although a small change in Bragg's angle does not indicate a change in the d-spacing from calculation due to truncation errors, Bragg's law can be used qualitatively to provide useful information; the larger the Bragg's angle, the smaller the d-spacing is.

4. EFFECT OF INTER-ELECTRODE DISTANCE

4.1 Electrochemical Characterization

The effect of the distance between the working and counter electrodes in electrochemical polymerization of thiophene on the properties of the resulting film has not been studied in detail. This parameter influences fundamental processes of the synthesis such as diffusion and transport of the monomer from the solution to the electrode surface and is important to consider for scaled up production of freestanding PTh films. Figure 4.1 shows cyclic voltammograms (CV) and chronoamperograms (CA) of 30 mM thiophene in BFEE at electrode distances of 5, 20, and 30 mm for electrodes with dimensions of 1.5 × 2 cm. The CA was performed with 1.3 V until the charge reached 1.5 C. As shown in the CV and CA plots in Figure 4.1, the current density decreased as the distance between electrodes increased because the solution resistance between the two electrodes increased. The increase in solution resistance results in a decrease in the diffusion rate of the monomer to the working electrode. Less monomer diffuses to the working electrode as the diffusion rate decreases, which results in a higher oxidation potential required to polymerize the monomer. The highest current density was produced at an electrode distance of 5 mm and the lowest current density was produced at an electrode distance of 30 mm. Shorter distances between electrodes also lead to faster nucleation stage (see inset of Figure 4.1b) and deposition time required to produce films of a fixed thickness.

4.2 In-Plane Conductivity

Figure 4.2 shows the electrical conductivity and charge efficiency of the PTh films grown at different electrode distances. In-plane conductivity decreases as the inter-electrode distance

increases. CA plot in Figure 4.1b shows that the deposition time to reach a fixed total charge is longer at a larger inter-electrode distance. Longer deposition time may produce more oligomers due to side reactions and form shorter chains [27], producing PTh films with lower electrical conductivity. Charge efficiency is the total current used to grow the PTh film relative to the total current passed in the cell, which can be calculated according to Eq. 4.1 [57] assuming the degree of polymerization is 100%,

$$\eta = [(nFW_p/M)/Q] \times 100\% \qquad \text{Eq. 4.1}$$

where η is the charge efficiency of polymerization, n is the number of electrons transferred per monomer attached to the polymer, which is estimated to be 2.17 [24], and F is the Faraday constant (96487 C mol^{-1}), Wp is the weight of the PTh film (g), M is the molar mass of the monomer (g/mol), and Q is the integrated charge passed through the cell during the film growth (1.5 C). The larger electrode distances (20 and 30 mm) with slower diffusion rates and longer deposition times have charge efficiency lower than the one calculated for 5 mm electrode distance as shown in Figure 4.2. The film growth at 5 mm electrode distance with the highest charge efficiency has the highest electrical conductivity because most of the charge in the cell was used to grow the film as opposed to oligomerization of the monomer in the solution or on the working electrode, which produced films that were thicker than films grown at 20 and 30 mm electrode distance. At 5, 20, and 30 mm distance, the film thickness was 0.93, 0.57, and 0.57 μm, respectively. Despite the fact that the thicker film had higher possibility of containing defects [55], the thickest PTh film synthesized at 5 mm distance had the highest conductivity indicating that PTh films synthesized at larger electrode distances contain more oligomers. In a different study, CA with 1.3 V for 90 min was performed and the total charge of 5 mm inter-electrode distance was 1.94 C and 20 mm and 30 mm distance were 1.58 C and 1.60 C, respectively.

Therefore, making PTh film at shorter electrode distance has higher charge efficiency, which would potentially reduce the cost of the energy input required to make the films.

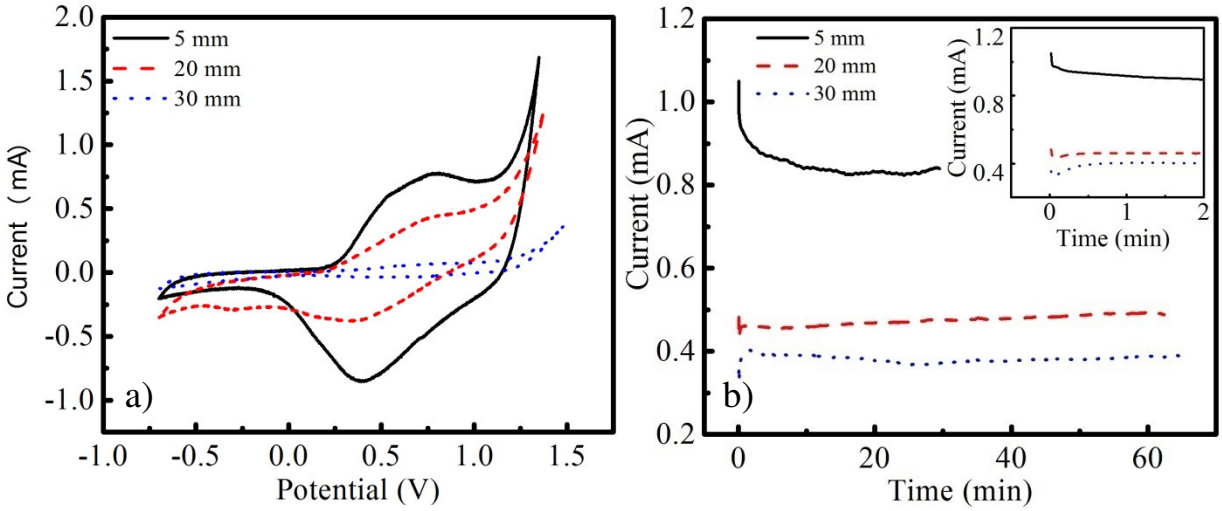

Figure 4.1: a) CV using scan speed of 200 mV/s and b) 1.3 V CA with total charge of 1.5 C using 30 mM thiophene in BFEE at different electrode distances.

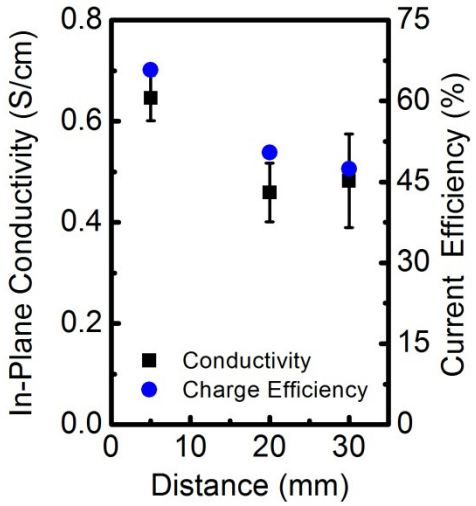

Figure 4.2: In-plane conductivity and charge efficiency of PTh films synthesized using 30 mM thiophene in BFEE at different electrode distance obtained using 1.3 V with 1.5 C total charge. Each data point is an average of four measurements on samples coming from two films.

4.3 Surface Morphology

The surface morphology of PTh films on the solution side (as opposed to the side in contact with the electrode) is influenced by the diffusion rate, which can be controlled by adjusting the electrode distance. The monomers or oligomers on the working electrode at 20 and 30 mm electrode distance are not as many as when the electrode distance is set at 5 mm because the diffusion rate at 20 and 30 mm is slower due to higher solution resistance. Because of the slower monomer diffusion rate, the solution side of the surface of PTh films synthesized at 20 and 30 mm electrode distance is smoother than the film surface synthesized at 5 mm electrode distance as shown in Figure 4.3. The slower diffusion rate can also reduce the quality of PTh films because overoxidation of the polymer can occur more rapidly than oxidation of the monomer when there is not enough monomer on the working electrode; this is a result of the PTh paradox discussed in Chapter 1.

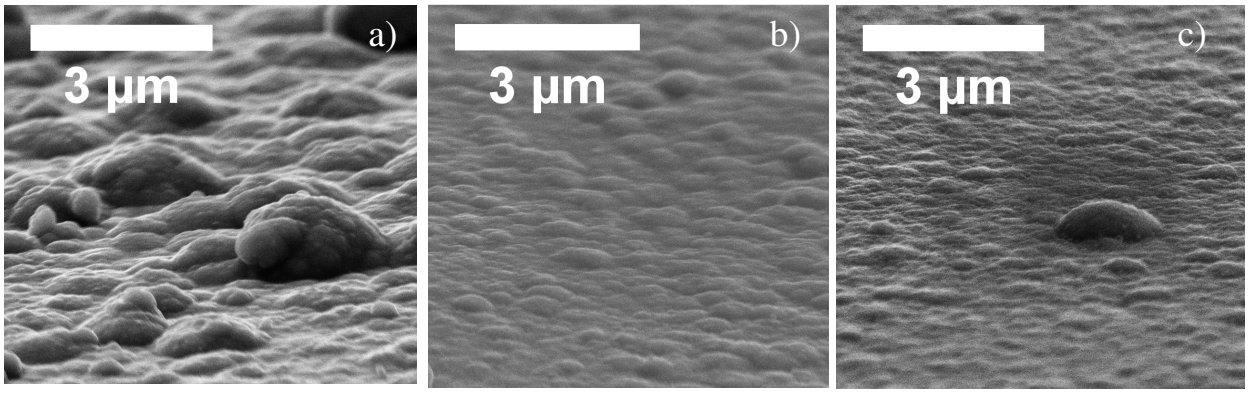

Figure 4.3: SEM images of PTh surface (solution side) electropolymerized at a) 5 mm, b) 20 mm, and c) 30 mm inter-electrode distance.

5. EFFECT OF THIOPHENE CONCENTRATION

5.1 Electrochemical Characterization

Monomer concentration has been known as one of the important parameters affecting the electrosynthesis properties and electrical conductivities of polymer films [27, 58]. The thiophene concentration affects the current density as shown in Figure 5.1a. The increased current density as thiophene concentration is increased is possibly due to the faster dimerization rate [44], which also affects the nucleation stage. The nucleation is faster with faster dimerization rate using higher thiophene concentration (see inset of Figure 5.1b). Figure 5.1b shows that the thiophene oxidation potential decreases as the thiophene concentration increases because more oligomers are available in the solution or at the working electrode surface and the oxidation potential of thiophene oligomers is lower than that of the monomer [59].

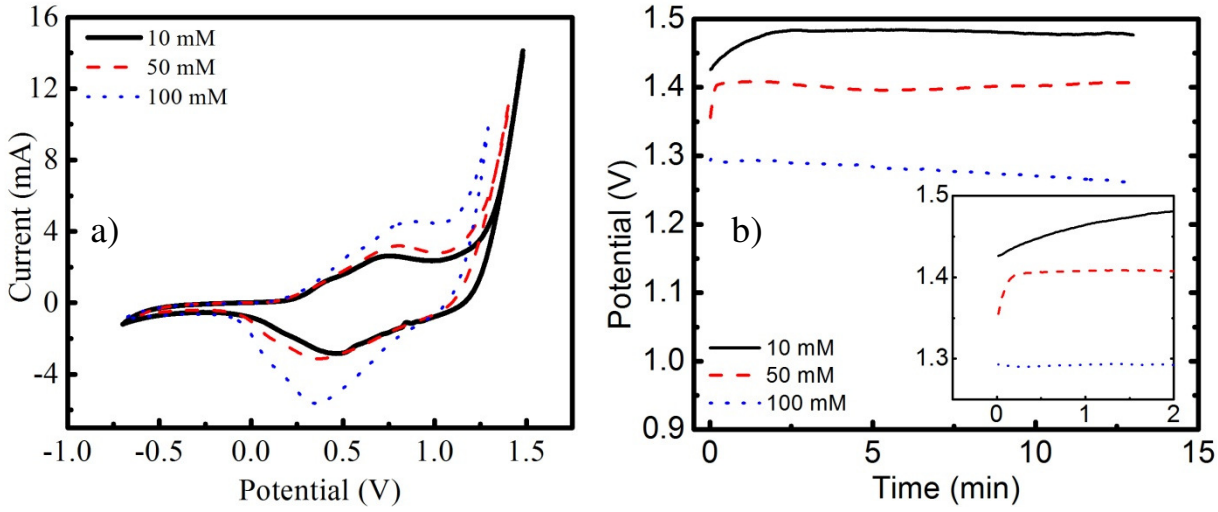

Figure 5.1: a) CV using scan speed of 200 mV/s and b) CP at 1 mA/cm^2 of different thiophene concentration in BFEE at 5 mm inter-electrode distance.

5.2 In-Plane Conductivity

There is a competition between overoxidation due to low thiopehe concentration [27] and high oligomerization from very high dimerization rate [44] to synthesize PTh film with different thiophene concentrations. Consequently, there will be a critical point of thiophene concentration for which the properties of the film are optimum. The electrical conductivity and deposition time of PTh films using different thiophene concentrations at 1.3 V and 1.5 × 2 cm electrodes is presented in Figure 5.2. The film made using 100 mM thiophene concentration has the highest electrical conductivity of 17.37 S/cm at 5 mm inter-electrode distance. The electrical conductivities of the films using 30 and 60 mM thiophene concentration is lower than films made by using 100 mM thiophene due to low thiophene concentration at the electrode surface. This reduction in electrical conductivity due to lower thiophene concentration at the electrode is also observed in the studies on the effect of inter-electrode distance presented in Chapter 4. PTh film synthesized using 150 and 200 mM of thiophene have lower conductivity than films produced using 100 mM thiophene due to oligomerization in the PTh films synthesized at 150 and 200 mM thiophene. The competition between overoxidation and high oligomerization can also be observed in the deposition time required to produce PTh films with the same thickness using different thiophene concentrations as shown in Figure 5.2. The deposition time is slower at 30 and 60 mM concentration because the dimerization rate is slower than at 100 mM concentration. However, the deposition time starts to slow down at 150 and 200 mM concentration, because the oligomers are more dominant in the PTh films growth using 150 and 200 mM concentration than the film growth using 100 mM thiophene. The oligomers produce films with lower conductivity and the diffusion of the monomer to the film is slower than the films synthesized using 100 mM thiophene. The deposition time at 150 and 200 mM thiophene is

comparable likely because 200 mM thiophene produces oligomers that reduce the diffusion rate, but it also has faster dimerization rate than 150 mM that increases the diffusion rate.

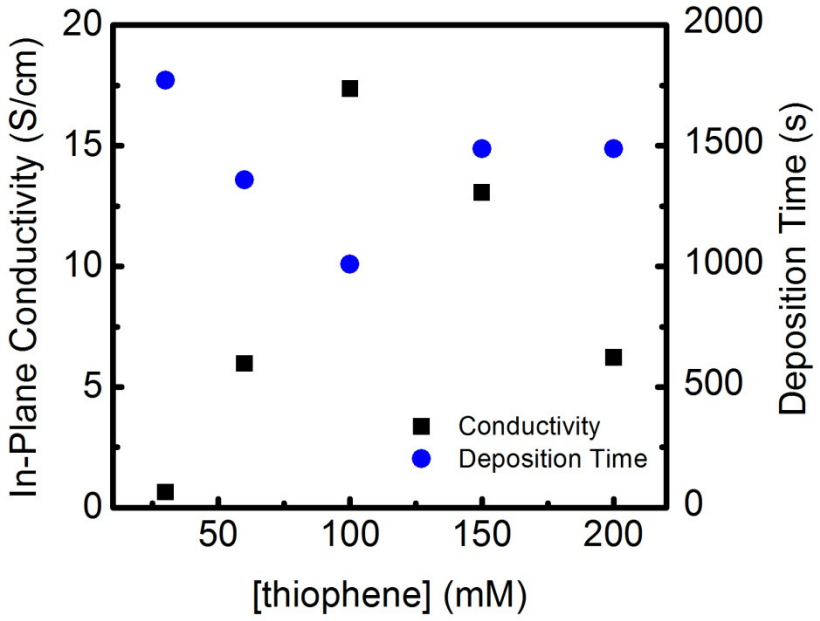

Figure 5.2: In-plane conductivity of PTh films with different thiophene concentration at 5 mm inter-electrode distance synthesized at 1.3 V with total charge of 1.5 C. The thickness of PTh films are 0.7 ± 0.1 µm.

In our system, CP produced better PTh films with higher electrical conductivity than CA as shown Figure 1.10a due to better process control using the CP method. Roncali in his review paper found that the conducting films grown using CP method are generally more homogeneous and more compact with high electrical conductivity than films made by the CA method [60]. Figure 5.3 shows the in-plane conductivity of PTh films synthesized using different thiophene concentrations with the CP method at 1 mA/cm^2. The in-plane conductivity increased with higher thiophene concentration. The low electrical conductivity of PTh films synthesized with 10 mM thiophene was likely due to the overoxidation of PTh film on electrode, which degraded the

quality of the film. The CP plot in Figure 5.1b shows that the oxidation potential is 1.48 V at a thiophene concentration of 10 mM which is larger than the potential required to overoxidize PTh (1.3 V) and leads to cross-linking, shorter chains, and low electrical conductivity. The electrical conductivity values at a thiophene concentration of 50 and 100 mM were close within the standard deviation of four measured PTh films. While the values produced at 50 and 100 mM were close, the highest conductivity of 41.17 S/cm was measured at 50 mM thiophene concentration. Thiophene concentration higher than 100 mM is needed to see a similar trend as that shown in Figure 5.2 for films synthesized with the CA method. Films produced at 50 mM thiophene concentration possess better structural order than those made at 100 mM thiophene concentration; this is discussed in the following section in detail.

Maintaining a 5 mm electrode distance will be challenging using a large electrode area in large scale process. The electrical conductivity of PTh films synthesized using 30 and 100 mM thiophene and 1.3 V at 20 mm electrode distance was measured to be 0.45 S/cm and 1.15 S/cm, respectively, which is a decrease from the measured conductivities of PTh films synthesized using the same experimental conditions at 5 mm electrode distance, 1.15 S/cm and 17 S/cm, respectively. Because the diffusion rate of the monomer can be controlled by adjusting the electrode distance and thiophene concentration, the need to use a larger inter-electrode distance can be compensated for by using larger thiophene concentrations. Further studies are required to see if this trend will exist at production scales.

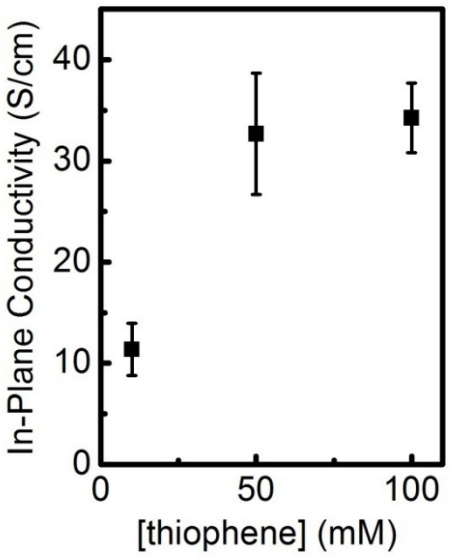

Figure 5.3: In-plane conductivity of PTh films with different thiophene concentrations at 5 mm inter-electrode distance synthesized with current density of 1 mA/cm^2 and total charge of 7.8 C. The thickness of PTh films are 1.3 ± 0.2 μm. Each data point is an average of eight measurements on samples coming from four films.

5.3 Mechanical Properties and Thermal Stability

The effect of thiophene concentration on the mechanical properties of PTh films is shown in Figure 5.4. The tensile modulus and strength of three different thiophene concentrations were comparable, yet the films synthesized using 50 and 100 mM of thiophene have larger elongation at break than the films synthesized at 10 mM of thiophene concentration. The PTh film synthesized using 50 mM of thiophene concentration has the highest tensile strength and Young's Modulus of 170 MPa and 3.5 GPa, respectively. The electrical conductivity results shown in Figure 5.3 suggest that PTh films synthesized using 50 and 100 mM of thiophene have longer conjugated chains than films synthesized using 10 mM of thiophene. The extended chain length and high entanglement of PTh films synthesized using 50 and 100 mM of thiophene are

expected to provide high strength, modulus, and elongation at break. The comparable tensile modulus and strength in the film synthesized using 10 mM of thiophene is likely the result of cross-linking. This film with the highest oxidation potential (1.48 V) is likely to have more cross-linking than films synthesized at 50 and 100 mM of thiophene [61]. Note that the standard deviation of elongation at break for the film synthesized using 10 mM of thiophene is very small, 0.33 (see Figure 5.4b). A high degree of cross-linking is known to produce brittle films [17].

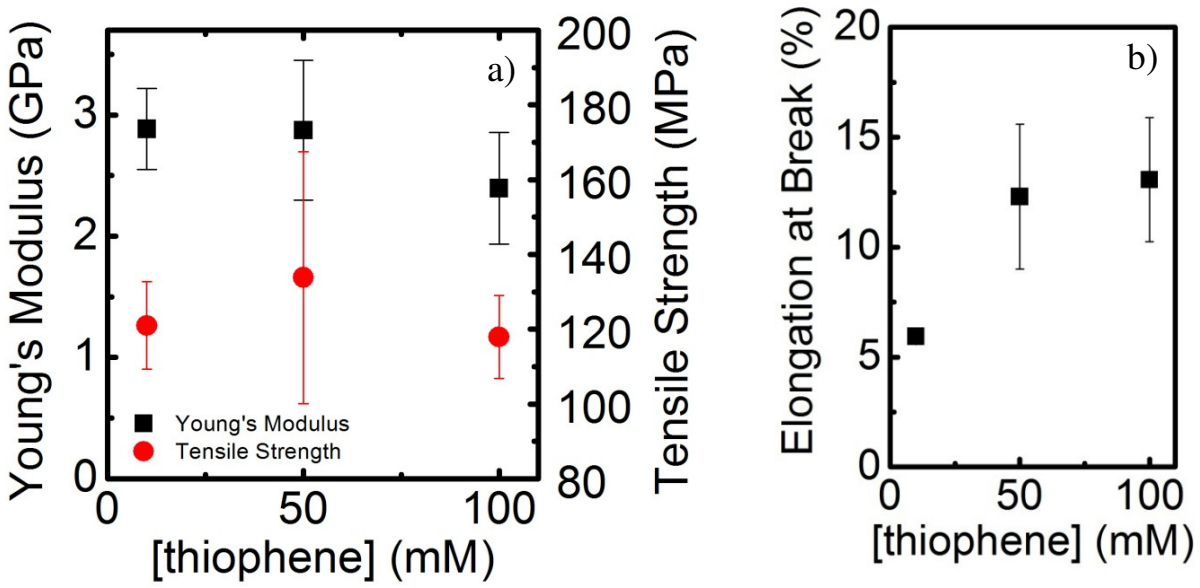

Figure 5.4: Mechanical properties of PTh films with different thiophene concentrations at 5 mm inter-electrode distance synthesized at 1 mA/cm^2 with total charge of 7.8 C in BFEE. The thickness of PTh films were 1.3 ± 0.2 µm. Each data point is an average of 16 measurements on samples coming from four films.

Figure 5.5 shows that the PTh film synthesized using 10 mM of thiophene has higher thermal stability than PTh films synthesized using 50 and 100 mM of thiophene. There are two decomposition steps [62]. The first decomposition at 190 ^{0}C represents the loss of dopant ions, which exist in larger amounts in films made at 50 and 100 mM of thiophene since films with

higher electrical conductivity have higher dopant concentration. The decomposition at 600 ^{0}C corresponds to the degradation of the PTh chain [22]. The, PTh made using 10 mM of thiophene only lost 15.6 % weight upon heating above 600 ^{0}C, while PTh films using 50 and 100 mM of thiophene lost 24.7 % and 25.5 % of the weight, respectively. The high thermal stability in cross-linking polymer network exhibited by PTh films made using 10 mM of thiophene comes from the delay of the thermal flow in the polymer.

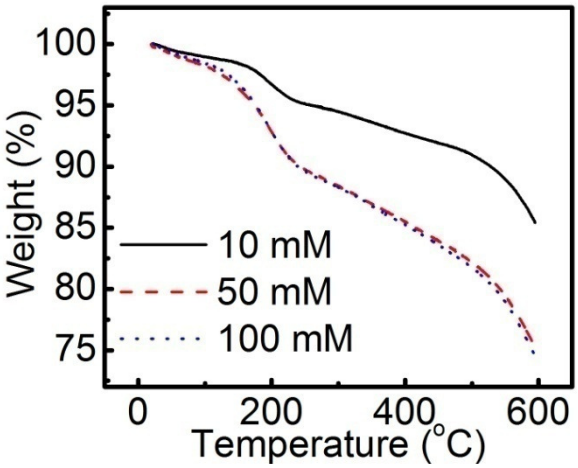

Figure 5.5: Thermogravimetric analysis (TGA) of PTh film with different thiophene concentration.

5.4 Structural Analysis

X-ray diffraction is used commonly to determine the molecular structure of PTh [31, 36]. Figure 5.6 shows three distinct peaks in the scattering pattern of PTh films synthesized at 10, 50, and 100 mM thiophene concentration. The three peaks represent inter-molecular spacing of *d*1, *d*2, and *d*3 as illustrated in Figure 5.7. The two molecular packing orientations for PTh chains shown in Figure 5.7 were proposed by Jin et. al., This packing results in highly anisotropic electrical transport in the films due to the orientation of thiophene rings on the electrode [36].

The peak observed at $2\theta = 38^{o}$ was not found in prior work. It is proposed here that the d3 distance represents the distance between two thiophene rings because the d3 peak is at the highest angles (i.e., shortest d-spacing) compared with the other two peaks. It is observed that the film made with 50 mM of thiophene exhibits the smallest d1/d3 and d2/d3 ratios indicating that the d3 peak in this film is more pronounced than the corresponding peak in the films made at 10 and 100 mM of thiophene. The result also suggests that the conjugated PTh chain is longer in the film made at 50 mM thiophene concentration. The X-ray data of line broadening at full width at half maximum intensity (FWHM) in Table 5.1 shows that PTh films made at 50 mM thiophene concentration has the narrowest d1 and d2 peaks, showing more molecular ordering compare to the PTh films made using 10 and 100 mM of thiophene. The PTh films made at 50 mM thiophene concentration also has good molecular packing as indicated by the low d1/d2 ratio. PTh films with larger cross-plane than in-plane spacing are expected to be more dense. The atomic-spacing calculated by Eq. 3.3 shows that the distance between crystallite will be shorter at larger Bragg's angles (2θ). The inter-atomic distance observed in Table 5.1 for the 50 mM film is the highest compare to that of films made with 10 and 100 mM of thiophene. The high elongation at break of PTh films made with 50 mM and 100 mM of thiophene can be explained according to the X-ray pattern, because a high elongation at break is consistent with the longer chain length of PTh films synthesized using 50 and 100 mM thiophene concentration than PTh film synthesized at 10 mM of thiophene as discussed above.

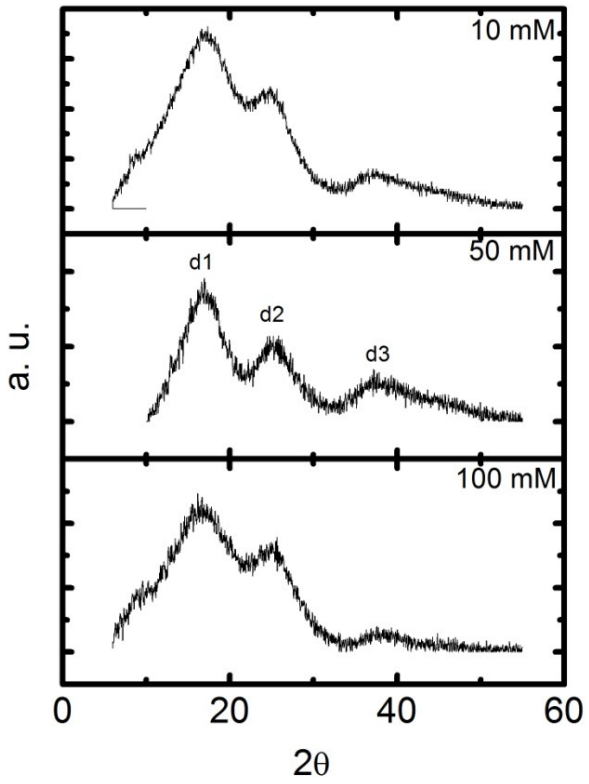

Figure 5.6: Wide angle X-ray scattering (WAXS) pattern in transmission mode of PTh films electrochemically synthesized at 1 mA/cm^2 with thiophene concentrations of 10, 50, and 100 mM.

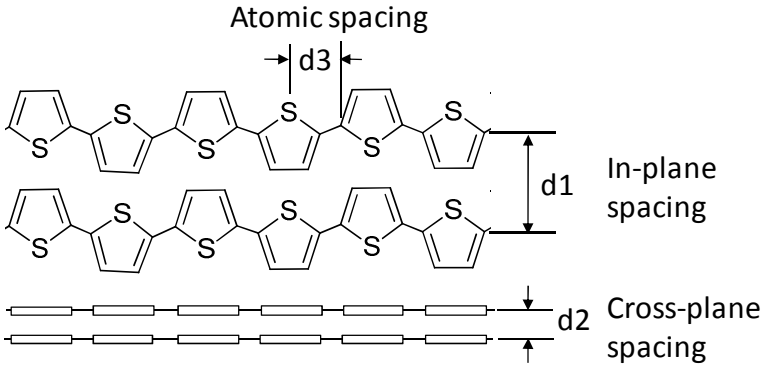

Figure 5.7: Illustration of three types molecular packing and inter-atomic spacing in PTh film.

Table 5.1: X-ray diffraction data of PTh films with different thiophene concentrations.

		2θ			FWHM			Peak intensity ratio		
	σ (S/cm)	d1	d2	d3	d1	d2	d3	d1/d2	d1/d3	d2/d3
10 mM	8.79 - 13.95	16.6	25.2	38.0	11.5	13.5	6.0	1.9	14.0	7.6
50 mM	26.69 - 38.69	16.8	25.5	38.1	6.6	7.4	8.8	1.9	3.7	1.9
100 mM	31.23 - 37.29	16.9	25.1	37.7	10.8	12.8	8.4	2.1	7.3	3.5

5.5 Surface Morphology

Images of the surfaces of the PTh films synthesized using different thiophene concentrations are presented in Figure 5.8. It was discussed in the section on the effect of electrode distance on film properties that the amount of thiophene on the surface of the working electrode affects the surface roughness of the film. This result is consistent with the trend observed when the inter-electrode distance is fixed and the concentration of thiophene is varied. Lower thiophene concentrations produced smoother films that were shinny metallic black.

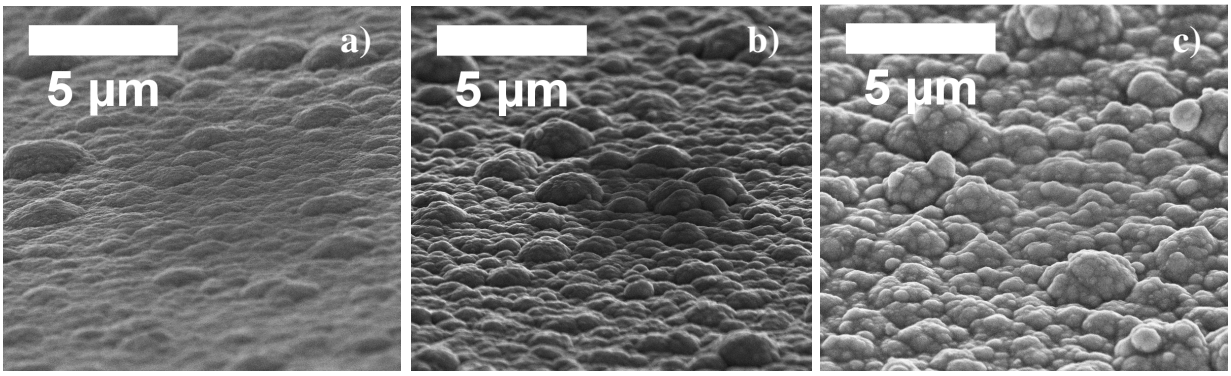

Figure 5.8: SEM images of PTh surface on solution side electropolymerized at 5 mm with a) 10 mM, b) 50 mM, and c) 100 mM thiophene in BFEE.

6. EFFECTS OF ANIONIC SURFACTANTS AND PROTON SCAVENGER

PTh is generally synthesized by electrochemical oxidation of thiophene or its oligomers in organic media such as acetonitrile [6, 27, 31] or BFEE due to its insolubility in aqueous solution and higher oxidation potential than that of water [63]. Several studies have been done to address this problem by using anionic surfactant solution that has the ability to increase the solubility of thiophene in water, providing an electrocatalytic effect during polymerization [37, 63-65] and modifying the characteristic of the metal/electrolyte interface [66]. Electrochemical synthesis of PTh in aqueous micellar medium using sodium dodecyl sulfonate (SDS) or sodium dodecylbenzene sulofante (SDBS) has been demonstrated to improve the electrochemical properties by reducing the oxidation potential of thiophene via the catalytic effect of the anionic surfactant (*29*). The radical cation of thiophene interacts with the anion of the surfactants (DS^- or DBS^-) and diffuses to the electrode electrostatically on the anodic polymerization route. A study has also demonstrated an improvement in polymer order using SDS in the electropolymerization of poly(3-alkylpyrrole)s in aqueous medium [67].

Although several studies of electrochemical polymerization have been done in aqueous solution with anionic surfactants, no studies were found on the effects of surfactant in organic solution and BFEE on the synthesis and properties of PTh films. PTh films produced in BFEE solution show great improvement in their electrical and mechanical properties because this Lewis acid reduces the oxidation potential of thiophene compared to deposition in a strong acidic or other non-aqueous solution, i.e. acetonitrile. The goal of using BFEE and anionic surfactants (SDS and SDBS) in this study is to understand the process of electrochemical polymerization of

PTh in surfactant/non-aqueous solution at different surfactant concentrations, and further improve the physical properties of PTh films while understanding the connection between improved structural order in the film and increased electrical conductivity and mechanical properties.

2,6-di-tert-butylypyridine (DTBP), a proton scavenger, was used by Jin et al., to eletropolymerize thiophene in BFEE producing films with conductivities as high as 1300 S/cm [36]. DTBP with its specificity toward protons from water removes defects in the thiophene ring during anodic polymerization. Using anionic surfactants and DTBP in BFEE as electrolyte is expected to increase the conductivity of the resulting film due to synergistic effects, i.e., the combination of the positive characteristics of both additives.

Based on optimal conditions revealed in the studies presented in previous chapters, PTh films were deposited at 0.5 mA/cm^2 for 90 min at 5 mm inter-electrode distance using 50 mM thiophene and film thickness of 4.1 ± 0.3 µm. Technical grade SDBS and SDS purchased from Sigma Aldrich were used.

6.1 Preparation of Anionic Surfactant/BFEE Electrolyte

The Bjerrum length is the charge separation between ions where the Coulombic interaction is comparable to the thermal energy $k_B T$, where k_B is the Boltzmann constant and T is absolute temperature in Kelvin. In water, ionic bonding is weak due to the short Bjerrum length of water, 0.7 nm [68]. Water has a dielectric constant, ε, of 80 which makes the ion-solvation highly probable. The ε of BFEE is 2.833 [69] and its Bjerrum length is 21.92 nm calculated by Eq. 6.1, where ion-solvation is not likely to occur [70].

$$\lambda_B = \frac{e^2}{4\pi\varepsilon_0\varepsilon_\tau k_B T} \qquad \text{Eq. 6.1}$$

where e is the elementary charge of an electron 1.60×10^{-19} C, ε_0 is the vacuum permittivity 8.85 $\times 10^{-12}$ F/m, and ε_τ is the dielectric constant of BFEE. The lengths of SDS and SDBS are 1.46 nm and 2.26 nm, respectively, calculated using a semi-empirical molecular program [71]. Consequently, anionic surfactants (SDS and SDBS) require external energy (e.g., sound, thermal, or light energy) to be solvated in BFEE. Table 6.1 and Eq. 6.2, where r is the radius of an ion, show that the Coulombic energy of SDS and SDBS in BFEE is approximately 10-fold larger than the thermal energy. Therefore, SDS and SDBS were sonicated for 30 min in BFEE to overcome this energy barrier and break the ionic bond. The solvation of SDBS and SDS is shown in Figure 6.1.

$$E_{Coulombic} = \frac{\lambda_B}{2r} k_B T \qquad \text{Eq. 6.2}$$

Table 6.1: Coulombic energy of SDBS and SDS in BFEE

	2r (nm)		$\lambda_B/2r$	
Bjerrum Length of BFEE (nm)	SDBS	SDS	SDBS	SDS
21.92	2.26	1.46	9.70	15.01

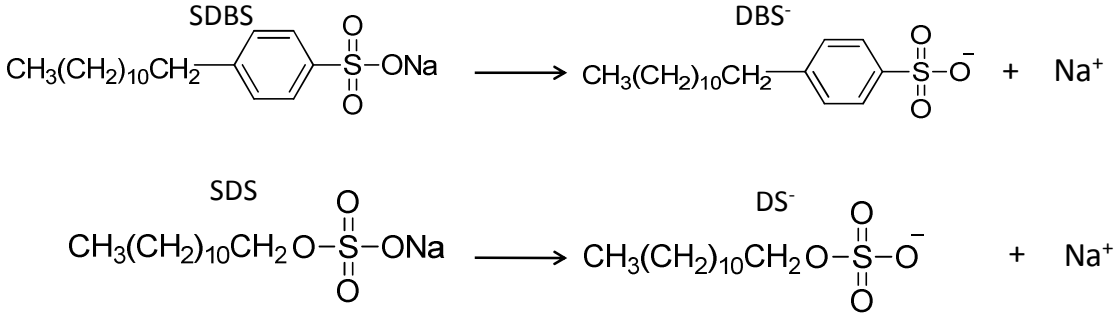

Figure 6.1: Solvation of SDBS and SDS

6.2 Electrochemical Behavior of Thiophene in Anionic Surfactant/BFEE Electrolyte

Figure 6.2 and Figure 6.3 show the CV of 50 mM thiophene in anionic surfactant/BFEE solution (SDBS and SDS respectively) with 5 mm inter-electrode distance for five consecutive cycles with 2 seconds delay between each cycle. The current density during the deposition of PTh without anionic surfactants is higher on the first two cycles because the diffusion of thiophene to the electrode surface is much faster than the diffusion of surfactant. The slower diffusion is the result of anionic surfactants being more than three times heavier than thiophene. Molecular weights of thiophene, SDBS, and SDS are 84.14 g/mol, 348.48 g/mol, and 288.38 g/mol, respectively. Consequently, DS^- and DBS^- molecules will need more time to diffuse into the polymer network. This conclusion is supported by the clear transition from lower to higher current over the five cycles when SDBS and SDS are included in electrolyte as shown in Figure 6.2 and Figure 6.3. A deposition rate of 0.5 mA/cm^2 and a longer film deposition time of 90 min were used to synthesize PTh films. The in-plane conductivities of the films grown with and without the presence of the surfactants were comparable when the deposition time was set to 13 min because sufficient time was not given for surfactant to diffuse into the film. The fact that the use of surfactants only affects the film conductivity after some critical deposition time supports the hypothesis that the solid-state polymerization process occurs until the polymerization is terminated, which means that “late-arriving” surfactant molecules can influence polymer order at the electrode-film interface.

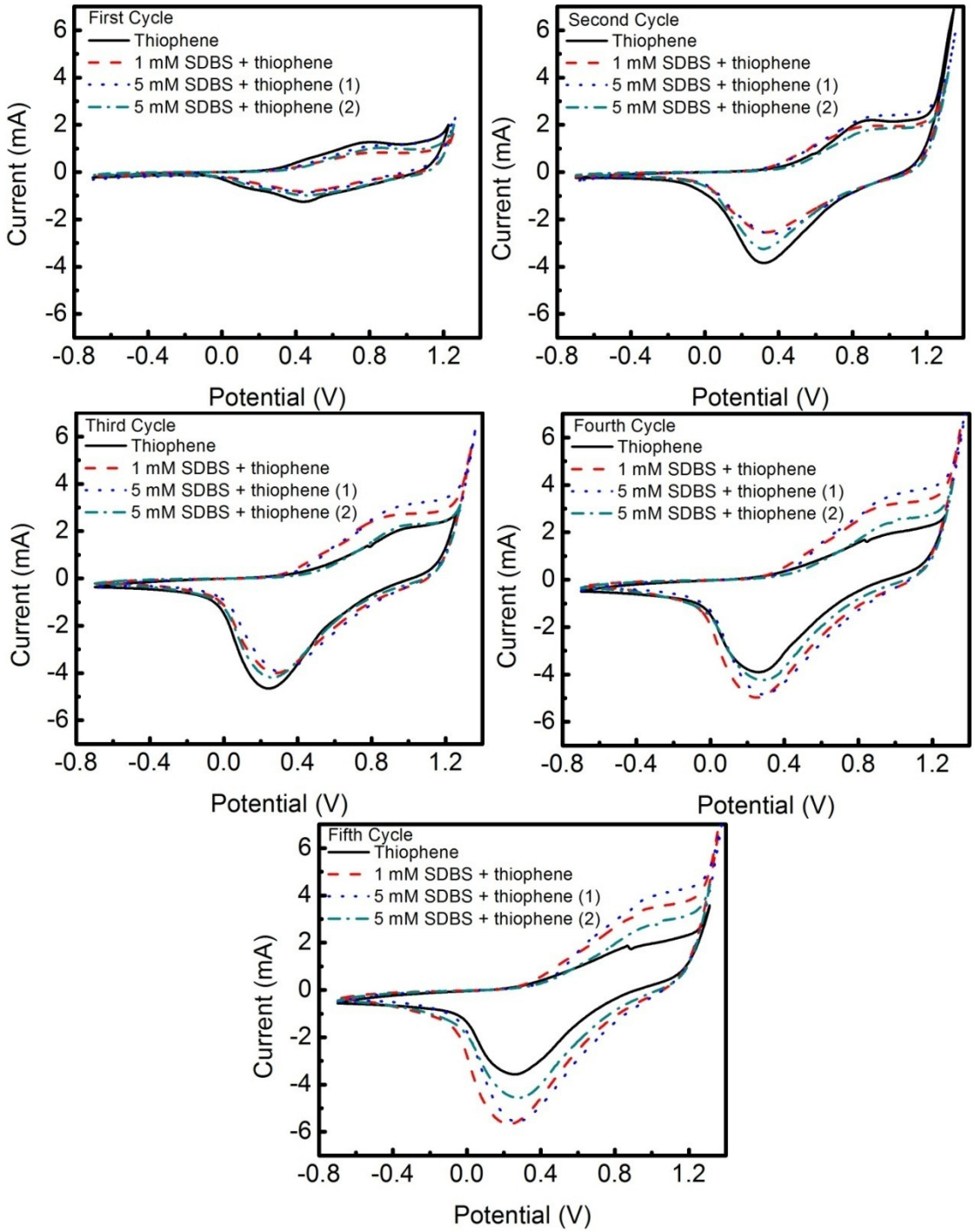

Figure 6.2: Five consecutive CV scans of 50 mM thiophene in SDBS/BFEE with scan speed of 20 mV/s.

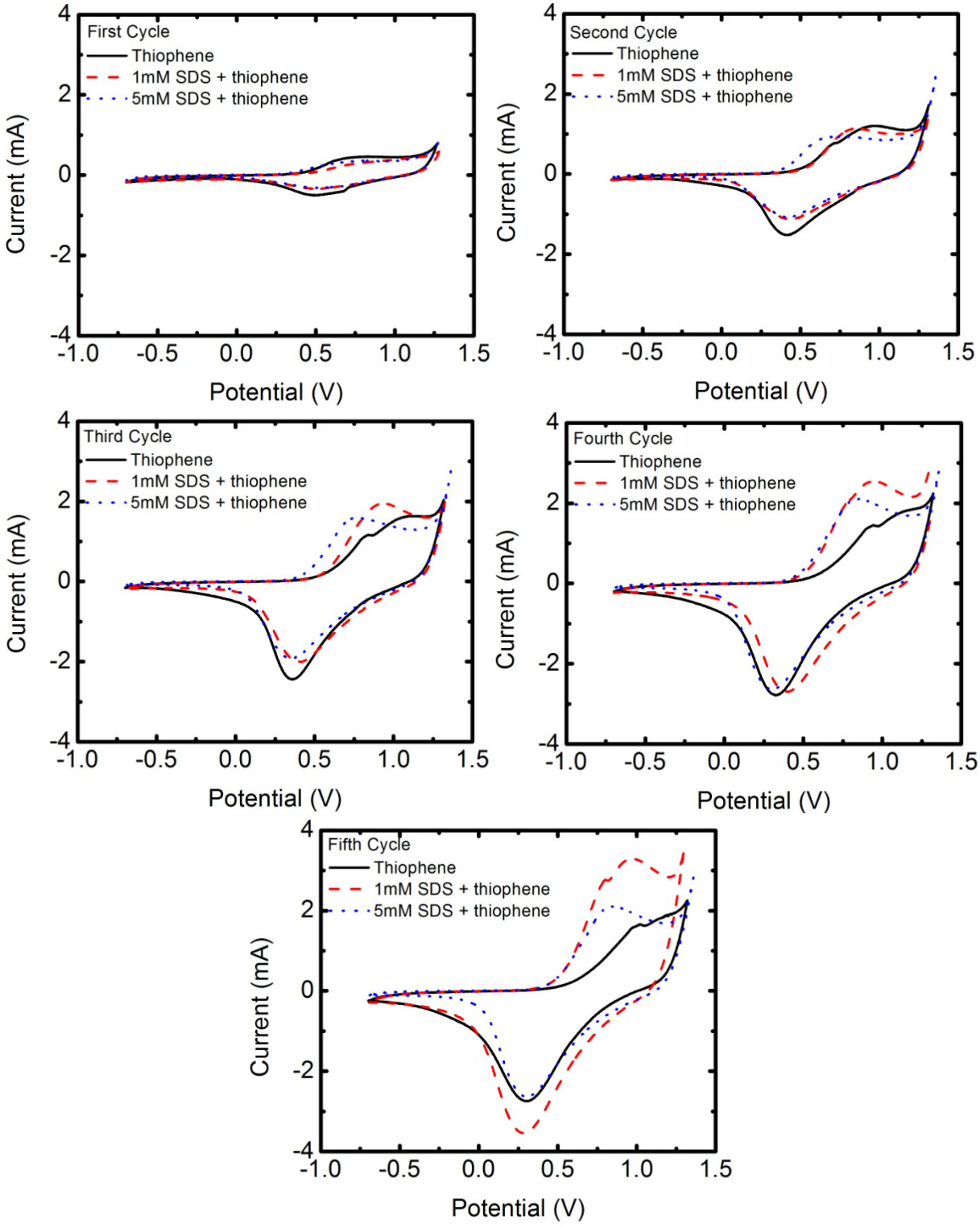

Figure 6.3: Five consecutive CV scans of 50 mM thiophene in SDS/BFEE with scan speed of 20 mV/s.

Changing the concentration of SDBS does not show a clear trend in the CV plots (see in particular the fifth CV cycle in Figure 6.2). The current density is expected to increase with increased concentration of SDBS due to additional charge provided by SDBS. However, the current density is expected to decrease when the SDBS concentration reaches the critical micelles concentration (CMC) because steric effects of the micelles in the solution will limit diffusion of SDBS to the electrode. The 5th CV cycle in Figure 6.3 supports the explanation given for the expected behavior in the CV plots using SDBS or surfactants in general. This cycle show clearly that the presence of SDS increases the current density, yet the concentration of 5 mM SDS has lower current density than 1 mM SDS suggesting the presence of micelles in BFEE.

Figure 6.4 shows the CP plots of 50 mM thiophene in SDS/BFEE and SDBS/BFEE at different concentrations of each surfactant. For both surfactants, the oxidation potential decreased as the concentration of the surfactant increased until a critical concentration was reached – likely CMC – and the oxidation potential begin to increase. The presence of surfactant in the solution increased the conductivity of the solution by providing additional charge, and this decrease in solution resistance under constant current deposition lowers the oxidation potential as shown in Figure 6.4. A decrease in thiophene oxidation potential in anionic surfactant medium can also be attributed to stabilization of the thiophene radical cation in the solvent due to the strong interaction of the thiophene radical cation with the anionic chain of the surfactants (DS^- and DBS^-) [72]. Once CMC is reached, the presence of micelles in the solution hinders monomer or oligomer diffusion into working electrode which increases the effective solution resistance and the oxidation potential. Fall et al. found the same trend in aqueous solution that increasing the concentration of anionic surfactant above CMC in anodic polymerization increased the

monomer oxidation potential [64]. The difference in oxidation potential magnitude between SDS and SDBS is attributed to the large batch-to-batch variability of the water content in BFEE received from Alfa Aesar.

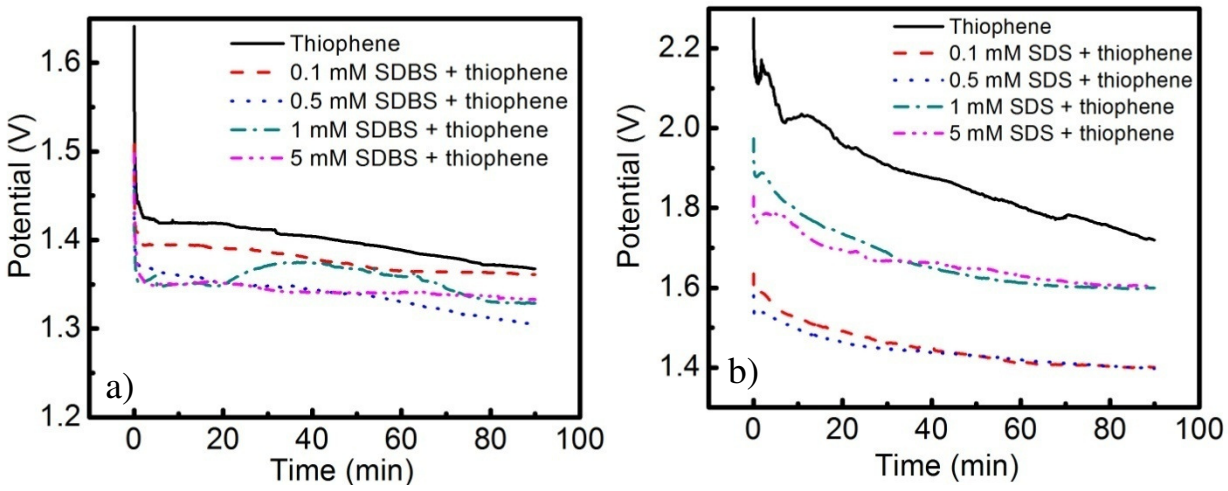

Figure 6.4: CP plot of 50 mM thiophene in BFEE at different concentration of a) SDBS and b) SDS.

Figure 6.5 shows the CV of 50 mM thiophene in SDBS/distilled BFEE and SDS/distilled BFEE with 5 mm inter-electrode distance. The most distinguishable feature in the CV scan is that the oxidation current density of the solution with surfactant is lower than it is without surfactant in the first cycle. This result is identical with the result for the first cycle in undistilled BFEE (see Figure 6.2 and 6.3), which was attributed to the slower diffusion of surfactant to the electrode compared to thiophene. The solutions with 0.5 mM SDS and 0.5 mM SDBS have comparable oxidation current density, which suggests that SDS and SDBS provide similar increase in solution conductivity. The current densities for solutions with 5 and 30 mM SDS are lower than that of the 0.5 mM SDS solution probably due to formation of micelles during

polymerization. The reduction current densities of 0.5 mM SDS and SDBS solutions at negative potential are higher than that of the thiophene solution. This can be attributed to reduction reactions occurring on PTh deposited during the first sweep at positive potentials or reduction of the positive charge from the surfactants on the working electrode. The oxidation current density of 50 mM thiophene solution under the same deposition condition in distilled BFEE is lower than it is in the undistilled BFEE (see Figure 5.1 and Figure 6.5). The presence of water in undistilled BFEE (< 0.1%) increases its conductivity leading to larger currents during deposition. Although the electrochemical characteristics of distilled BFEE are not as favorable as the characteristics of undistilled BFEE, the distilliation process offers more control in the PTh synthesis leading to reproducible results.

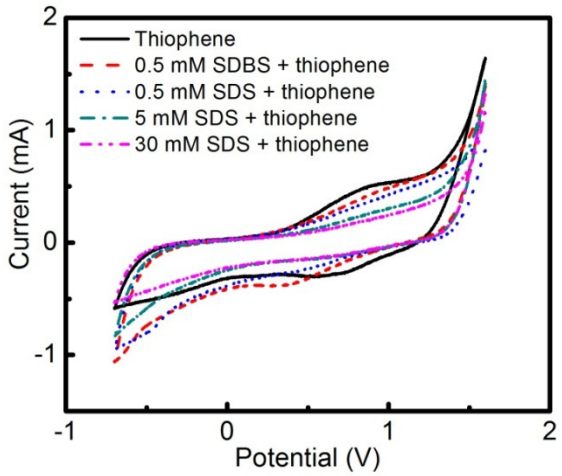

Figure 6.5: First cycle of CV of 50 mM thiophene in freshly anionic surfactant/distilled BFEE electrolyte at 5 mm inter-electrode distance with 20 mV/s scan rate.

The oxidation potential of 50 mM thiophene in anionic surfactant/distilled BFEE electrolyte in Figure 6.6 shows that the presence of surfactant in the solution helps the polymerization by reducing the oxidation potential. The oxidation potential of 0.5 mM SDS/distilled BFEE solution is lower than oxidation potential of 0.5 mM SDBS/distilled BFEE

solution. DS^- possibly provides more charge into BFEE and has stronger interaction with the thiophene radical cation than DBS^- does. In both distilled and undistilled BFEE, anionic surfactants reduce the oxidation potential, and the oxidation potential increases with surfactant concentration, yet is still lower than that of the solution without anionic surfactants.

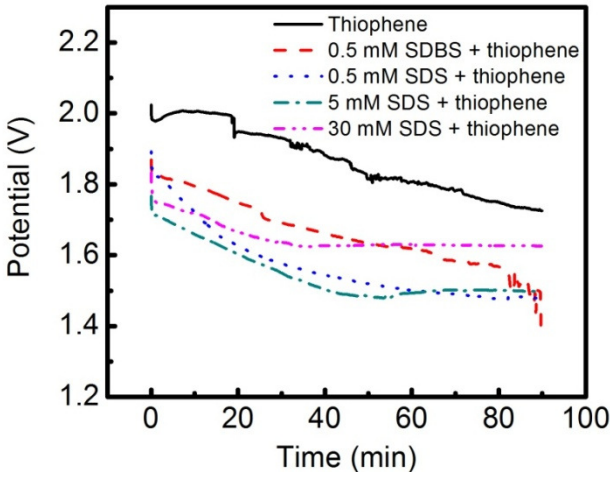

Figure 6.6: CP plot of 50 mM thiophene in anionic surfactant/distilled BFEE.

BFEE is a solvated Lewis acid which has a strong interaction with the radical cation of thiophene [26]. The low oxidation potential of thiophene in BFEE is due to the presence of counter ions from BFEE (i.e., $[(C_2H_5)_3O^+]BF_4^-$ [47] or $H^+BF_3OH^-$) that stabilize the radical thiophene cation and decrease the aromaticity of the thiophene ring. The presence of DBS^- and DS^- from the SDBS and SDS anionic surfactants can also stabilize the radical cation of thiophene in BFEE because of the steric interaction between thiophene and the dodecyl chain of anionic surfactants. Additionally, the conductivity of the BFEE solution is increased by the addition of DBS^- or DS^-, which reduces the oxidation potential of thiophene in BFEE. The molecular weight of the dopants $[(C_2H_5)_3O^+]BF_4^-$ [47] or $H^+BF_3OH^-$ that exist in BFEE solutions are 189.95 g/mol

and 85.79 g/mol, respectively, which makes them much lighter than DBS^- and DS^-. These dopants also exist in much higher concentrations than DBS^- and DS^- so they are expected to play a larger role in determining electron density derived from doping in the PTh films.

A mechanism for the diffusion of anionic surfactant into the working electrode is proposed in Scheme 6.1a. The diffusion of the thiophene to the electrode is faster than the diffusion of the surfactant anion. The surfactant is "late-arriving" due to its larger weight compare to thiophene monomer. Hydrophobic interactions between the dodecyl chain of the surfactant (DS^- and DBS^-) and the thiophene monomers may add more weight. These interactions lead to chain alignment in the polymer network because the dodecyl chain acts as a template for polymerization. Scheme 6.1b shows PTh electropolymerization on the working electrode in the presence of anionic surfactant indicating surfactant-mediated molecular ordering that will be explained further later in this chapter.

The lower oxidation potential of surfactant/BFEE electrolyte results from the additional charge and the radical cation stability in the solution. The oxidation potential increases due to the presence of micelles in the solution. The hydrophobic chain inside the micelle may trap some thiophenes reducing the thiophene presence in the solution and on the working electrode as shown in Scheme 6.2, resulting in microemulsion polymerization [73] and likely shorter conjugated polymer chains. PTh films are deposited layer-by-layer, so if there is any contamination on film (i.e. surfactant micelles), the PTh layer wraps around the object as shown in Figure 6.7. The presence of micelles in the PTh film network can degrade the quality of the film because the thiophene may polymerize around the perimeter of the micelles, reducing the compactness of the film.

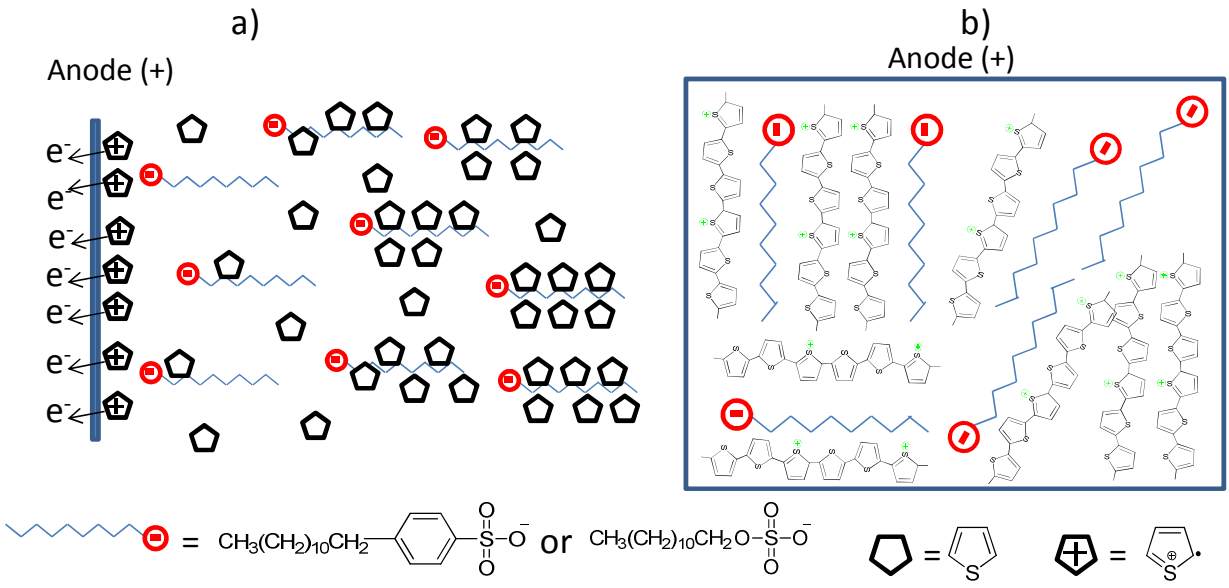

Scheme 6.1: a) Diffusion illustration in anionic surfactant/BFEE electrolyte and b) molecular ordering in PTh film using anionic surfactant/BFEE electrolyte.

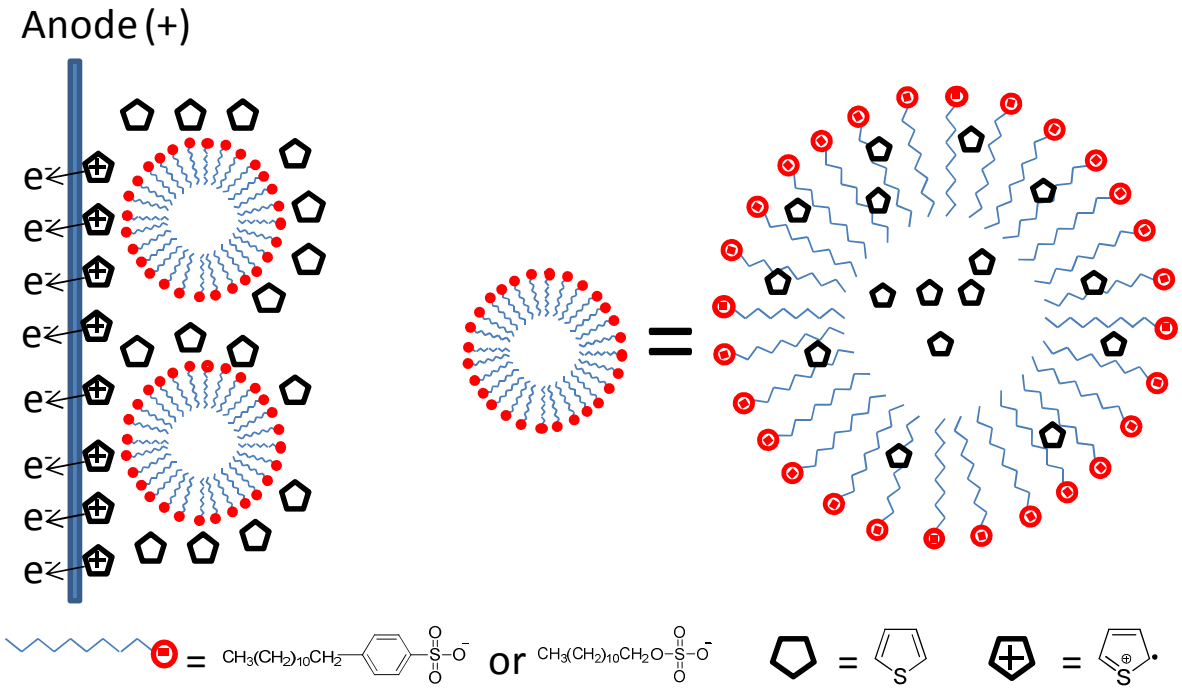

Scheme 6.2: Presence of micelles in electropolymerization of thiophene in anionic surfactant/BFEE electrolyte. PTh is shown to polymerize around the micelles on the surface.

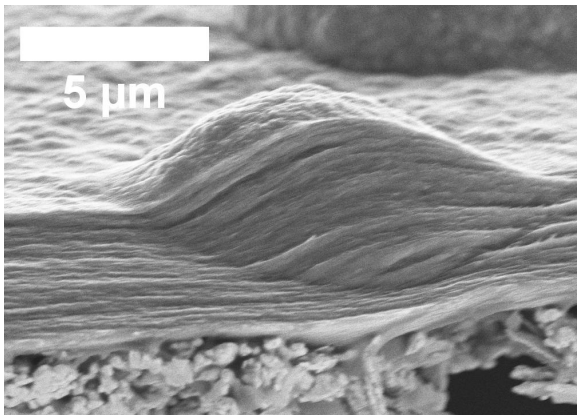

Figure 6.7: SEM image of PTh growing around an object (e.g., micelle) in the film.

6.3 Role of DTBP in Anodic Polymerization of Thiophene in Distilled BFEE

The dimerization of PTh shown in the Figure 1.6 with its 2,2-bithiophene coupling as proposed by Diaz is the desired route to have a long and linear conjugated length. However, bithiophene has three resonances as shown in Figure 6.8. With 3,3` and 2,3`-bithiophene, the conjugated chain will be non-linear and short -bb. The occurrence of 3,3` and 2,3`-bithiophene is more probable if protons at the 3-position of the radical cation are more acidic than at the 2-position [74]. 2,6-di-tert-butylpyridine (DTBP) purchased from Sigma Aldrich (≥ 97%), which has a very high specificity toward protons during cationic polymerization as shown in Figure 6.9, can play an important role as a proton scavenger because it prevents deprotonation of 3'-cationic radical by taking the H^+, which reduces the acidity of the solution. The probability of having 2,2-bithiophene in the polymer structure increases when DTBP is used. Recent work has shown that inclusion of DTBP during the polymerization of PTh in BFEE produces film with electrical conductivities as high as 1300 S/cm [36]. Here, DTBP will be used with surfactant additives as a potential method to improve the electrical and mechanical properties of PTh films.

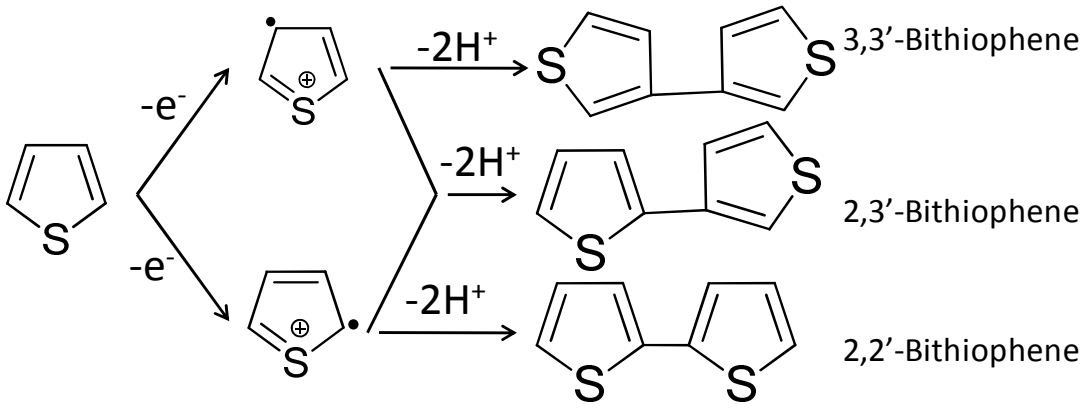

Figure 6.8: Resonance of bithiophene.

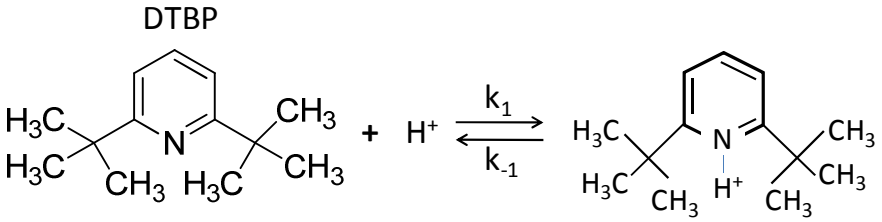

Figure 6.9: DTBP protonation.

DTBP forms a stable cation after reacting with a proton, and such formation of a stable cation increases the conductivity of distilled BFEE electrolyte as indicated by the increase in current compare to BFEE without DTBP shown in the CV plot of Figure 6.10a. As expected the current density increased as the concentration of DTBP increased. The CV observations are confirmed by the reduction in oxidation potential with increasing DTBP concentration at 5 mm inter-electrode distance shown in Figure 6.10b. The oxidation potential was the same for 25 mM and 50 mM DTBP after approximately 20 min of film growth because the proton supply in the solution was exhausted at this time and in this concentration range. DTBP may also assist the deprotonation process for thiophene (i.e., the last step in dimerization), which would reduce the oxidation potential during anodic polymerization of PTh.

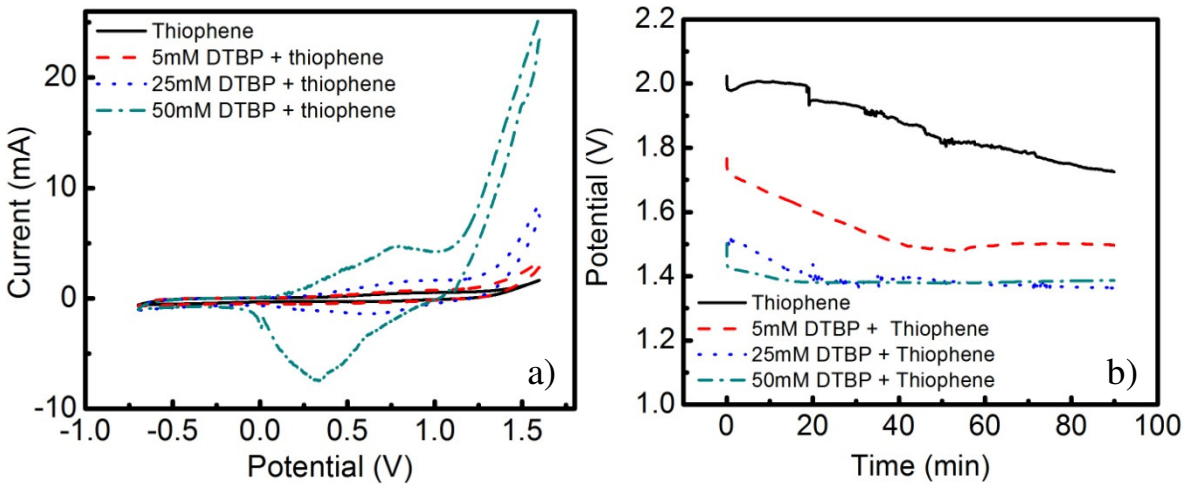

Figure 6.10: a) CV using 200 mV/s and b) CP using 0.5 mA/cm^2 of 50 mM thiophene with different DTBP concentration in distilled BFEE.

There is a maximum concentration of DTBP that can be used during polymerization of thiophene, because excess DTBP reduces the rate of polymerization via the deprotonation reaction with intermediate cation radicals. Previous work has shown that no polymer film is produced at very large concentrations of DTBP [49]. Figure 6.11 shows that the maximum electrical conductivity of a PTh film synthesized in distilled BFEE was produced with a DTBP concentration of 25 mM. This concentration of DTBP is therefore taken as the maximum concentration for improving the electrochemical properties of the electrolyte.

The mechanical properties of PTh films synthesized in distilled BFEE using various DTBP concentrations are shown in Figure 6.12. The effect of the DTBP concentrations on the mechanical properties of the PTh films is not clear due to overlapping of the error bars. However, slightly higher average values of mechanical properties were achieved for films synthesized at 25 mM DTBP.

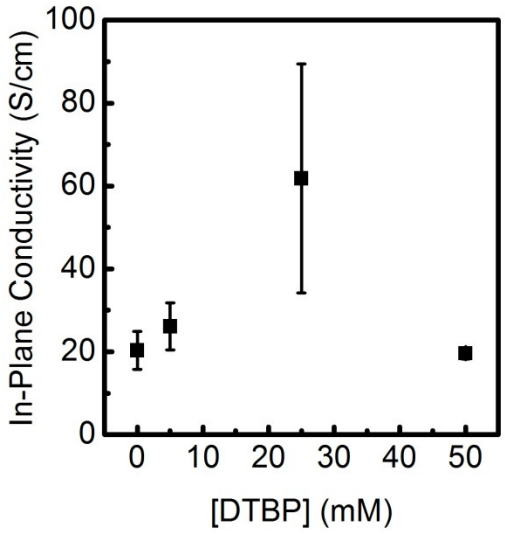

Figure 6.11: In-plane conductivity of PTh films synthesized in distilled BFEE using 0.5 mA/cm^2 for 90 min at 5 mm inter-electrode distance with different DTBP concentration. Each data point is an average of four measurements on samples coming from two films. The films thickness is 3.8 ± 0.5 µm.

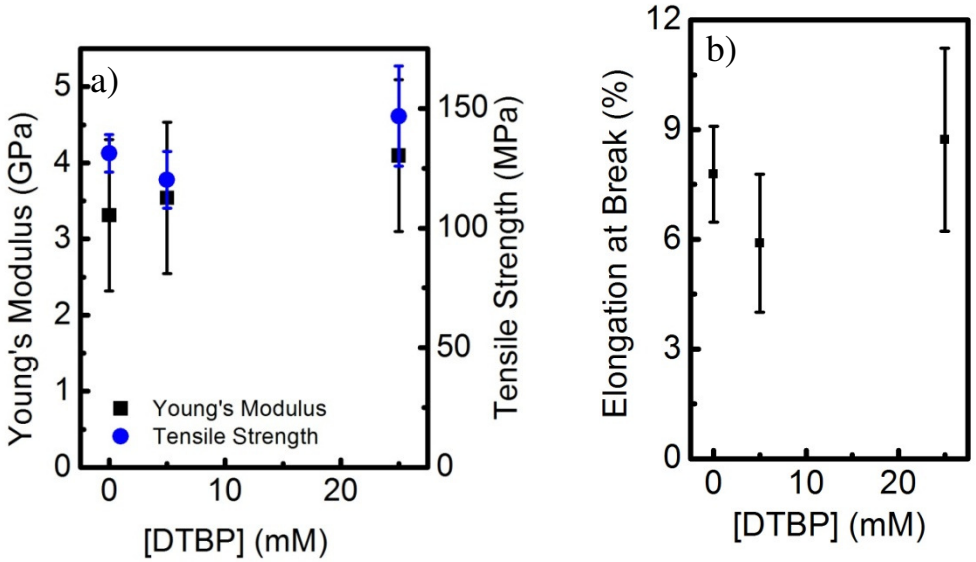

Figure 6.12: Mechanical properties of PTh films in distilled BFEE with different DTBP concentration. Each data point is an average of eight measurements on samples coming from two films. The films thickness is 3.8 ± 0.5 µm.

Jin et al. reported that PTh films electropolymerized in a DTBP/BFEE electrolyte using a constant current of 1 mA/cm^2 produced electrical conductivities of 800-1300 S/cm measured 30 minutes after deposition, and a Young's modulus of 46 GPa [36] due to a low number of defects from hydrogenated thiophene rings. In this study, a lower current density of 0.5 mA/cm^2 was used to synthesized PTh film in DTBP/BFEE electrolyte, and these films exhibited electrical conductivities as high as 180 S/cm 45 minutes after deposition, and a Young's modulus of 3.5 ± 0.8 GPa. The oxidation potential is higher at higher current density, so the rate of polymerization is higher than the rate of deprotonation thiophene assisted by DTBP. This may produce a higher doping level in the films produced by Jin et al., leading to the reported higher conductivity value (it is also not clear if the films synthesized by Jin et al. were exposed to air, which leadings to lose of dopants, before electrical conductivity measurements as the films here were). The use of higher current density in this work as proposed by Jin et al., led to films with reduced electrical conductivity presumably due to increased cross-linking in the film at the higher oxidation potential used during deposition. Further work is required to clarify the reasons for the lower conductivities measured in our work compared to the prior study.

6.4 Electrochemical Polymerization of PTh in Anionic Surfactant/DTBP/BFEE

Electrochemical polymerization of thiophene in solvated Lewis acid BFEE reduces the oxidation potential by reducing the aromaticity of the thiophene ring, which promotes the deposition of high quality PTh films. The molecular order and electrical conductivity of PTh films are shown later in this thesis to be improved significantly by adding anionic surfactants to the BFEE electrolyte. Motivated by these results and the demonstrated improvement to the PTh chain structure using DTBP, here we synthesize PTh film in an anionic surfactant/DTBP/BFEE

mixture to further improve the molecular structure of PTh films by combining the merits of the surfactant and DTBP additives.

The first cycle of a CV scan with anionic surfactant/DTBP/distilled BFEE mixture is presented in Figure 6.13. The previously determined optimal concentrations of SDS, SDBS, and DTBP were used to create various mixtures in freshly distilled BFEE. The current density was the highest for the DTBP/distilled BFEE mixture because of the presence of the stabilized cation of DTBP. Similar values of current density are observed for the anionic surfactant/DTBP/distilled BFEE mixtures and the anionic surfactant/distilled BFEE electrolyte. It is possible that the effects of the DTBP cation are cancelled by the anion of the surfactant (the reverse of this as well). The oxidation potential of the three mixtures was lower than that of the surfactant/distilled BFEE mixture and distilled BFEE alone. This observation was confirmed by the trends observed in the CP plots shown in Figure 6.14. The DTBP was more effective for proton elimination in the surfactant/DTBP/distilled BFEE mixture because the amount of water is lower than in the undistilled BFEE. The oxidation potential in the distilled BFEE was higher than in the undistilled BFEE due to higher water percentage in the undistilled BFEE. Figure 6.15 shows CP plots of the anionic surfactant/DTBP/undistilled BFEE mixture for comparison with the mixture in distilled BFEE. The oxidation potential of this mixture in undistilled BFEE is more comparable to that of the surfactant/undistilled BFEE electrolyte because more water is present in the solution, making the DTBP virtually ineffective.

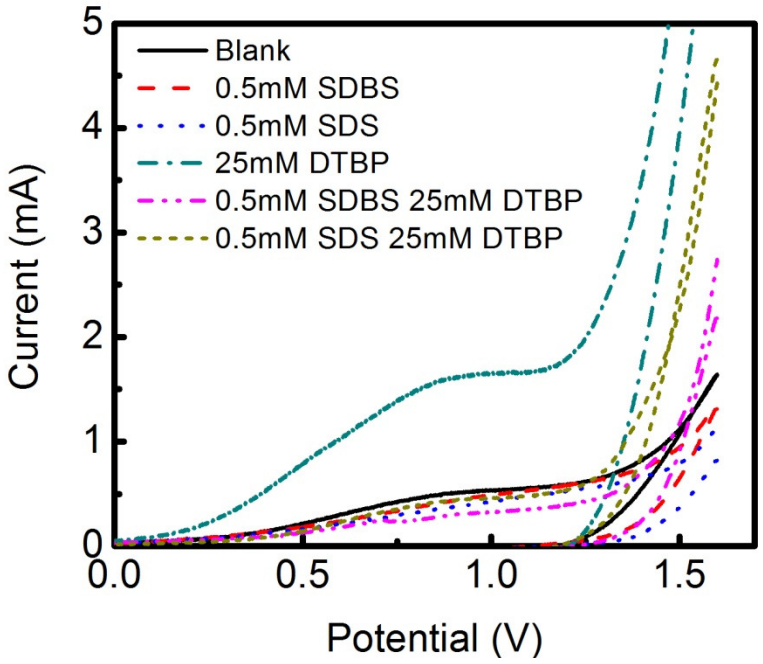

Figure 6.13: CV plot of 50 mM thiophene in anionic surfactant/DTBP/distilled BFEE electrolyte with 200 mV/s scan rate.

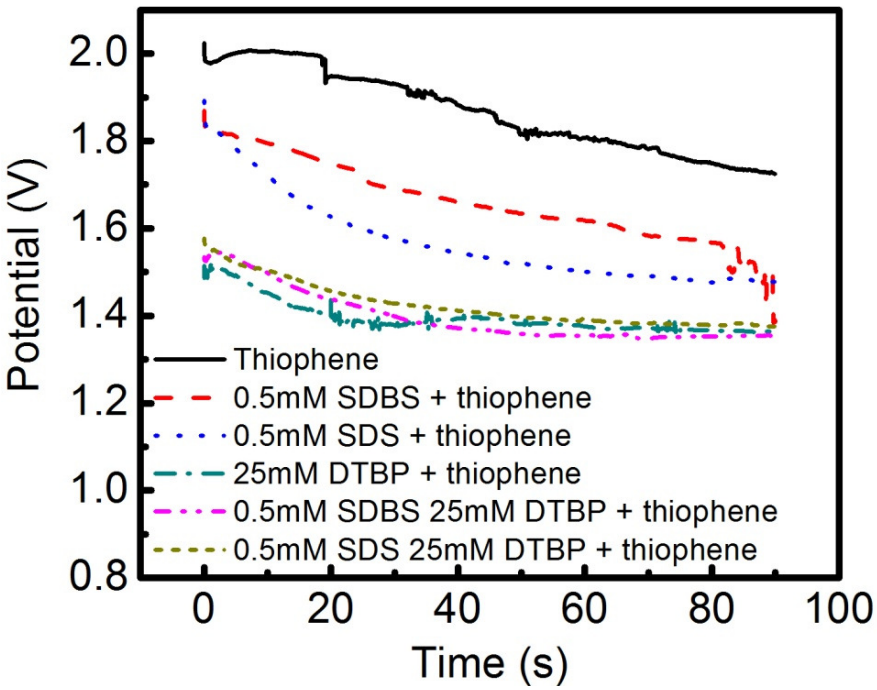

Figure 6.14: CP using 0.5 mA/cm^2 of 50 mM thiophene in anionic surfactant/DTBP/distilled BFEE electrolyte at 5 mm inter-electrode distance.

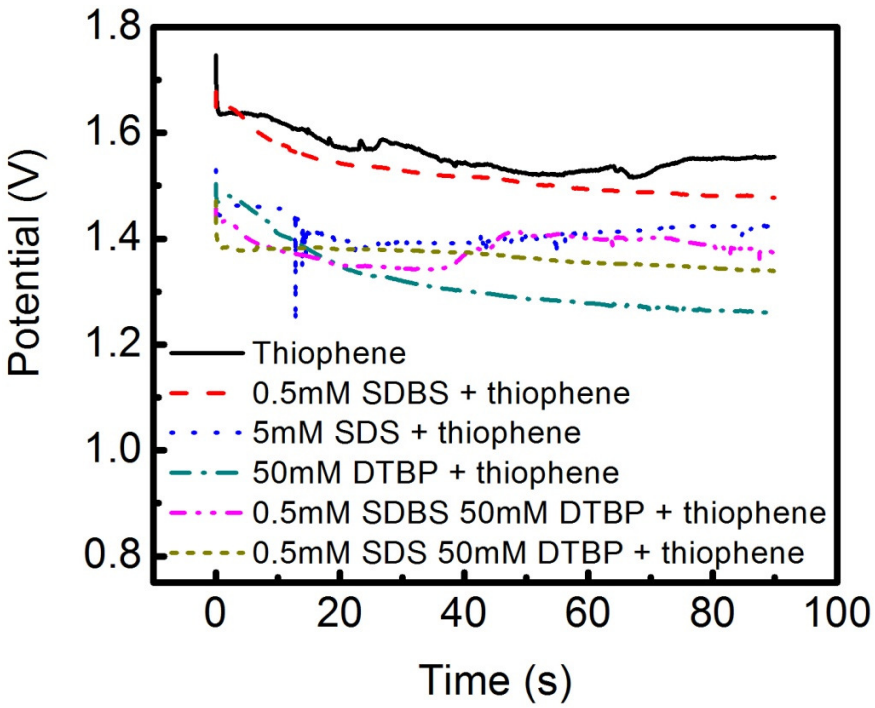

Figure 6.15: CP using 0.5 mA/cm^2 of 50 mM thiophene in anionic surfactants/DTBP/undistilled BFEE electrolyte at 5 mm inter-electrode distance.

6.5 In-Plane Conductivity

The conductivity of a PTh film can be predicted from its electrochemical behavior (i.e., CV and CP plots). Figure 6.16a shows that the critical concentration of PTh film synthesized in SDBS is at 0.5 mM. This behavior agrees with the CP in Figure 6.4a where the oxidation potential during polymerization increases at 1 and 5 mM SDBS suggesting the presence of micelles. However, this is not the case for PTh films synthesized in SDS. Although the CP in Figure 6.4b predicts the micelles presence at 1 and 5 mM SDS, the electrical conductivity of the PTh films synthesized at these concentration still increases (see Figure 6.16b). The lower critical concentration for SDBS is likely the result of the larger DBS^- anion and the presence of the benzene ring in SDBS compared to the DS^- anion in SDS, which may produce steric hindrance to

polymerization at high concentration of SDBS. The addition of SDS improved the electrical conductivity of PTh films by a higher percentage compared with the addition of SDBS into PTh films. This was the case for growth in undistilled and distilled BFEE (see Figure 6.16). PTh films synthesized in 0.5 mM SDS and 0.5 mM SDBS in distilled BFEE has 200% and 300% increase respectively with the respect to the PTh films made without surfactants. The critical concentration of SDS reduced to 0.5 mM when freshly distilled BFEE was used (see Figure 6.16c). The critical concentration of SDBS in distilled BFEE appears to be the same (or possibly higher) as that in undistilled BFEE. The change in critical concentration of SDS is likely caused by the reduced water content in distilled BFEE, which reduced reactions between SDS and water. The electrical conductivities of films synthesized using distilled BFEE were lower than those of films synthesized in undistilled BFEE. This might be due to the lower solution conductivity of distilled BFEE because of less water content, which increased the oxidation potential during film growth.

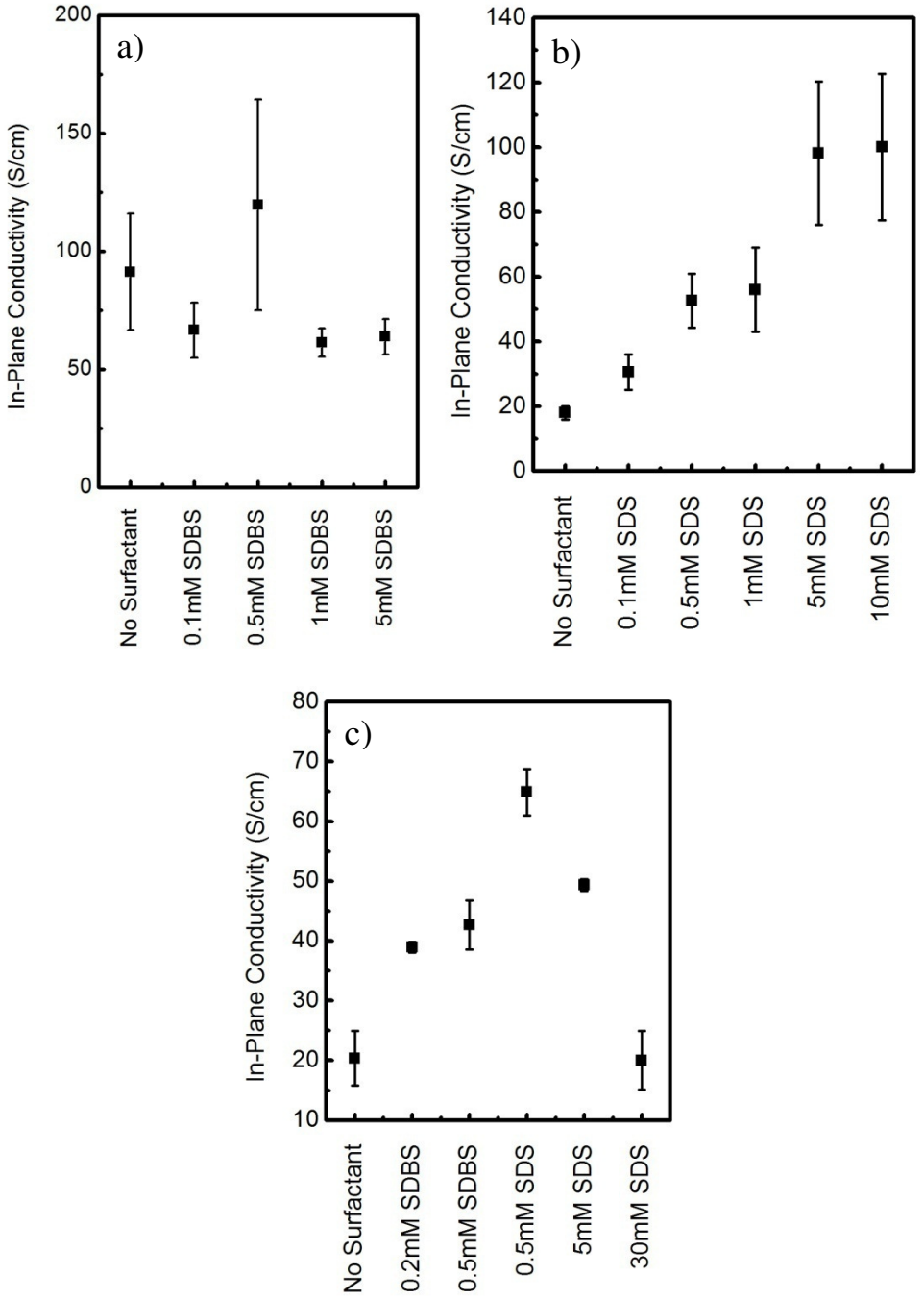

Figure 6.16: In-plane conductivity of PTh films growth by CP at 0.5 mA/cm^2 for 90 min using 50 mM thiophene in a) SDBS/undistilled BFEE/, b) SDS/undistilled BFEE, and c) SDS/distilled BFEE and SDBS/distilled BFEE. Each data point is an average of four measurements on samples coming from two films. The film thickness is 4.1 ± 0.3 µm.

Figure 6.17 suggest that the use of surfactants allowed a higher amount of dopants to enter the film, thus the higher electrical conductivity measured on the next day of deposition (i.e. day 1). Literature has shown that increased molecular order will allow a high packing density of dopants [75, 76]. The conductivity may converge due to "less trapped" dopants escaping the film first, followed by the slow decay of dopants that are trapped more in the bulk of the polymer. Further studies are required to understand the mechanism of dopant loss from the films clearly.

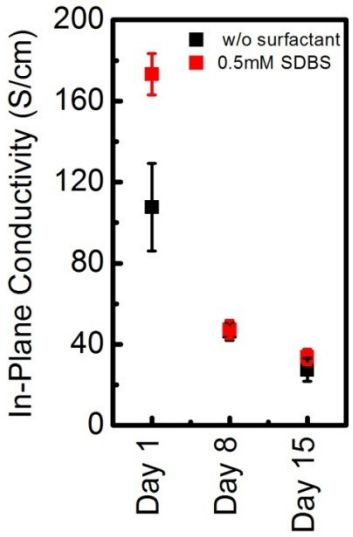

Figure 6.17: Conductivity stability of PTh film synthesized in SDBS/undistilled BFEE electrolyte.

The electrical conductivities of PTh films made from anionic surfactant/DTBP/distilled BFEE mixtures are shown in Figure 6.18. The conductivities of PTh films with additives were higher than that of films without additives for all electrolyte mixtures used in the synthesis of the films. The electrical conductivity of PTh films synthesized using the three mixtures are within the standard deviation of the electrical conductivity of the film synthesized using DTBP/distilled BFEE. The presence of DTBP cation may cancel the charge from DBS^- and DS^- anions reducing the solution conductivity. This can result in a smaller amount of dopants from the dodecyl chain

of the surfactants which improves molecular ordering because anionic surfactants require longer times and high solution conductivities to diffuse into the working electrode due to their relatively large weight.

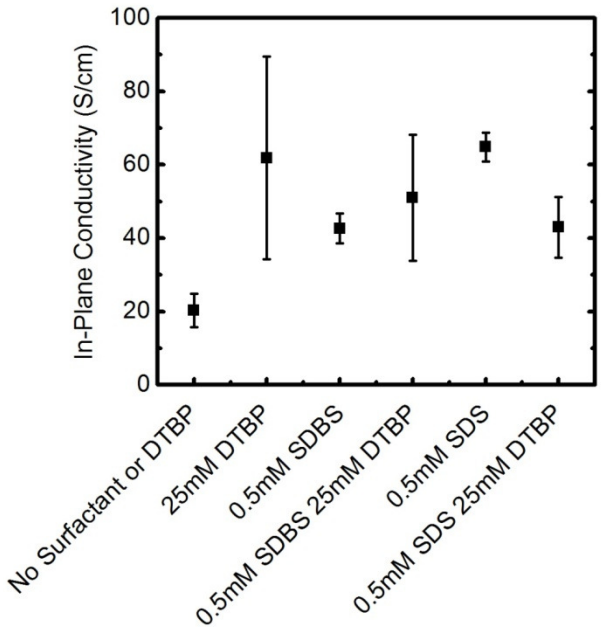

Figure 6.18: In-plane conductivity of PTh films synthesized using 0.5 mA/cm^2 with 50 mM thiophene at 5 mm inter-electrode distance in anionic surfactant/DTBP/distilled BFEE electrolyte. Each data point is an average of four measurements on samples coming from two films.

The PTh films synthesized in anionic surfactant/DTBP/undistilled BFEE have higher conductivities than the films synthesized in anionic surfactant/undistilled BFEE and DTBP/undistilled BFEE as shown in Figure 6.19. In the anionic surfactant/DTBP/undistilled BFEE, anionic surfactant appears to be the dominant factor as shown in Figure 6.15. The oxidation potentials of the mixtures are comparable to the oxidation potentials of the anionic surfactant/undistilled BFEE system after several minutes of film deposition. The DTBP cation may still cancel the charge of the dodecyl chain, but higher water content in the undistilled BFEE

promotes a faster diffusion rate of the DBS- and DS- to the working electrode. Therefore, the PTh films synthesized in anionic surfactant/DTBP/undistilled BFEE have higher electrical conductivities than the films synthesized in anionic surfactant/undistilled BFEE and DTBP/BFEE. Using the anionic surfactant/DTBP mixtures in undistilled BFEE to synthesize the PTh films offers the advantage of reducing the defects due to DTBP and increasing the molecular ordering due to the anionic surfactants.

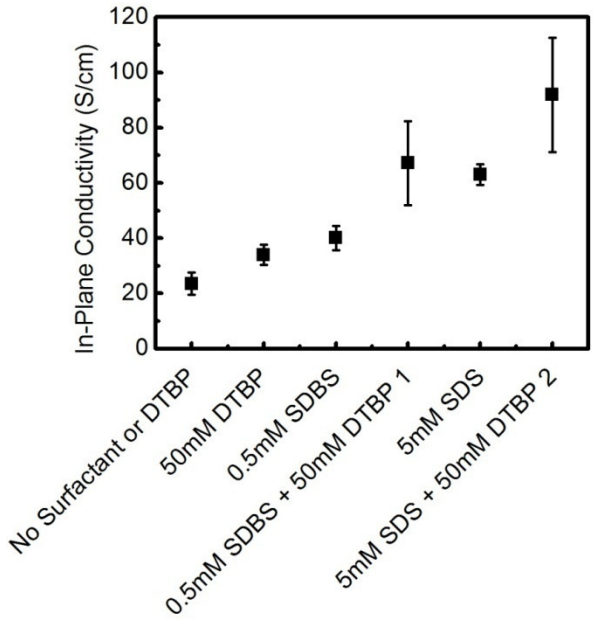

Figure 6.19: In-plane conductivity of PTh films synthesized using 0.5 mA/cm^2 with 50 mM thiophene at 5 mm inter-electrode distance in anionic surfactant/DTBP/undistilled BFEE electrolyte. Each data point is an average of four measurements on samples coming from two films.

6.6 Mechanical Properties

Mechanical properties of PTh films synthesized in SDBS/undistilled BFEE solution are shown in Figure 6.20. The Young's modulus and tensile strength of PTh films without surfactant, with 0.1 mM SDBS, and with 0.5 mM SDBS were comparable within the spread of

eight measured 0.5 × 2 cm strips. There was little difference in the electrical conductivity and oxidation potential of films synthesized with no surfactant and with 0.1 mM SDBS solution, so similar mechanical properties were expected for those films. The tensile modulus and strength of films synthesized with 0.5 mM SDBS were expected to be higher than that of films synthesized with no surfactant and 0.1 mM SDBS because the electrical conductivity was higher and the oxidation potential was lower for films synthesized at 0.5 mM SDBS. The molecular weight of SDBS is lower compare to that of the PTh structure; therefore, films made with SDBS could have lower molecular weights than films made without surfactant. Steric effects from the use of surfactants could also cause the films to be less compact, so increased chain length and alignment may compete with reduced effective molecular weight when surfactants are added to PTh films. Because of these competing factors, it is difficult to draw clear conclusions about the mechanisms responsible for the tensile modulus and strength data of films made with no surfactant, 0.1 mM and 0.5 mM SDBS concentrations. However, it is clear that the tensile strength and Young's modulus of PTh films reduces slightly when the SDBS concentration is increased. Out of the eight strips that were cut from two films and used for testing for each surfactant concentration (0.1, 0.5, and 5 mM SDBS), almost half exhibited necking behavior as shown in the stress-strain curves in Figure 6.21. Necking indicates that the polymer network is at least partially aligned because of the presence of surfactant. However, the short necking period without drawing steps suggest that the conjugated chain lengths are short. No necking was observed in films that were synthesized without surfactant and with 1 mM SDBS solution. Overall, the inclusion of SDBS increased the maximum strain of PTh films. This improvement is likely the results of increased molecular order, which is discussed further in the next section. Note that the reported strain measurement assumes uniform deformation. Assuming necking with

uniform deformation can overestimate the true strain values. PTh films synthesized in BFEE by Jin et al. produced lower tensile strength and elongation at break than PTh films synthesized with surfactants in this study [24]. The mechanical properties measured here would be even higher at the slower strain rate used by Jin et al. because the polymer has more time to overcome the stress.

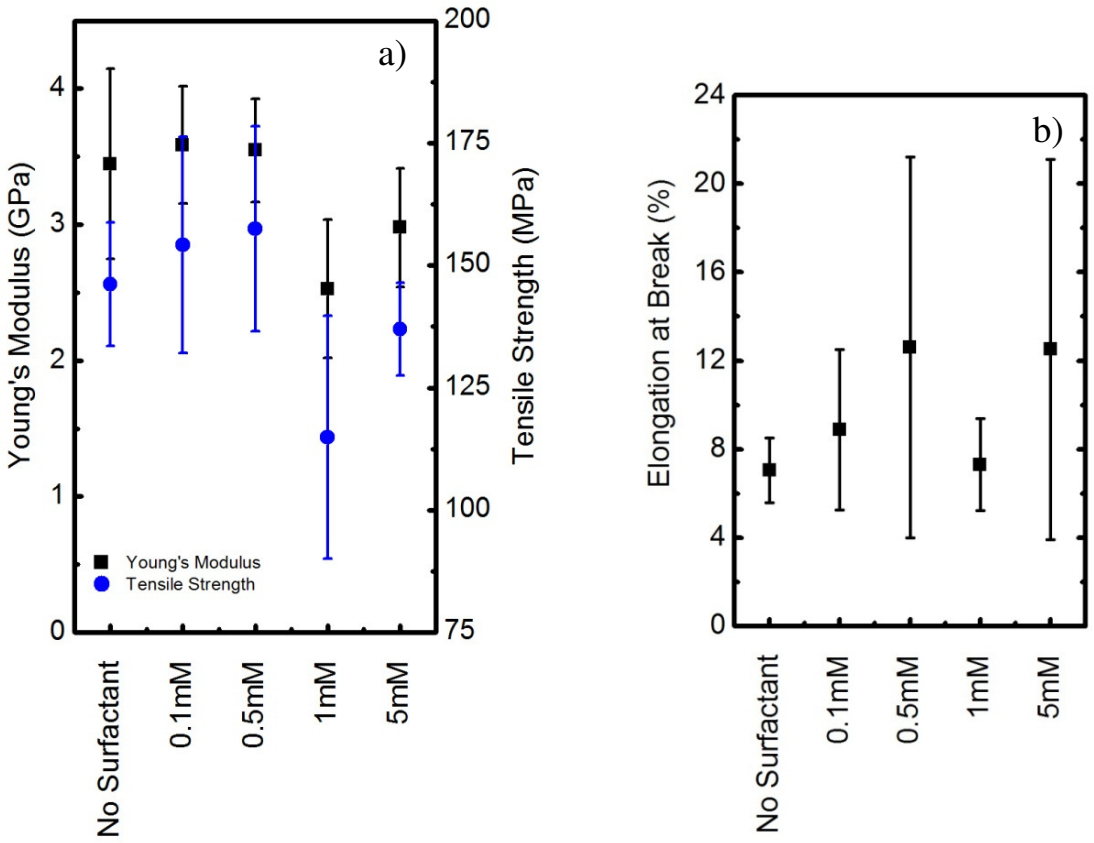

Figure 6.20: Mechanical properties of PTh films synthesized at different SDBS concentrations in BFEE. Each data point is an average of eight measurements on samples coming from two films. The film thickness is 4.1 ± 0.3 µm.

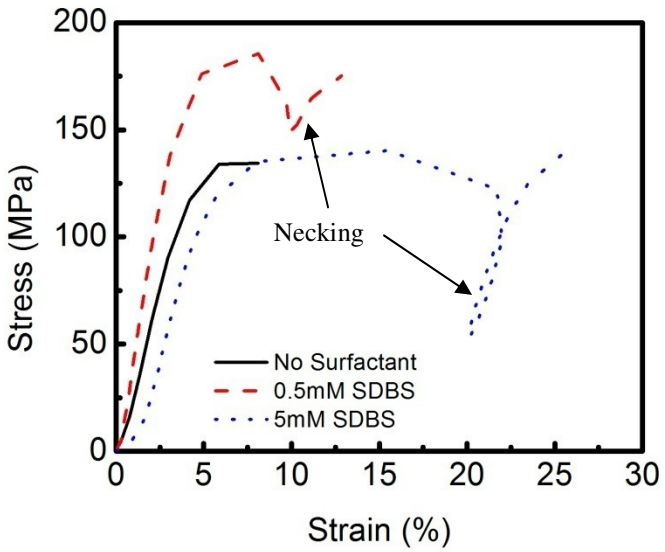

Figure 6.21: Stress-strain curve of PTh in SDBS/BFEE electrolyte.

Figure 6.22 displays the mechanical properties of PTh synthesized in SDS/BFEE electrolyte. Unlike PTh films synthesized in SDBS/BFEE, the Young's modulus and tensile strength at all concentration were comparable within the data spread. The in-plane electrical conductivity of PTh films with SDS increased with SDS concentration (see Figure 6.16b), which suggest increased molecular ordering with the addition of SDS. Therefore, the near constant mechanical strength and tensile modulus are most probably the result of reduced molecular weight with increased SDS concentration (there is balancing act between increased molecular order and reduced molecular weight similar to the case with SDBS). There was directionality in the elongation at break data for films synthesized with SDS where the transverse direction exhibited higher elongation than the longitudinal direction with the respect to the direction of electron flow into the lead wire attached to the electrode as shown in Figure 2.5. A possible reason for this behavior is uneven film growth experienced with these samples. This anisotropic behavior was not observed in the mechanical properties of films made with SDBS.

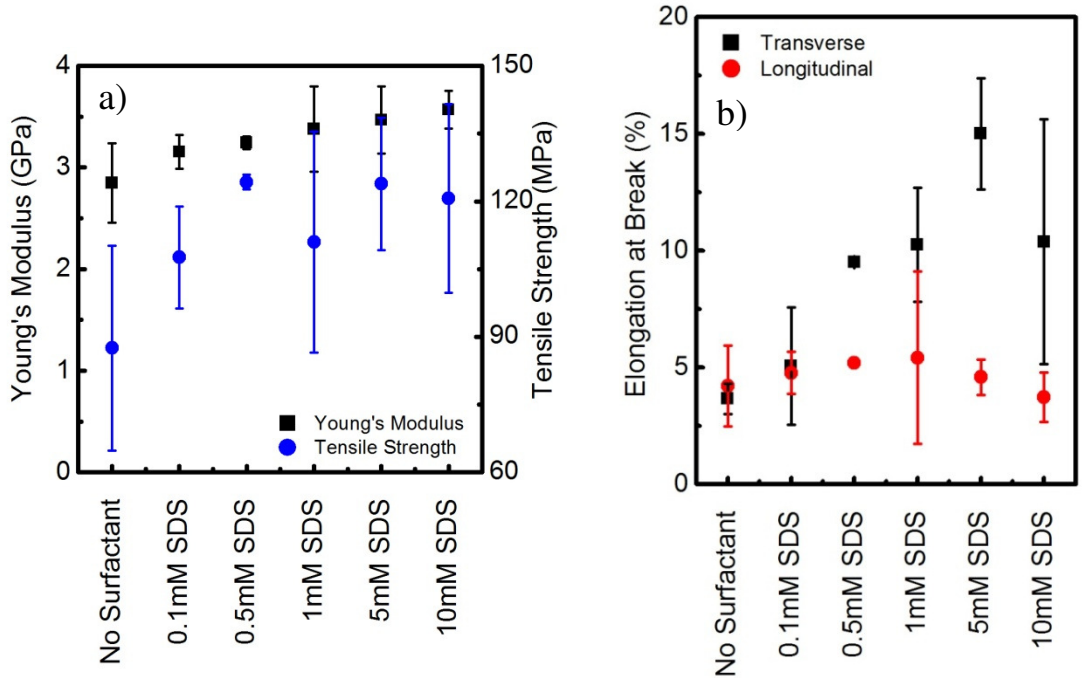

Figure 6.22: Mechanical properties of PTh films synthesized at different SDS concentrations in BFEE. Each data point is an average of eight measurements (four for each direction) on samples coming from two films.

In distilled BFEE, the mechanical properties of the films synthesized in presence of various concentrations of either SDS or SDBS showed no difference as shown in Figure 6.23. There was no directionality in the elongation at break, and 4 out of 12 strips of films made with SDBS and 6 out of 16 strips of films made with SDS exhibited necking behavior, most likely due to chain alignment in the film. This result highlights that improved experimental consistency is achieved with distilled BFEE because the films made with each surfactant are more uniform without any directionality compared with films made using undistilled BFEE.

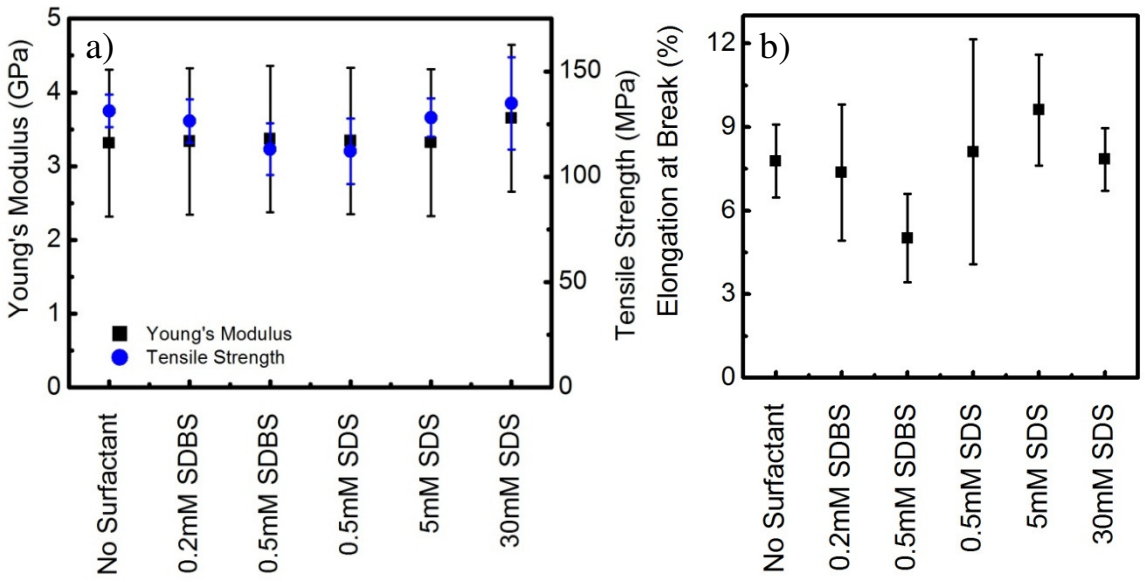

Figure 6.23: Mechanical properties of PTh films synthesized in anionic surfactant/distilled BFEE. Each data point is an average of eight measurements on samples coming from two films.

Tensile modulus and strength of PTh films in SDS/DTBP/undistilled BFEE presented in Figure 6.24 are comparable, which also exhibit the highest absolute and average value, with the results obtained from films made using SDS/undistilled BFEE and DTBP/undistilled BFEE electrolytes. Tensile strength and Young's modulus of the films synthesized in the mixtures of three solutions is comparable to the films synthesized in no additive, DTBP/BFEE, and SDS/BFEE because the addition DTBP and anionic surfactants in BFEE does not produce significant changes in tensile strength and Young's modulus of the films (see Section 6.3Figure 6.22a). Although the films synthesized in SDS/DTBP/undistilled BFEE have higher electrical conductivities than the films synthesized in anionic surfactant/undistilled BFEE and DTBP/undistilled BFEE as shown in Figure 6.19, the effect of anionic surfactant is more dominant as suggested by the CP plot in Figure 6.15 creating competition between enhancement of molecular structure and decreasing molecular weight. This trend is identical to that observed

for the Young's modulus and tensile strength of PTh films synthesized in distilled BFEE mixtures, and the Young's modulus and tensile strength of the PTh films synthesized in anionic surfactant/DTBP/distilled BFEE are comparable to the values obtained with the same additives in distilled BFEE (see Figure 6.25). Surfactant/DTBP mixtures in distilled and undistilled BFEE produced absolute and average Young's modulus and tensile strength values that are higher than values achieved with films made using SDS/distilled BFEE and DTBP/distilled BFEE electrolytes. The slightly higher Young's modulus and tensile strength of the films synthesized in the three mixture solutions show that mixing anionic surfactant and DTBP in distilled or undistilled BFEE produce synergistic results. The elongation at break of the films made with anionic surfactant/DTBP/distilled and undistilled BFEE is shown in Figure 6.26 and Figure 6.27, respectively. It is noted that these values are comparable to the values measured for films made in several different electrolyte combinations. The variance in the measurements standard deviation is likely due to the variability in thickness of the PTh films.

The mechanical properties (tensile modulus, strength, and elongation at break) of the films synthesized in distilled solution are slightly better than those of films synthesized in undistilled BFEE. This is likely because of the higher polymerization rate in distilled BFEE that results from the higher oxidation potential. This explanation is supported by structural analysis data that is discussed in the following section.

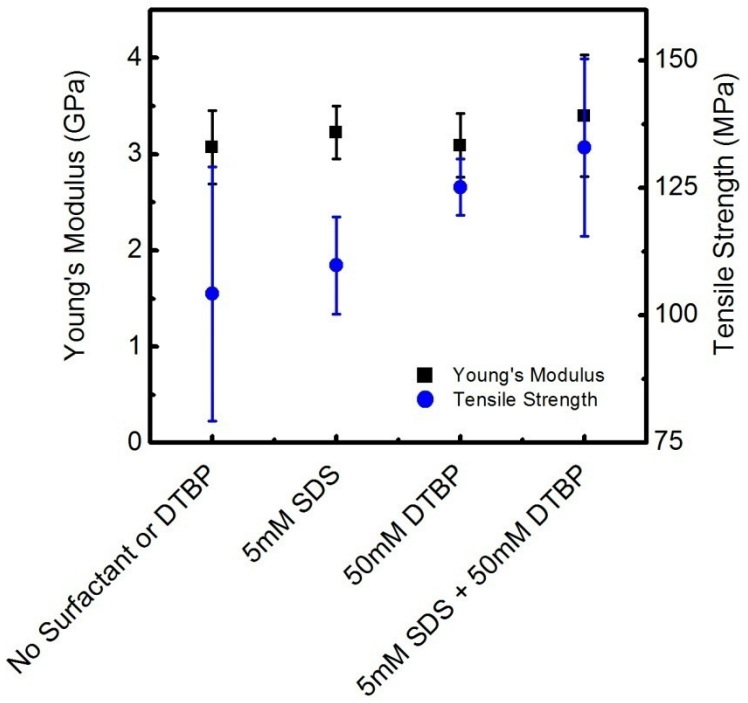

Figure 6.24: Tensile modulus and strength of PTh films synthesized using 0.5 mA/cm^2 with 50 mM thiophene at 5 mm inter-electrode distance in SDS/DTBP/undistilled BFEE electrolyte. Each data point is an average of eight measurements on samples coming from two films.

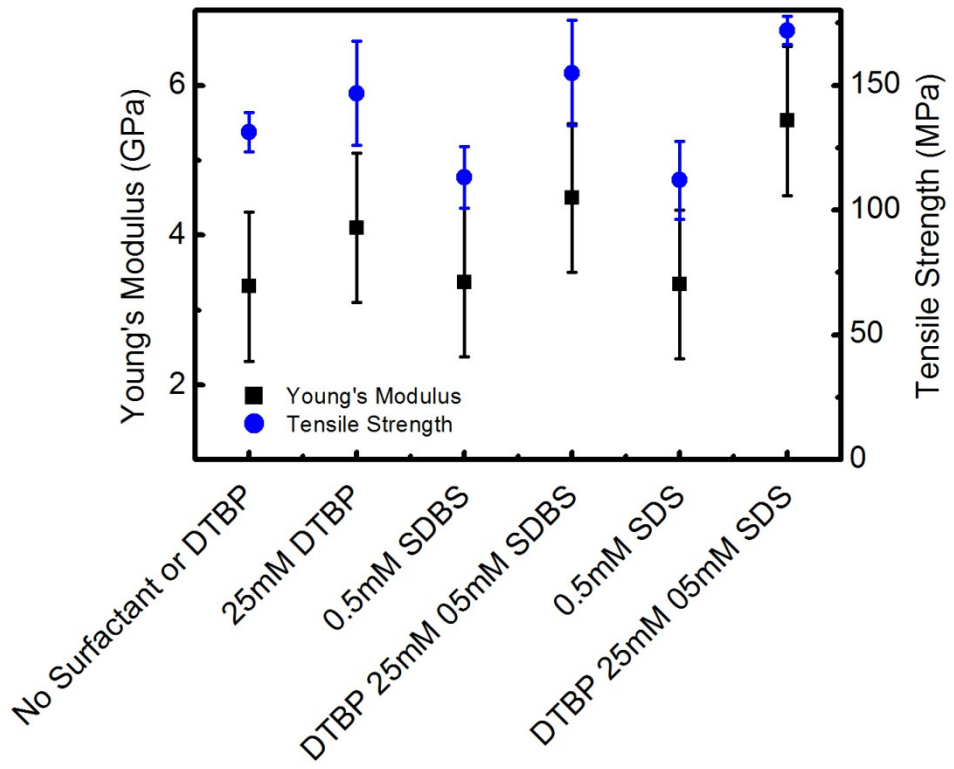

Figure 6.25: Tensile modulus and strength of PTh films synthesized using 0.5 mA/cm^2 with 50 mM thiophene at 5 mm inter-electrode distance in anionic surfactant/DTBP/undistilled BFEE electrolyte. Each data point is an average of eight measurements on samples coming from two films.

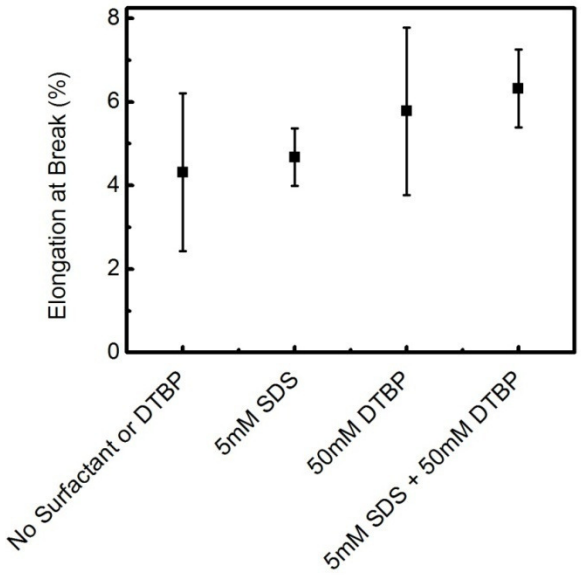

Figure 6.26: Elongation at break of PTh films synthesized using 0.5 mA/cm^2 with 50 mM thiophene at 5 mm inter-electrode distance in anionic surfactant/DTBP/undistilled BFEE. Each data point is an average of eight measurements on samples coming from two films.

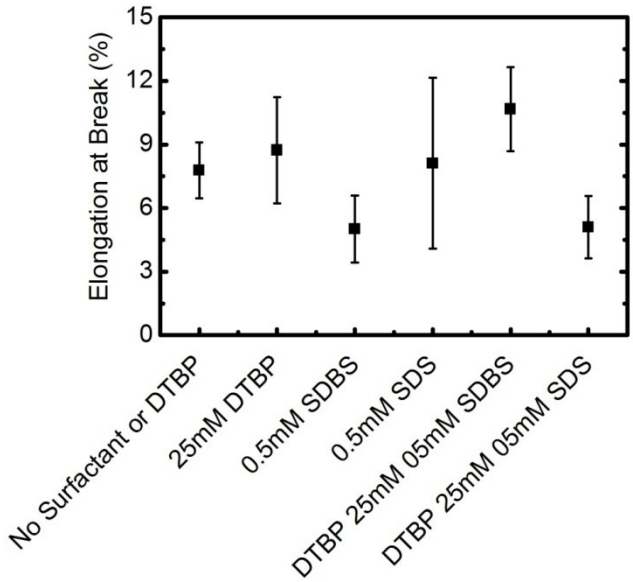

Figure 6.27: Elongation at break of PTh films synthesized using 0.5 mA/cm^2 with 50 mM thiophene at 5 mm inter-electrode distance in anionic surfactant/DTBP/distilled BFEE. Each data point is an average of eight measurements on samples coming from two films.

6.7 Structural Analysis

The PTh films synthesized with SDBS and SDS were analyzed with X-ray photoelectron spectroscopy (XPS) to confirm the incorporation of DS^- and DBS^- anions in the PTh films. Figure 6.28 displays the high-resolution spectra of O1s and S2p recorded for PTh films made with different concentrations of SDBS and SDS. A small hump located at 168.4 eV in concentrations higher than 1 mM SDS and 1 mM SDBS in S2p scans is the signature of [S=O] from [$=SO_4^-$] of SDS and [$=SO_3^-$] of SDBS, which indicate the incorporation of DS^- and DBS^- anions in the film (see Figure 6.28b and d). This hump does not appear when the SDBS and SDS concentration is lower than 5 mM because the relative concentration of SDBS and SDS to the concentration of thiophene was low. The hump might appear at low SDBS and SDS concentrations with additional scans to compensate for the low concentration. The peaks in the S2p scan at 163.9 eV, and the shoulder at 165.6 eV, are the signature of doublets from the thiophene sulfur atom [$S(2p)_{3/2}$, $S(2p)_{1/2}$] [77]. The O1s peak in the XPS in Figure 6.28a and c shows that there is oxygen in the PTh film structure. This oxygen is attributed to the oxygen from air [78], because the thiophene structure does not have oxygen and oxidized thiophene may react with atmospheric oxygen. The O1s peaks are shifted to lower binding energies at concentrations higher than 1 mM SDBS and 1 mM SDS (see Figure 6.28 a and c) because of the presence of [O-S=O] from DS^- and DBS^- anions in the film as shown in Figure 6.29. The C-O-C is likely from the diethyl ether trapped in the PTh film. The O1s peak of 0.1 mM SDBS shifted to a higher binding energy possibly because of [C=O] in the film that has a signature at approximately 535.7eV. The [C=O] is likely a contaminant in the thiophene chain from CO_2 [37].

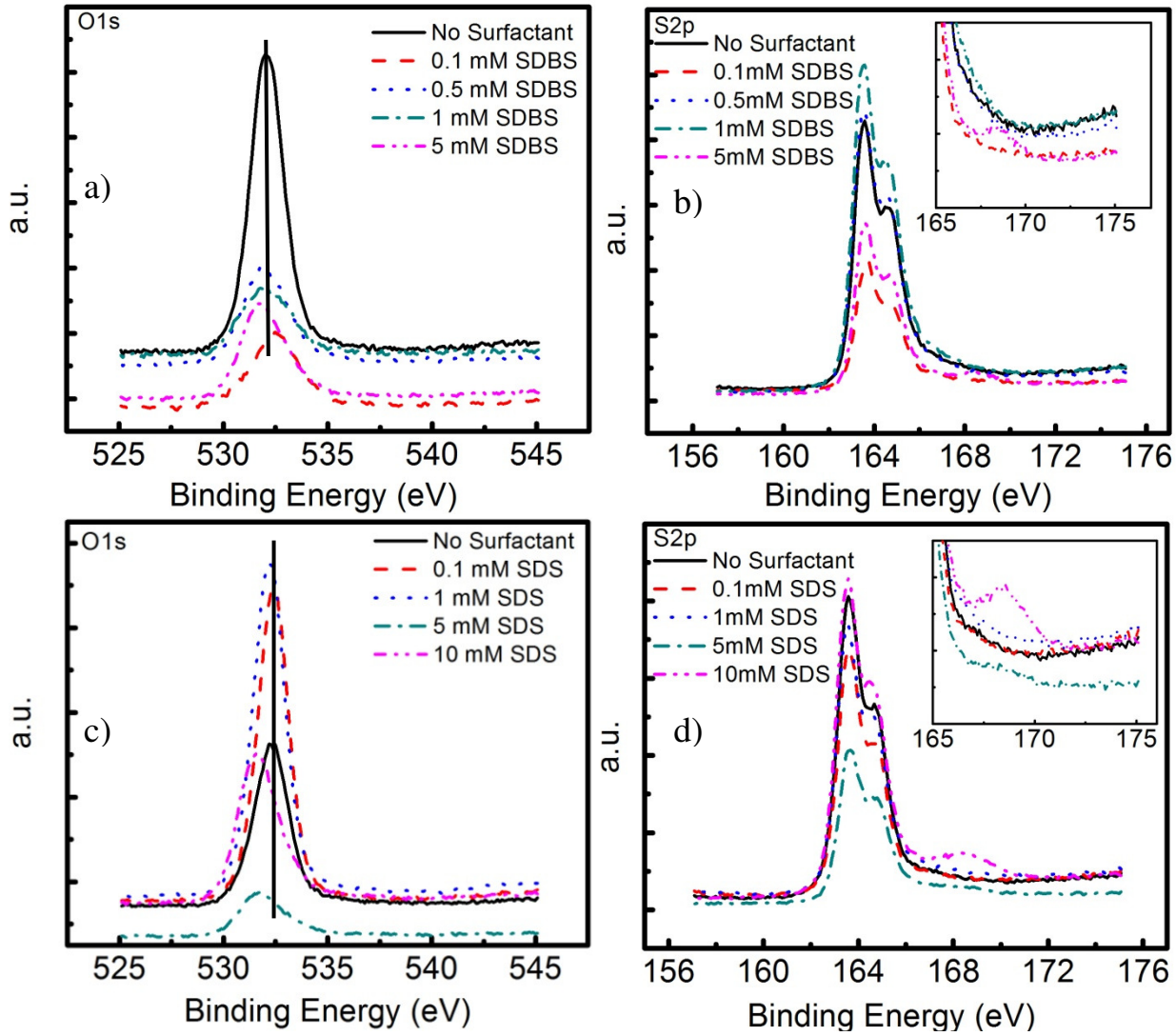

Figure 6.28: O1s and S2p high resolution XPS spectra of 50 mM thiophene in undistilled BFEE with different concentration of a, b) SDBS and c, d) SDS.

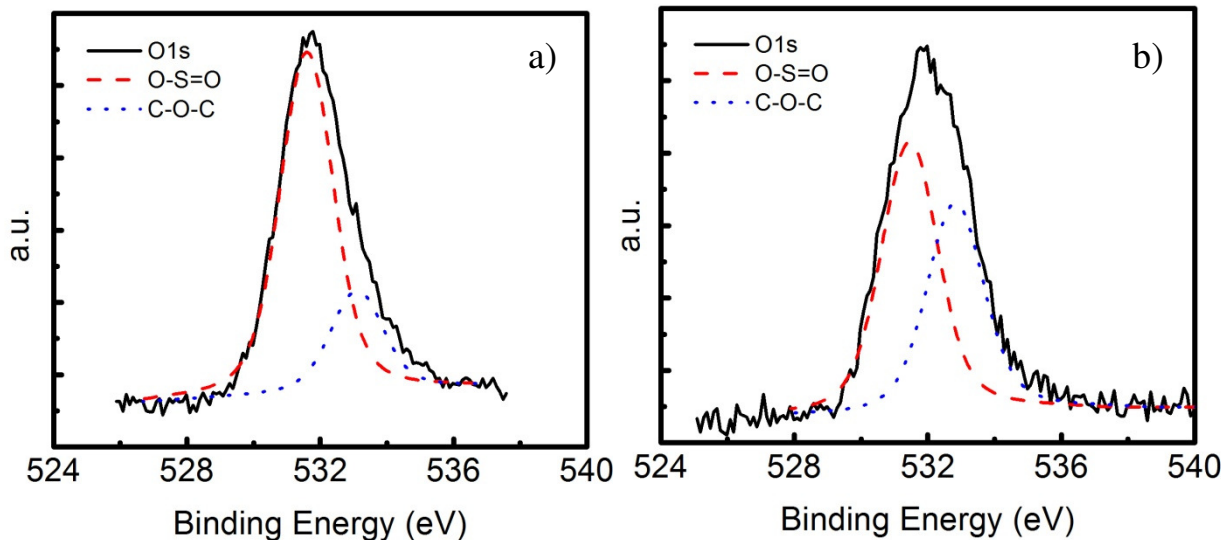

Figure 6.29: Fitted PTh O1s peaks of 50 mM thiophene in undistilled BFEE with a) 5 mM SDS and b) 5 mM SDBS.

Current density controls the diffusion rate of the monomers or oligomers to the working electrode. The wide-angle X-ray scattering (WAXS) spectra of PTh films made without the presence of surfactant and deposited using 0.5 mA/cm^2 with 50 mM thiophene are shown in Figure 6.30c and d and reveal enhanced molecular ordering in the films. This is indicated by the sharper peaks in these films compared to films in Figure 5.6 that were deposited using 1 mA/cm^2. The films grown with 0.5 mA/cm^2 are also thicker than the films grown using 1 mA/cm^2. This suggests that a slower deposition rate provides more time to rearrange monomers and oligomers on the working electrode.

WAXS data for PTh films made with and without SDBS and SDS anionic surfactants are shown in Figure 6.30 and Table 6.2. The broad peaks in the WAXS pattern of the PTh films synthesized in the presence of SDBS and SDS (see Figure 6.30) show that the PTh films are amorphous. As discussed in the prior section, the anion tail from the surfactant is thought to create steric effects that reduce the packing density of PTh chains in the film. This hypothesis is

supported by the larger d1 and d2 spacing (i.e., larger full width at half maximum for the d1 and d2 peaks) for films synthesized with 5 mM SDS (Figure 6.30d) compared to films synthesized without surfactant (Figure 6.30a) that have similar values of electrical conductivity. The films made with SDS and SDBS increased electrical conductivity by 479% and 61%, respectively, with respect to the films synthesized without surfactant additives. The PTh films in Figure 6.30a and b were produced with a different BFEE batch than the one used to produce the films in Figure 6.30c and d so it is only useful to compare the percent improvement in electrical conductivity achieved using SDBS or SDS in the respective batches. The Bragg's angles and full width at half maximum (FWHM) of peaks in the WAXS spectrum of the films made with SDBS are comparable to the angles and peaks for films made with no surfactant as shown in Figure 6.30a and b. The important differences are that the ratio of d1/d2 is closer to one when SDBS is in the PTh film, which means that the thiophene ring has approximately the same periodicity of d1 and d2 packing, and that the FWHM of the d3 peak is significantly lower. The sharper d3 peak in films made with 0.5 mM SDBS suggest increased ordering, and possibly chain length, compared to films synthesized without surfactants. Films made with SDS produced a more than 400% increase in electrical conductivity compare to films made with no surfactant. The FWHM of the d2 and d3 peaks are narrower in films synthesized with 5 mM SDS than in films made with no surfactant. The films with 5 mM SDS also show larger d1/d3 and d2/d3 peak ratios. The sharper d2 peak suggest closer out-of-plane packing of polymer chains and the sharper d3 peak suggest increased conjugation length; this hypothesis as based on assigning the d3 peak to the unit spacing between thiophene rings.

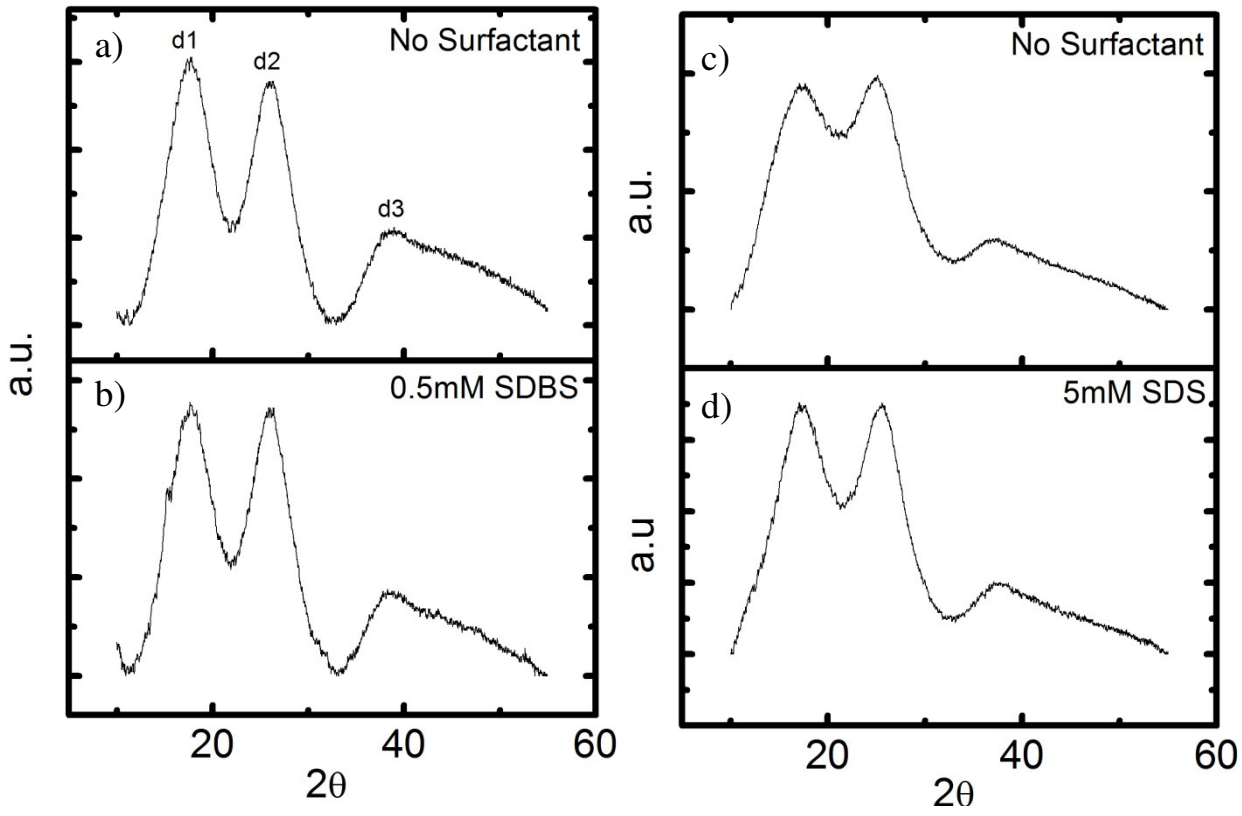

Figure 6.30: WAXS pattern in transmission mode of PTh film electrochemically synthesized using 50 mM thiophene with current density of 0.5 mA/cm^2 at 5 mm inter-electrode distance in anionic surfactants/undistilled BFEE electrolyte.

Table 6.2: X-ray diffraction data of PTh films in undistilled anionic surfactant/undistilled BFEE electrolyte.

ID		σ (S/cm)	2θ			FWHM			Peak intensity ratio		
			d1	d2	d3	d1	d2	d3	d1/d2	d1/d3	d2/d3
a	No Surfactant	86.02 - 129.18	17.6	26.0	38.7	5.1	4.6	13.2	1.1	3.0	2.7
b	0.5mM SDBS	162.96 - 183.52	17.7	26.0	38.3	5.2	4.8	10.8	1.0	3.5	3.4

ID		σ (S/cm)	2θ			FWHM			Peak intensity ratio		
			d1	d2	d3	d1	d2	d3	d1/d2	d1/d3	d2/d3
c	No Surfactant	18.07 - 20.74	17.0	24.9	37.2	6.3	7.2	12.7	1.0	3.6	3.7
d	5mM SDS	89.56 - 135.24	17.3	25.5	36.8	6.3	5.9	12.0	1.0	4.1	4.0

Figure 6.31 and Table 6.3 present the WAXS data for PTh films synthesized in anionic surfactant/DTBP/distilled BFEE, anionic surfactant/distilled BFEE, and DTBP/distilled BFEE. The PTh films synthesized in the distilled BFEE show increased molecular close-plane packing that probably results in more dense films compared to the films synthesized in the undistilled BFEE because the lower d1/d2 peak ratio in distilled BFEE suggest closer d2 spacing relative to d1 spacing (see Table 6.2 and Table 6.3) . This may result from the slower diffusion of the thiophene to the working electrode in distilled BFEE that can cause the PTh film on the working electrode to be oxidized more than it would in undistilled BFEE where the thiophene diffusion is faster. The electrical conductivities of PTh films synthesized in anionic surfactant/distilled BFEE, DTBP/distilled BFEE, and anionic surfactant/DTBP/distilled BFEE electrolytes are comparable to each other, but higher than the conductivities of films without additives as shown in Figure 6.18. It is difficult to find clear support of the trends observed in the electrical conductivity data in the WAXS data in Table 6.3 because several competing factors (some of the clear ones were discussed above) must be considered when attempting to interpret WAXS data for films with different combinations of additives. However, the d1 spacing is clearly larger in films synthesized in distilled BFEE without additives, and this suggest increased disorder of polymer chains in the plane in which electrical conductivity was measured. Further studies are required to isolate the effect each additive has on the WAXS spectra so a clear understanding of their influence on molecular ordering in the film can be developed.

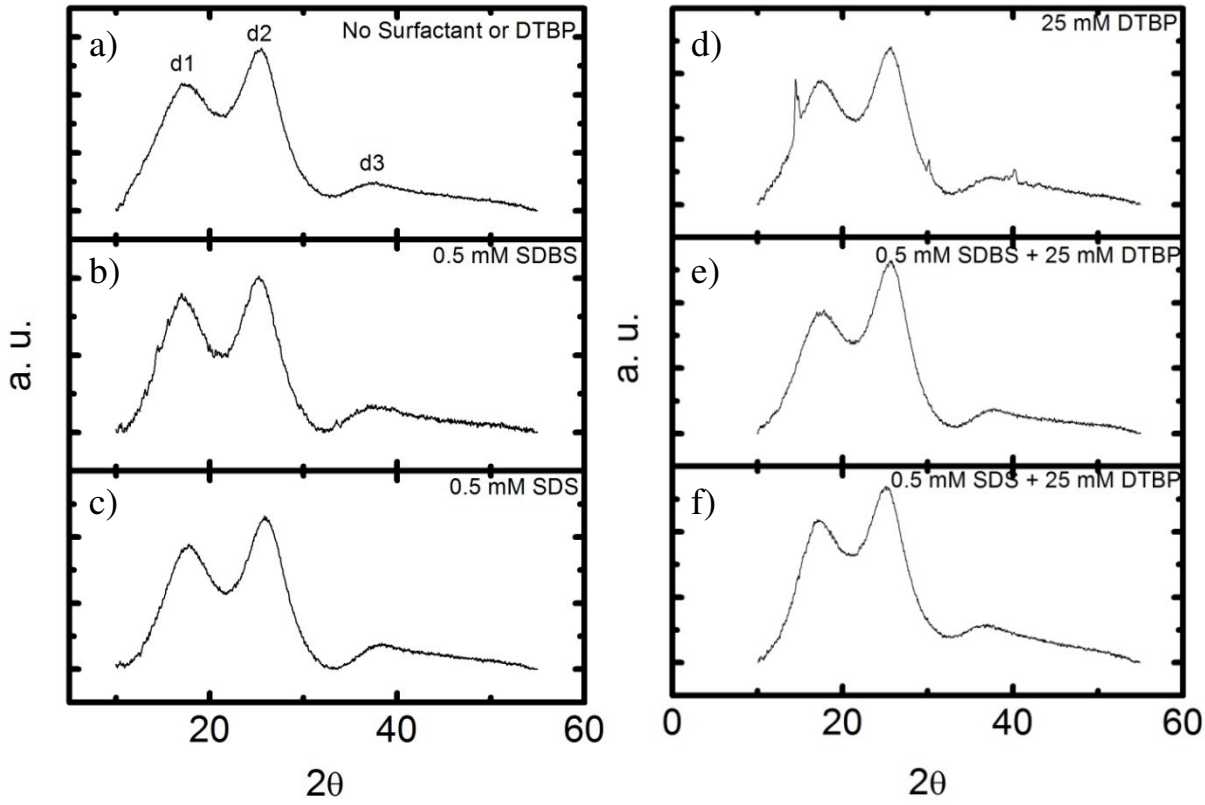

Figure 6.31: WAXS pattern in transmission mode of PTh films electrochemically synthesized using 50 mM thiophene with current density of 0.5 mA/cm^2 at 5 mm inter-electrode distance in distilled BFEE with DTBP and anionic surfactants additives.

Table 6.3: X-ray diffraction data of PTh films synthesized in anionic surfactant/DTBP/distilled BFEE electrolyte.

		2θ			FWHM			Peak intensity ratio		
	σ (S/cm)	d1	d2	d3	d1	d2	d3	d1/d2	d1/d3	d2/d3
No surfactant or DTBP	20.62-29.05	17.4	25.3	38.0	6.9	5.4	12.1	0.8	5.9	7.3
0.5mM SDBS	40.60-46.96	17.2	25.2	37.3	5.7	4.9	9.8	0.9	6.4	7.3
0.5mM SDS	66.33-67.77	17.9	25.8	38.7	6.0	4.9	9.9	0.8	6.1	7.5
25mM DTBP	64.53-99.12	17.6	25.5	37.7	6.4	5.2	11.2	0.8	5.2	6.5
0.5mM SDBS + 25mM DTBP	47.69-61.87	17.7	25.5	37.8	6.5	5.1	11.1	0.7	6.8	9.5
0.5mM SDS + 25mM DTBP	43.48-55.10	17.4	25.0	35.8	5.6	6.2	12.5	0.8	4.6	5.6

The films synthesized with SDS/DTBP additives in undistilled BFEE produced the highest electrical conductivities compared with films synthesized with other electrolyte combinations (see Figure 6.19). XRD analysis suggest that these films have best molecular ordering because they have the highest combination of d1, d2, and d3 Bragg's angles, the narrowest combination of d1 and d2 peaks, and a d1/d2 ratio close to one as shown in Figure 6.32 and Table 6.4. The data also suggest that films synthesized using SDBS/DTBP additives have better molecular packing than films made in DTBP/undistilled BFEE because of larger average Bragg's angles and smaller average FWHM, but molecular packing comparable with that of films made in SDBS/undistilled BFEE because the Bragg's angles and FWHM in Table 6.4 are comparable. This result is expected because the percent difference in conductivity of films synthesized in SDBS/DTBP/undistilled BFEE to the SDBS/undistilled BFEE film is not as high as the difference in conductivity between films synthesized in DTBP/undistilled BFEE and films synthesized in SDBS/DTBP/undistilled BFEE. Note that the 25 mM DTBP spectra in Figure 6.31 has some distortion that is likely due to some contamination on the surface. The films with anionic surfactants SDS and SDBS have better molecular ordering (smaller FWHM of d1, d2, and d3) than the films synthesized without additives in undistilled BFEE; identical results were observed with films synthesized in distilled BFEE (see Figure 6.31 and Table 6.3). Electropolymerized PTh films in anionic surfactant/DTBP/undistilled BFEE exhibit very promising mechanical and electrical properties as well as significantly enhanced molecular packing.

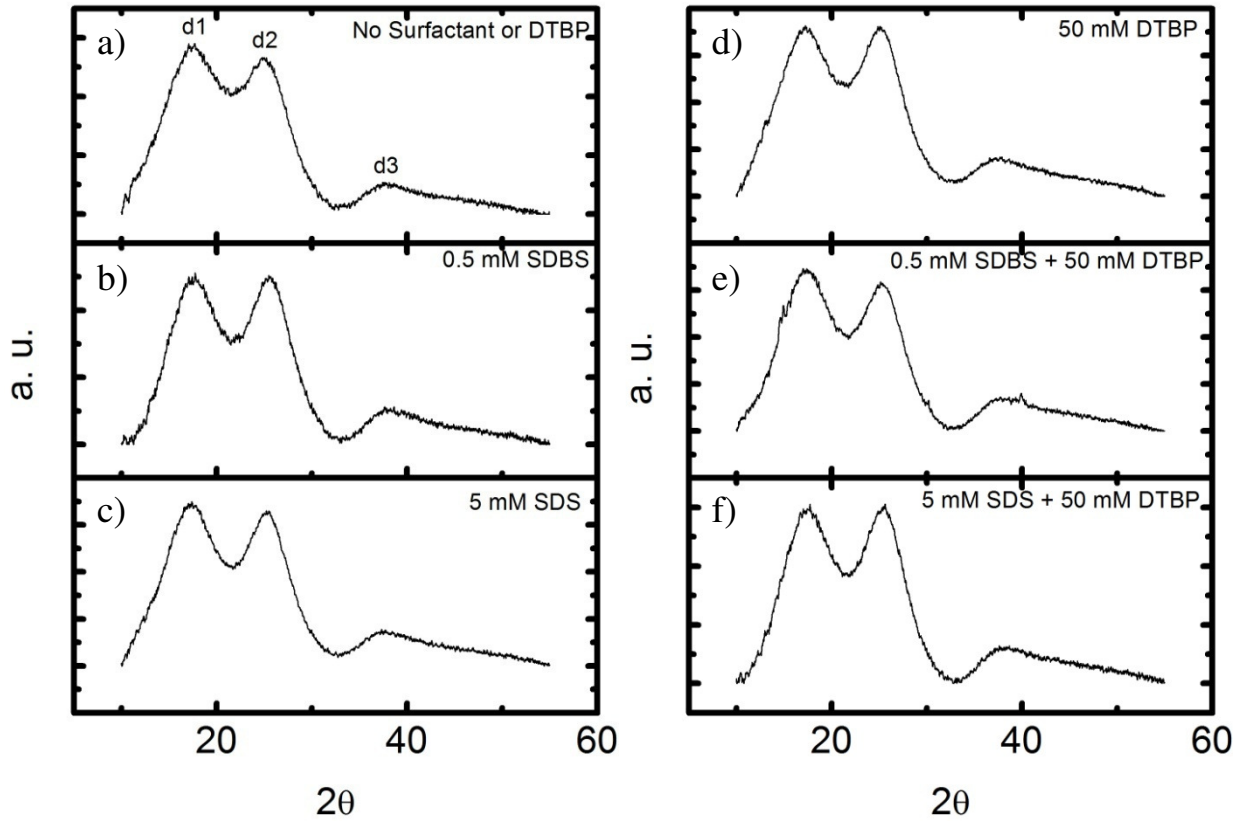

Figure 6.32: WAXS pattern in transmission mode of PTh film electrochemically synthesized using 50 mM thiophene with current density of 0.5 mA/cm^2 at 5 mm inter-electrode distance in undistilled BFEE with DTBP and anionic surfactants additive.

Table 6.4: X-ray diffraction data of PTh films synthesized in anionic surfactant/DTBP/undistilled BFEE electrolyte

		2θ			FWHM			Peak intensity ratio		
	σ (S/cm)	d1	d2	d3	d1	d2	d3	d1/d2	d1/d3	d2/d3
No surfactant or DTBP	25.76-26.8	17.5	25.1	38.6	7.3	5.5	9.1	1.2	7.1	6.2
0.5mM SDBS	36.85-46.04	17.7	25.5	37.9	6.4	5.2	9.4	1.0	6.0	5.8
5mM SDS	59.28-66.78	17.3	25.3	37.6	6.6	5.4	10.7	1.1	5.9	5.3
50mM DTBP	30.66-36.12	17.2	25.1	37.3	6.7	5.6	10.8	1.0	5.3	5.1
0.5mM SDBS + 50mM DTBP	53.45-84.71	17.4	25.3	37.9	6.0	5.4	9.4	1.2	5.7	5.0
5mM SDS + 50mM DTBP	87.89-119.7	17.6	25.4	38.3	6.1	5.2	10.4	1.0	6.0	5.8

7. CONCLUSIONS

This thesis has demonstrated the effects of several important processing parameters in the synthesis of PTh films and has shown for the first time that surfactant additives can be used in Lewis acid electrolytes such as BFEE to improve the molecular ordering and physical properties of ICP films such as PTh. Different parameters in the electrochemical polymerization of PTh in BFEE were studied to reveal and understand the conditions for improved experimental reproducibility, and to improve the molecular structure of PTh films and explain the mechanisms responsible for the improvements. The use of anionic surfactants SDS and SDBS and proton scavenger DTBP as additives in BFEE electrolyte were demonstrated to enhance molecular ordering in PTh films synthesized by electrochemical polymerization, and such enhancements produced improved in-plane electrical conductivities and mechanical properties. PTh films made with SDS and SDBS increased electrical conductivity by 479% and 61%, respectively, compared to films made without additives. All films in this work had Young's modulus in the range 1-8 GPa and tensile strength in the range 100-175 MPa; however, films fabricated with SDS and SDBS showed increased necking and elongation at break during density testing, which suggest increased alignment of constituent polymer chains using these additives. The findings in this study can be extended to improve the electrochemical processing of ICPs similar to PTh towards enhanced structural order and improved physical properties, and a high degree of experimental consistency.

The following steps and comments summarize key finding in this work and are presented to facilitate the fabrication of PTh films with enhanced electrical conductivity and mechanical properties:

1. Selection and preparation of electrodes: The electrode must be stable in the potential range of the process and have few surface defects, which can be removed with polishing to a mirror finish. Measures should be taken to minimize the contact resistance between the electrode and the lead wire; this will provide higher current efficiency during deposition.
2. Inter-electrode distance: The shortest distance is preferred to maximized current density. An optimal thiophene concentration of 50 mM was revealed for a distance of 5 mm. This critical concentration was determined using galvanostat and potentiostat techniques. The thiophene concentration should be increased to attain PTh films with similar properties using larger inter-electrode spacing.
3. Electrochemical method: The galvanostatic method is the preferable route for electrochemical synthesis of PTh, because it produces more compact, uniform films, and allows easier control of the total charge (i.e., film thickness). The current density needs to be optimized. High current density may produce films with more cross linking due to high oxidation potential, whereas low current density may produce oligomers in the PTh film.
4. Effect of surfactants: Anionic surfactants (SDS and SDBS) were demonstrated here as additives that improve the molecular ordering of PTh films. It was found that solvation of SDS and SDBS in BFEE requires external energy (i.e. sound, thermal, or light) to occur due to the low dielectric constant of BFEE. The concentration needs to be optimized, because the presence of micelles at high concentrations may hinder the polymerization process. Since SDS and SDBS are heavier than the thiophene, longer deposition times are necessary to compensate for “late-arriving” surfactant. PTh films

fabricated in SDS/BFEE electrolyte exhibit higher electrical conductivity than the films fabricated in SDBS/BFEE because of the steric effect of the benzene ring in SDBS.

5. Effect of proton scavenger: The addition of DTBP as an additive to BFEE led to reduction of defects in the polymer film. DTBP shows inhibiting effects because it reacts with intermediate radical cations, so its concentration needs to be optimized.
6. Combined effect of anionic surfactants and DTBP: An optimum concentration of anionic surfactants and DTBP added to undistilled BFEE produced PTh films with the highest electrical conductivities and best mechanical properties due to enhanced molecular order and reduced defects. Presence of water in BFEE improved the polymerization by increasing the diffusion rate.

7.1 Recommendations

Several studies have shown that the presence of water could improve the properties of polypyrroe by increasing the rate of polymerization [32, 79, 80]. In this study, water has been suggested to increase the polymerization rate, but no quantitative data were obtained because there was a technical limitation on measuring the content of water in BFEE. Coulometric Karl Fischer titration was performed, but the titrant, Hydernal-1, reacted with BFEE and failed to give any reading. Alternatively, the water content could be measured qualitatively by performing CV or CP and recording changes in current density. Using a distillation process, the water content in the BFEE could be highly controlled and characterized experimentally in order to determine the optimum conditions. Further work is suggested to study the role of water content in BFEE on the

electrochemical growth of PTh films. Using a molecular sieve pad can also be useful to control the water level in the BFEE electrolyte.

Additional studies, employing a wider variety of structural characterization techniques, are warranted to increase understanding of the mechanisms by which different processing conditions and electrolyte additives affect molecular ordering in PTh films. Studies that explore the effects of scaling electrode areas, spacing, and thiophene concentrations to find optimal conditions for large-scale production of PTh films would be very useful as well.

REFERENCES

[1] Chiang, C. K., Fincher, C. R., Park, Y. W., Heeger, A. J., Shirakawa, H., Louis, E. J., Gau, S. C., and MacDiarmid, A. G., 1977, "Electrical conductivity in doped polyacetylene," Physical Review Letters, 39(17), pp. 1098-1101.

[2] Shirakawa, H., and Ikeda, S., 1971, "Infrared spectra of polyacetylene," Polymer Journal, 2(2), pp. 231-244.

[3] Patil, A. O., Heeger, A. J., and Wudl, F., 1988, "Optical properties of conducting polymer," Chemical Review, 88, pp. 183-200.

[4] Bao-Yang, L., Cong-Cong, L., Shan, L., Jing-Kun, X., Feng-Xing, J., Yu-Zhen, L., and Zhuo, Z., 2010, "Thermoelectric performances of free-standing polythiophene and poly(3-Methylthiophene) nanofilms," Chinese Physics Letters, 27(5), p. 057201.

[5] Bubnova, O., Khan, Z. U., Malti, A., Braun, S., Fahlman, M., Berggren, M., and Crispin, X., 2011, "Optimization of the thermoelectric gigure of merit in the conducting polymer poly(3,4-ehylenedioxythiophene)," Nature Materials, 10, pp. 429-433.

[6] Garnier, F., Tourillon, G., Gazard, M., and Dubois, J. C., 1982, "Organic Conducting polymer derived from substituted thiophene as electrochromic material," Journal of Electroanalytical Chemistry, 148, pp. 299-303.

[7] Alkan, S., Cutler, C. A., and Reynolds, J. R., 2003, "High quality electrochromic polythiophene via $BF_3.Et_2O$ electropolymerization," Advanced Functional Materials, 13(4), pp. 331-336.

[8] Romero, D. B., Schaer, M., Zuppiroli, L., Cesar, B., and Franc¸ois, B., 1995, "Effects of doping in polymer light-emitting diodes," Applied Physics Letter, 67(12), pp. 1659-1661.

[9] Ding, A.-L., Pei, J., Lai, Y.-H., and Huang, W., 2001, "Phenylene-functionalized polythiophene derivatives for light-emitting diodes: their synthesis, characterization and properties," Journal of Materials Chemistry, 11(12), pp. 3082-3086.

[10] Vangeneugden, D. L., Vanderzande, D. J. M., Salbeck, J., Hal, P. A. v., Janssen, R. A. J., Hummelen, J. C., Brabec, C. J., Shaheen, S. E., and Sariciftci, N. S., 2001, "synthesis and characterization of a poly(1,3-dithienylisothianaphthene) derivative for bulk heterojunction photovoltaic cells," The Journal of Physical Chemistry, 105, pp. 11106-11113.

[11] Valaski, R., Canestraro, C. D., Micaroni, L., Mello, R. M. Q., and Roman, L. S., 2007, "Organic photovoltaic devices based on polythiophene films electrodeposited on ITO substrates," Solar Energy Materials and Solar Cells, 91(8), pp. 684-688.

[12] Lu, J., Pinto, N. J., and MacDiarmid, A. G., 2002, "Apparent dependence of conductivity of a conducting polymer on an electric field in a field effect transistor configuration," Journal of Applied Physics, 92(10), p. 6033.

[13] Zou, Y., Sang, G., Wu, W., Liu, Y., and Li, Y., 2009, "A polythiophene derivative with octyloxyl triphenylamine-vinylene conjugated side chain: synthesis and its applications in field-effect transistor and polymer solar cell," Synthetic Metals, 159(3-4), pp. 182-187.

[14] Paoli, M.-A. D., and Gazotti, W. A., 2002, "Electrochemistry, polymers, and opto-electronic devices: a combination with a future," Journal of the Brazilian Chemical Society, 13(4), pp. 410-424.

[15] Krebs, F. C., 2009, "Fabrication and processing of polymer solar cell: a review of printing and coating techniques," Solar Energy Materials and Solar Cells, 93(4), pp. 394-412.

[16] Fichou, D., 1999, Handbook of oligo- and polythiophenes, Wiley VCH, Weinheim, New York, Chochester, Brisbane, Singapore, Toronto.

[17] Landel, L. E. N. a. R. F., 1994, Mechanical Properties of Polymers and Composites Marcel Dekker.

[18] Tourillon, G., and Garnier, F., 1992, "New electrochemically generated organic conducting polymers," Journal of Electroanalytical Chemistry, 135, pp. 173-178.

[19] Pelizzetti, E., and Pramauro, E., 1985, "Analytical applications of organized molecular assemblies," Analytica Chimica Acta, 169, pp. 1-29.

[20] Ryu, and K., 2004, "The electrochemical performance of polythiophene synthesized by chemical method as the polymer battery electrode," Materials Chemistry and Physics, 84(2-3), pp. 380-384.

[21] Shakouri, A., and Li, S., "Thermoelectric power factor for electrical conductive polymer," Proc. 18th International Conference on Thermoelectrics, pp. 402-406.

[22] Mohammad, F., Calvert, P. D., and Billingham, N. C., 1995, "Thermal stability of electrochemically prepared polythiophene and polypyrolle," Bulletin of Materials Science, 18(3), pp. 255-261.

[23] Chiu, H. T., LIN, J. S., and HUANG, L. T., 1992, "The processing and mechanical properties of polypyrrole-poyluerathan alloy film," Journal of Applied Electrochemistry, 22, pp. 528-534.

[24] Shi, G., Jin, S., Xue, G., and Li, C., 1995, "A conducting polymer film stronger than aluminum," Science, 267, pp. 994-996.

[25] Li, C., Shi, G., Liang, Y., and Ye, W., 1998, "High-strength metallic plastic sheet prepared by electrochemical polymerization of thiophene on stainless steel," Journal of Applied Polymer Science, 68, pp. 1027-1029.

[26] Jin, S., and Xue, G., 1997, "Interaction between thiophene and solvated lewic acids and the low-potential electrochemical deposition of a highly anisotropic conducting polythiophene film," Macromolecus, 30, pp. 5753-5757.

[27] Li, X., and Li, Y., 2003, "Electrochemical preparation of polythiophene in acetonitrile solution with boron fluoride-ethyl ether as the electrolyte," Journal of Applied Polymer Science, 90, pp. 940-946.

[28] Tsukamoto, J., Takahashi, A., and Kawasaki, K., 1990, "Structure and electrical properties of polyacetylene yielding a conductivity of 10^5 S/cm," Japanese Journal of Applied Physics, 29(1), pp. 125-130.

[29] Gok, A., Omastova, M., and Yavuz, A., 2007, "Synthesis and characterization of polythiophenes prepared in the presence of surfactants," Synthetic Metals, 157(1), pp. 23-29.

[30] Zotti, G., 1997, Handbook of organic conductive molecules and polymers, conductive polymers: Synthesis and Electrical Properties, Wiley, New York.

[31] Tourillon, G., and Garnier, F., 1983, "Effect of fopant on the physicochemical and electrical properties of organic conducting polymers," The Journal of Physical Chemistry, 87, pp. 2289-2292.

[32] Downard, A. J., and Pletcher, D., 1986, "A Study of the conditions for the electrodeposition of polythiophene in acetonitrile," Journal of electroanalytical chemistry, 206, pp. 147-152
.

[33] Krische, B., and Zagorska, M., 1989, "The polythiophene paradox," Synthetic Metals, 28, pp. C263-C268.

[34] Dong, S., and Zhang, W., 1989, "Study on conducting polythiophene electrochemically polymerized in phosporic acid and aqueous solution," Synthetic Metals, 30, pp. 359-369.

[35] Bazzaoui, E. A., Aeiyach, S., and Lacaze, P. C., 1994, "Low potential electropolymerization of thiophene in aqueous perchloric acid," Journal of electroanalytical chemistry, 364, pp. 63-69.

[36] Jin, S., Cong, S., Xue, G., Xiong, H., Mandsdorf, B., and Cheng, S. Z. D., 2002, "Anisotropic polythiophene films with high conductivity and good mechanical properties via a new electrochemical synthesis," Advanced Materials, 14(20), pp. 1492-1496.

[37] Sakmeche, N., Aeiyah, S., Aaron, J.-J., Jouini, M., Lacroix, J. C., and Lacaze, P.-C., 1999, "Improvement of the electrosynthesis and physicochemical properties of poly(3,4-

ethylenedioxythiophene) esing a sodium dodecyl sulfate micellar aqueous medium," Langmuir, 15, pp. 2566-2574.

[38] Rusling, J. F., and Kamau, G. N., 1985, "Electrocatalytic reactions in organized assemblies part II. electrocatalytic reduction of allyl chloride by tris (2,2'-bipyridyl) cobalt (II) in micelles of dodecylsulfate," Journal of Electroanalytical Chemistry, 187, pp. 355-359.

[39] Naoi, K., Oura, Y., Maeda, M., and Nakamura, S., 1995, "Electrochemistry of surfactant-doped polypyrolloe film (I): formation of columnar structure by electropolymerization," Journal of the Electrochemical Society, 142(2), pp. 417-422.

[40] Bredas, J. L., and Street, G. B., 1985, "polarons, bipolarons, and solitons in conducting polymers," Accounts of Chemical Research, 18, pp. 309-315.

[41] Bredas, J. L., Themans, B., Andre, J. M., Chance, R. R., and Silbey, R., 1984, "The role of mobile organic radicals and ions (solitons, polarons, and bipolarons) in the transport properties of doped conjugated polymers," Synthetic Metals, 9(2), pp. 265-274.

[42] Brédas, J., Thémans, B., Fripiat, J., André, J., and Chance, R., 1984, "Highly conducting polyparaphenylene, polypyrrole, and polythiophene chains: an ab initio study of the geometry and electronic-structure modifications upon doping," Physical Review B, 29(12), pp. 6761-6773.

[43] Heinze, J., Frontana-Uribe, B. A., and Ludwigs, S., 2010, "Electrochemistry of conducting polymers-persistent models and new concepts," Chemical Reviews, 110, pp. 4724-4771.

[44] Andrieux, C. P., Audebert, P., Hapiot, P., and Saveant, J.-M., 1990, "Observation of the cation radicals of pyrrole and of some substituted pyrroles in fast-scan cyclic voltammetry. Standard potentials and lifetimes," Journal of the American Chemical Society, 112, pp. 2439-2440.

[45] Andrieux, C. P., Audebert, P., Hapiot, P., and Saveant, J. M., 1991, "Identification of the first steps of the electrochemical polymerization of pyrroles by means of fast potential step techniques," The Journal of Physical Chemistry, 95, pp. 10158-10164.

[46] Chen, W., and Xue, G., 2005, "Low potential electrochemical syntheses of heteroaromatic conducting polymers in a novel solvent system based on trifluroborate–ethyl ether," Progress in Polymer Science, 30(7), pp. 783-811.

[47] Plesch, P. H., 1963, The chemistry of cationic polymerization, Macmillan, New York.

[48] Topchiev, A. V., Zavgorodnii, S. V., and Paushkin, Y. M., 1959, Boron fluoride and its compounds as catalysts in organic chemistry, Pergammon Press, New York.

[49] Visy, C., Lukkari, J., and Kankare, J., 1994, "Study of the role of the deprotonation step in the electrochemical polymerization of thiophene-type monomers," Synthetic Metals, 66, pp. 61-65.

[50] Tanaka, K., Shichiri, T., Wang, S., and Yamabe, T., 1988, "A study of electropolymerization of thiophene," Synthetic Metals, 24, pp. 203-215.

[51] Schlesinger, M., and Paunovic, M., 2010, "Modern electroplating," John Wiley and Sons, Inc., Hoboken, New Jersey.

[52] Zhou, W., Zhai, C., Du, Y., Xu, J., and Yang, P., 2009, "Electrochemical fabrication of novel platinum-poly(5-nitroindole) composite catalyst and its application for methanol oxidation in alkaline medium," International Journal of Hydrogen Energy, 34(23), pp. 9316-9323.

[53] Smits, F. M., 1958, "Measurement of sheet resistivites with the four-point probe," The Bell System Technical Journal pp. 711-718.

[54] Li, Y., and Qian, R., 1993, "Stability of conducting polymers from the electrochemical point of view," Synthetic Metals, 53, pp. 149-154.

[55] Wang, X.-S., and Fen, X.-Q., 2002, "Effect of thickness on mechanical properties of conducting polythiophene films," Journal of material science letters, 21, pp. 715-717.

[56] Nevedov, V. I., 1988, X-ray photoelectron spectroscopy of solid surfaces, VSP Books, Zeiss.

[57] Zytner, Y. D., and Makarov, K. A., 1980, "Current effiecienty and thermal effieciency of initiation during electrochemical polymerization," Polymer Science, 22(11), pp. 2866-2869.

[58] Otero, T. F., and Larreta-Azelain, E. d., 1988, "Electrochemical generation of polythiophene films on platinum electrode," Polymer - Plastics Technology and Engineering, 29, pp. 1522-1528.

[59] Audebert, P., Catel, J. M., Coustumer, G. L., Duchenet, V., and Hapiot, P., 1998, "Electrochemistry and polymerization mechanism of thiophene-pyrrole-thiophene oligomers and terthiophens. Experimental and theoritical modeling studies," The Journal of Physical Chemistry B, 102, pp. 8661-8669.

[60] Roncali, J., 1992, "Conjugated poly(thiophenes): Synthesis, functionalization, and applications," Chemical Reviews, 92, pp. 711-738.

[61] Satoh, M., Kaneto, K., and Yoshino, K., 1986, "Depedences of electrical and mechanical properties of conducting polypyrrole films on conditions of electrochemical polymerization in an aqueous medium," Synthetic Metals, 14, pp. 289-296.

[62] Sari, B., Talu, M., Yildirim, F., and Balci, E. K., 2003, "Synthesis and Characterization of polyurethane/polythiophenne Conducting copolymer by electrochemical method," Applied Surface Science, 205, pp. 27-38.

[63] Sakmeche, N., Bazzaoui, E. A., Fall, M., Aeiyach, S., Jouini, M., Lacroix, J. C., Aaron, J. J., and Lacaze, P. C., 1997, "Appliation of sodium dodecylsulfate (SDS) micellar solution as an organized medium for electropolymerization of thiophene derivates in water," Synthetic Metals, 84, pp. 191-192.

[64] Fall, M., J. J, A., Sakmeche, N., Dieng, M. M., Jouini, M., Aeiyach, S., Lacroix, J. C., and Lacaze, P. C., 1998, "Electrochemical and spectroscopic properties of poly(3-methoxythiophene) electrosynthesized in an aqueous micellar medium," Synthetic Metals, 93, pp. 175-179.

[65] Sakmeche, N., Aaron, J. J., Fall, M., Aeiyach, S., Jouini, M., Lacroix, J. C., and Lacaze, P. C., 1996, "Anionic micelles; a new aqueous medium for electropolymerization of poly(3,4-ethylenedioxythiophene) films on Pt electrodes," Chemical Communications(24), p. 2723.

[66] Jaschke, M., Butt, H. J., Gaub, H. E., and Manne, S., 1997, "Surfactant Aggregates at a metal surface," Langmuir, 13, pp. 1381-1384.

[67] Barr, G. E., Sayre, C. N., Connor, D. M., and Collard, D. M., 1996, "Polymerization of hydrophobic 3-alkylpyrroles from aqueous solutions of sodium dodecyl sulfate," Langmuir, 12, pp. 1395-1398.

[68] Espinosa, C. E., Guo, Q., Singh, V., and Behrens, S. H., 2010, "Particle charging and charge screening in nonpolar dispersions with nonionic surfactants," Langmuir, 26(22), pp. 16941-16948.

[69] Osthoff, R. C., Brown, C. A., and Hawkins, J. A., 1951, "The dipole moments of some boron trifluorides etherates," Journal of the American Chemical Society, 73(11), p. 5480.

[70] Hoeven, P. C. V. D., and Lyklema, J., 1992, "Electrostatic stabilization in non-aqueous media," Advances in Colloid and Interface Science, 42, pp. 205-277.

[71] Yang, K., Zhu, L., and Xing, B., 2007, "Sorption of sodium dodecylbenzene sulfonate by montmorillonite," Environmental Pollution, 145(2), pp. 571-576.

[72] McIntire, G. L., and Blount, H. N., 1979, "Electrochemistry in ordered systems. 1. Oxidative electrochemistry of 10-methylphenothiazine in anionic, cationic, nonionic micellary systems," Journal of the American Chemical Society, 101, p. 7720.

[73] Lagrost, C., Jouini, M., Tanguy, J., Aeiyach, S., Lacroix, J. C., Chane-Ching, K. I., and Lacaze, P. C., 2001, "Bithiophene electropolymerization in aqueous media: A Specific effect of SDS and β-cyclodextrin," Electrochimica Acta, 46, pp. 3985-3992.

[74] Takakubo, M., 1989, Journal of Electroanalytical Chemistry, 258, p. 303.

[75] Li, C., and Imae, T., 2004, "Electrochemical and optical properties of the poly(3,4-ethylenedioxythiophene) film electropolymerized in an aqueous sodium dodecyl sulfate and lithium tetrafluoroborate medium," Macromolecus, 37, pp. 2411-2416.

[76] Fu, M., Shi, G., Chen, F., and Hong, X., 2002, "Doping level change of polythiophene film during its electrochemical growth process," PCCP, 4(12), pp. 2685-2690.

[77] Heeg, J., Kramer, C., Wolter, M., Michaelis, S., Plieth, W., and Fischer, W. J., 2001, "Polythiophene - O_3 surface reaction studied by XPS," Applied Surface Science, 180, pp. 36-41.

[78] Wu, C. R., Nilsson, J. O., Inganas, O., Salaneck, W. R., Osterholm, J. E., and Bredas, J. L., 1987, "Electronic structure of polythiophene," Synthetic Metals, 21, pp. 197-202.

[79] Zotti, G., Schiavon, G., Berlin, A., and Pagani, G., 1989, "The role of water in the electrochemical polymerization of pyrroles," Electrochimica Acta, 34(6), pp. 881-884.

[80] Beck, F., Oberst, M., and Jansen, R., 1990, "On the mechanism of the filmforming electropolymerization of pyrrole in acetonitrile with water," Electrochimica Acta, 35(11), pp. 1841-1848.